



SPE 145080

Reservoir Engineering for Unconventional Gas Reservoirs: What Do We Have to Consider?

C.R. Clarkson, University of Calgary; J.L. Jensen, University of Calgary and T.A. Blasingame, Texas A&M University

Copyright 2011, Society of Petroleum Engineers

This paper was prepared for presentation at the SPE North American Unconventional Gas Conference and Exhibition held in The Woodlands, Texas, USA, 14–16 June 2011.

This paper was selected for presentation by an SPE program committee following review of information contained in an abstract submitted by the author(s). Contents of the paper have not been reviewed by the Society of Petroleum Engineers and are subject to correction by the author(s). The material does not necessarily reflect any position of the Society of Petroleum Engineers, its officers, or members. Electronic reproduction, distribution, or storage of any part of this paper without the written consent of the Society of Petroleum Engineers is prohibited. Permission to reproduce in print is restricted to an abstract of not more than 300 words; illustrations may not be copied. The abstract must contain conspicuous acknowledgment of SPE copyright.

Abstract

The reservoir engineer involved in the development of unconventional gas reservoirs (UGRs) is required to integrate a vast amount of data from disparate sources, and to be familiar with the data collection and assessment. There has been a rapid evolution of technology used to characterize UGR reservoir and hydraulic fracture properties, and there currently are few standardized procedures to be used as guidance. Therefore, more than ever, the reservoir engineer is required to question data sources and have an intimate knowledge of evaluation procedures.

We propose a workflow for the optimization of UGR field development to guide discussion of the reservoir engineer's role in the process. Critical issues related to reservoir sample and log analysis, rate-transient and production data analysis, hydraulic and reservoir modeling and economic analysis are raised. Further, we have provided illustrations of each step of the workflow using tight gas examples. Our intent is to provide some guidance for best practices. In addition to reviewing existing methods for reservoir characterization, we introduce new methods for measuring pore size distribution (small-angle neutron scattering), evaluating core-scale heterogeneity, log-core calibration, evaluating core/log data trends to assist with scale-up of core data, and modeling flow-back of reservoir fluids immediately after well stimulation. Our focus in this manuscript is on tight and shale gas reservoirs; reservoir characterization methods for coalbed methane reservoirs have recently been discussed.

Introduction

The primary functions of a reservoir engineer, according to Dake (1978) are "estimation of hydrocarbons in place, the calculation of a recovery factor and the attachment of a time scale to the recovery". For modern reservoir engineers, this process will include estimating fluids-in-place and forecasting fluid production for play and prospect analysis, asset valuation, resource and reserves estimation, and field development planning. For conventional reservoirs, there are "tried and true" methods for performing these duties that are an outcome of relatively well understood fluid storage and transport mechanisms for these reservoir types. Many techniques for quantifying key reservoir properties controlling storage and flow, calculating hydrocarbons in place, establishing recovery and forecasting production have a long history of development and refinement. The reality for unconventional gas reservoirs (UGRs), including low-permeability (tight gas), coalbed methane (CBM) and shale gas reservoirs, is that fluid storage and transport mechanisms are poorly understood, and we are at an early stage for some reservoir types (ex. shale gas) in the development of such methods. Further, it is not just necessary to characterize the reservoir in unconventional plays but also the induced hydraulic fracture(s) or fracture network, that have a large impact on well performance, yet methods for evaluating hydraulic fracture properties are also in their infancy. Indeed there are new methods for unconventional reservoir and hydraulic fracture analysis (ex. microseismic monitoring and analysis) that are considered critical to the evaluation process that have only routinely been used for oilfield applications in the past decade; it is the job of the UGR engineer to keep on top of new developments, understand the uncertainties and the consequent impact on their evaluations.

Perhaps more than any other technical discipline related to petroleum geosciences and engineering, the reservoir engineer is required to interrogate, integrate and assimilate data from a vast array of sources. One only needs to think about all the inputs required to perform a field-scale reservoir simulation to see that this is true. Inputs include fluid, rock and reservoir properties, structural information about the reservoir, hydraulic fracture properties (for individual well performance modeling), wellbore architecture and current and historical completion (event sequences) information, production data and flowing pressures, wellbore tubulars and production strings, surface hydraulic networks and associated constraints. All data

sources need to be intensely scrutinized to yield meaningful results. The reservoir engineer is usually involved in the design of data gathering programs (for example a surveillance program), so an awareness of cost and value of information is also necessary. Finally, the conscientious reservoir engineer will need to evaluate all methods for arriving at critical inputs (ex. permeability and porosity), and understand sources of uncertainty. Because uncertainty in key reservoir and hydraulic fracture properties for UGRs is often great, this aspect of the reservoir engineer’s role is particularly critical.

The purpose of this manuscript is to discuss a primary function of the reservoir engineer in the context of unconventional gas: understanding data sources, data uncertainty and evaluation methods specifically for UGRs. To guide this discussion a workflow is given to demonstrate one approach to optimizing field development (Fig. 1). The reservoir engineer also has an active role in the exploration process, but this will not be discussed here. The evaluation process starts at small scales (core or finer) and proceeds to progressively larger scales (Fig 1).

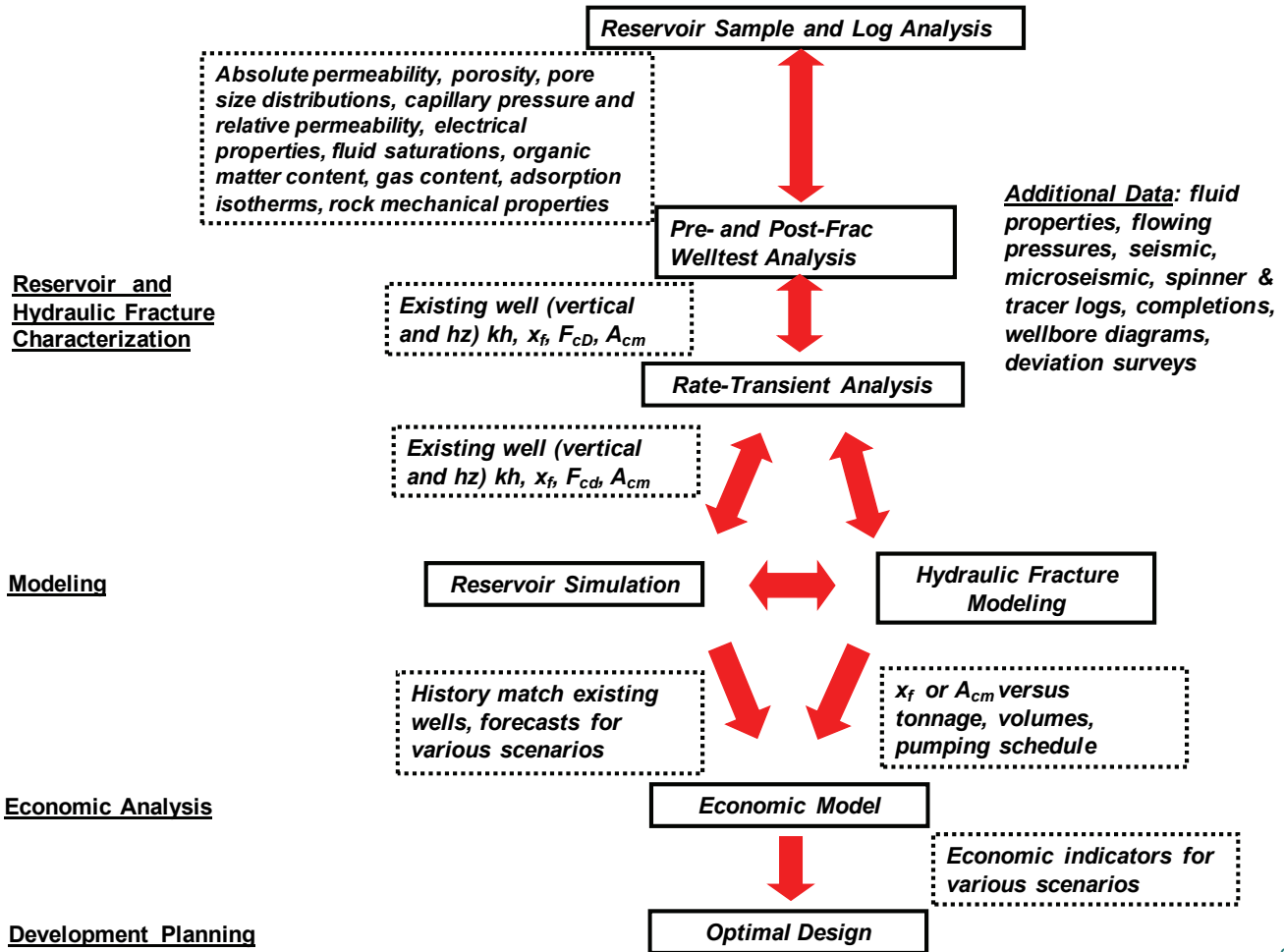


Fig. 1 — Illustration of a workflow used to optimize field development in unconventional gas reservoirs.

Typically field development optimization involves a reservoir and hydraulic fracture characterization step, where key fluid, reservoir (Table 1) and hydraulic fracture property (Table 2) data are estimated and integrated for the purpose of providing input to reservoir and hydraulic fracture models. This stage involves not only data collection and property estimation, but also critical decisions on the types of models needed to describe the reservoir, as will be discussed below.

<i>Reservoir Property</i>	<i>Data Source</i>
Porosity	Helium gas expansion, mercury injection capillary pressure (MICP), nuclear magnetic resonance (NMR), log analysis (calibrated to core)
Permeability	Core Analysis: Steady-state and unsteady state (pressure- and pulse-decay), MICP Well-test Analysis: (pre- and post-fracture) Injection/falloff (IFOT), diagnostic fracture injection test (DFIT), post-fracture flow and buildup (FBU) Production Analysis: Rate-transient analysis (RTA), simulation history-matching
Pore Pressure	IFOT, “dip-in”, perforation inflow diagnostic (PID), perforation inflow test analysis (PITA), various openhole tests
Water saturation	Core extraction (Dean Stark, Retort), capillary pressure, log analysis (using lab-based electrical property measurements)
Free and sorbed gas	Desorption canister testing & adsorption isotherms, calibrated log analysis
Total Organic Carbon	Leco TOC & RockEval (calculated)
Thermal Maturity	Vitrinite reflectance (Ro), RockEval (calc)
Rock composition	X-Ray Diffraction (XRD), Fourier-Transform Infrared (FTIR) visual point count (for optically-resolvable grains), EDAS (SEM), electron microprobe
Rock mechanical properties	Core measurements, log-derived (dipole sonic, (DSI))
Fracture and closure stress	Mini-frac tests, DFIT, log-based (DSI) calibrated to core
Fluid properties	Mud log, produced gas and water analysis (PVT properties)
Temperature	Openhole logs, “dip-in” pressure/temperature, production logs

Table 1. Common sources for key reservoir, fluid and rock properties for UGRs. Modified from Sondergeld et al. (2010a).

<i>Hydraulic Fracture Properties</i>	<i>Data Source</i>
Propp'd hydraulic fracture length and conductivity (static)	Post-fracture net-pressure analysis (hydraulic fracture modeling), post-fracture flow and buildup
Propp'd hydraulic fracture length and conductivity (flowing)	Rate-transient analysis
Created hydraulic fracture length, height and geometry (complexity)	Microseismic, tiltmeter survey, 4D seismic

Table 2. Common sources for hydraulic fracture properties for UGRs.

Data for different scales (reservoir sample sizes) are involved in the characterization step – it is best to consider these scales in the context of fluid transport pathways from reservoir to wellbore (**Fig. 2**). Each characterization method is designed to sample different reservoir sizes and estimate different properties. For example, well-test and rate-transient analysis are designed to sample meso- (10s of meters) and macro-scale properties (100s of meters) of the reservoir, and averaging of important properties (ex. permeability) is performed at this scale. All other methods represent progressively finer reservoir sizes.

We now discuss each step in the field development optimization workflow (**Fig. 1**) for UGR evaluation and address some of the primary reservoir engineering considerations. In some cases, we will also discuss new techniques that may prove useful for future UGR evaluation. This review is not meant to be exhaustive, but rather serves to highlight some of the key issues related to UGR evaluation. We illustrate the steps and techniques using tight gas reservoir examples from the same formation, but different geographic regions (Areas A and B) in Western Canada.

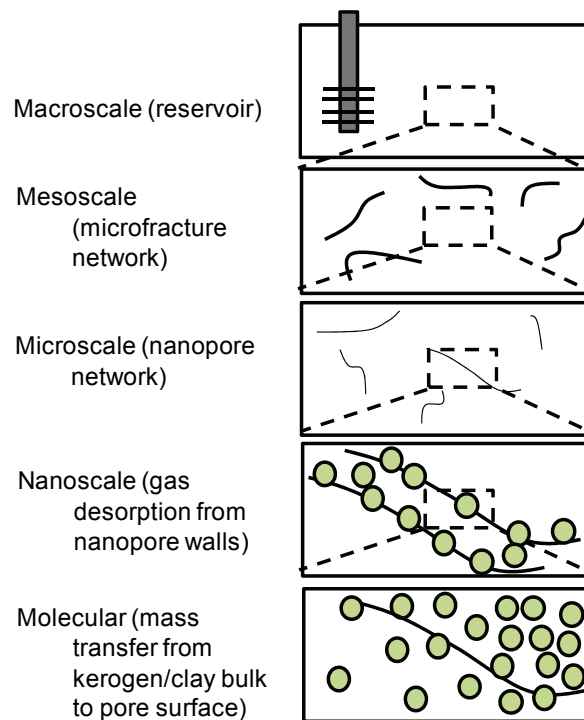


Fig. 2 — Illustration of the impact of scale on transport mechanisms in shale gas reservoirs. Flow to the wellbore is first initiated at the macroscale, followed by flow at progressively finer scales, including molecular transport through nanoporosity in kerogen. Modified from Javadpour et al. (2007).

Reservoir Sample Analysis

Reservoir sample analysis includes the evaluation of full-diameter core, core plugs, cuttings and other reservoir samples (including outcrops), to establish reservoir properties such as absolute permeability, porosity and sorption characteristics. There has been a rapid evolution in technologies for reservoir sample analysis to account for UGR properties, including ultra-fine (ex. nanopore) matrix pore structure, ultra-low permeability (ex. nano-darcy), gas storage by sorption (CBM and organic-rich shales), stress-sensitive porosity and permeability, multi-phase flow, compositional heterogeneity, and fluid sensitivity. There are typically no standards developed for evaluating key reservoir properties, and the reservoir engineer must be cognizant of the variability in estimated properties depending upon sample capture, storage and preparation techniques, and analytical method used. Some techniques, such as focused ion beam/scanning electron microscopy (FIB/SEM) are brand new, and helpful for understanding fluid storage and transport at the micro-/nano-scale, but sample only a very small (microns) portion of the reservoir.

Table 1 provides an overview of the techniques currently used for UGRs, which will be briefly reviewed below. First we begin with a discussion of the importance of sample collection, handling/preparation and type.

Sample Handling and Type. Of primary concern when performing reservoir sample analysis is the state of the sample (preserved or subject to atmospheric conditions), the size of the sample (full-diameter core, core plug, cuttings etc.) and hence the volume over which properties are averaged, the mud system used and the impact of mud invasion on measured properties, whether or not the sample(s) are representative of the interval of interest, and the ability to recreate *in-situ* conditions (ex. stress and fluid saturation). All of these factors will have an impact on the measured reservoir or rock properties of interest. If samples are not preserved then fluid loss or gain in the sample will result – fluid flow of gas in UGRs is extremely sensitive to water saturation (S_w), as is gas sorption on organic matter. Standardized tests (ASTM) have been created to reproduce *in-situ* water content in coal, but to our knowledge, these do not exist for tight gas or shale. For the latter, it is best to use preserved cores if possible. **Fig. 3** illustrates the impact of sample size on dehydration times for a tight gas reservoir, and the importance of proper core handling. Two samples were analyzed: one was crushed to powder; the other is a core plug. Both samples were subject to atmospheric pressure and 20°C; short (< 12 hours) exposure of the crushed sample led to a reduction of S_w from 40% to 2%, whereas the core plug S_w decreased after a much longer period. Clearly sample size plays a role in the rate of dehydration, and even modest exposure can affect S_w estimates. Wherever possible, use preserved samples.

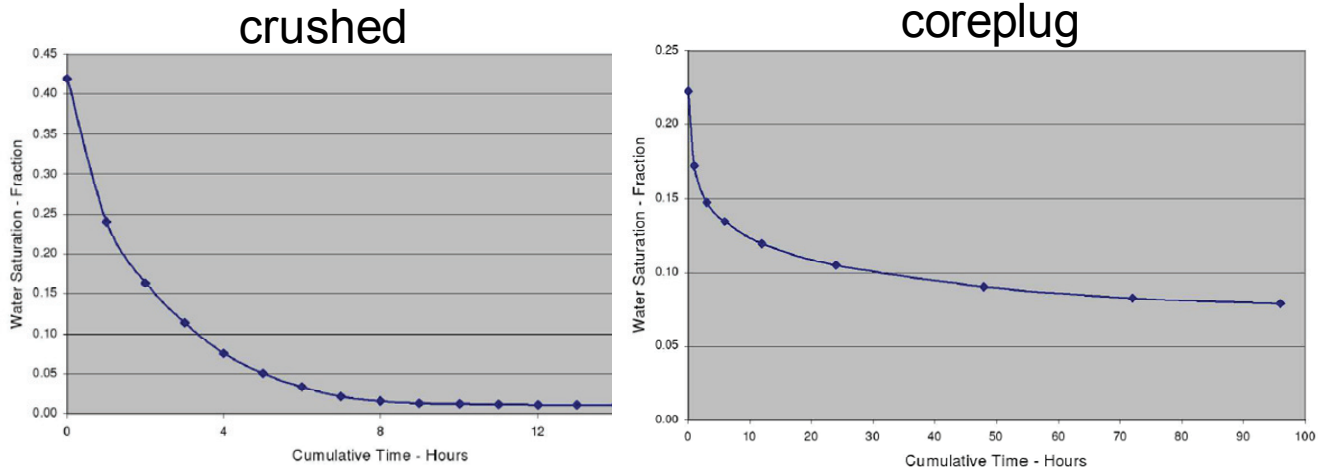


Fig. 3 — Illustration of the effect of sample size on dehydration time for a tight gas sample from study area A.

Sample size affects the volume over which properties such as porosity and permeability are averaged. Methods for averaging multiple samples is specific to the type of measurement performed (ex. porosity or permeability) and will be discussed in a later section. Whole (full-diameter) core may be more representative than smaller samples particularly if fine-scale heterogeneities are present such as laminations, but whole core may be more susceptible to drilling mud invasion (and hence property alteration) and may be more difficult to clean. Core plugs and sidewall cores allow for more precise estimates of properties of specific lithofacies that are at a finer scale than full-diameter core, improving correlations between porosity and permeability, but there is a possibility of sampling bias. On inspection of full-diameter core, core plugs are often taken from intervals that look best on logs or are visually the best reservoir – such sampling practices place a statistical bias on the sampling program, causing problems with log-core analysis. Care must be taken in cutting core plugs from full-diameter cores when swelling clays are present; for this purpose, either brine, or preferably liquid nitrogen should be used as a lubricant. Percussion sidewall cores can lead to loss of sample integrity and fracturing, and cuttings are problematic due to possible contamination with non-reservoir lithologies, and difficulty in accurate determination of the original sample depth. Mavor (1996) discusses sampling protocols for coalbed methane to improve core-log calibration for gas content determination, some of which are applicable to organic-rich shales.

To crush or not to crush: there is a fundamental philosophical difference between commercial labs as to whether it is better to crush samples before permeability and porosity measurement, or to perform the measurements on core plugs or full diameter core – the differences in results between the 2 methods are tremendous (Sondergeld et al. 2010a). There are advantages and disadvantages to both, but we note that there are variable procedures between labs regardless of what sample sizes are used. The process of reservoir sampling often causes stress-relief fracturing to occur in the samples. Some labs prefer to crush samples to remove these microfractures that were not present *in-situ* and to provide access to more non-connected porosity. There are several disadvantages to this method, including the inability to provide stress to crushed samples and the fact that permeability is a function of particle size (Cui et al. 2009). Core plugs sample a larger volume of reservoir, and hence measurement involves averaging over a larger scale. If fine laminations or fractures occur in the samples, then orientation of the plug relative to the heterogeneities has a large impact on the permeability. With core plugs, measurements tend to take longer, and stress-relief fractures may be present. Measurements at elevated confining pressure may close the artificially-induced fractures.

An issue of critical importance for UGRs is the recreation of *in-situ* conditions in the lab. Byrnes (2006) notes that all petrophysical properties that are measured are a function of the pressure (pore and confining pressure), volume/scale, temperature and time/history, and composition (rock and fluid) (PVTxt). Lab measurement conditions directly influence the property being measured. For example, permeability and porosity are a function of the pore/confining pressure and method for application of stress (uniaxial, hydrostatic conditions etc.), current temperature of measurement, temperature and pressure history while collecting (most properties exhibit some form of hysteresis due to cyclic loading/unloading), and fluid type used to measure the property (if fluid invasion techniques are used). The reservoir engineer must always question the conditions of lab measurement and understand the sensitivity of those properties being measured to PVTxt. We discuss specific measurements performed as part of the reservoir sample analysis step in Fig. 1 and issues relative to the measurement that the reservoir engineer should know.

Matrix Fluid Saturation and Moisture Content. Fluid saturation and moisture content affect free gas and sorbed gas storage (coals, some shales) in UGRs. Common methods for saturation measurement in tight gas and shale reservoirs are Dean-Stark extraction and retort; crushed samples are often used for extraction from shale. Both Dean Stark and retort

methods have been standardized (API – RP40, API 1998). These API standards are applicable to conventional and tight reservoirs with permeabilities down to 1 μ D (Sondergeld et al. 2010a). The Dean Stark method involves heating a solvent to its boiling point, which then vaporizes water from the sample. The solvent and water, which may be miscible or immiscible, depending on the solvent used, rise to a condensing tube, then collect in an overflow or collection tube. High-temperature and low-temperature extraction methods, which use different solvents, have been applied and can lead to different results. High-temperature methods have the advantage that the solvent used (usually toluene) is immiscible with water allowing for easy measurement of water yield, but may cause clay dehydration (depending hydration temperature of the clay), artificially inflating the Sw. If the samples contain oil, oil volume cannot be directly measured with this method as it is miscible in toluene. Low temperature extraction, while not posing a problem for clay dehydration, is not as effective for extraction of liquid hydrocarbons, and the solvent used is usually miscible in water, so the water yield cannot be measured directly.

The retort method involves the removal of 30-100 g of sample from core, which is then crushed and retorted at 425-650°C to vaporize water and oil (if present). The vapor is captured (condensed) in a cold trap and measured volumetrically. Separate chip samples are then tested for gas saturation by injecting mercury to a pressure of 750-1000 psi – the injected mercury is assumed to occupy space formerly occupied by gas. The total pore volume is then obtained from summation-of-fluids. This technique can also lead to errors, depending on the lithology and the nature of the organic matter (Byrnes 2006). As with Dean Stark, the principal source of error is the saturation changes experienced by the core during coring operations, retrieval and preparation. The use of different samples for mercury injection and retort can lead to errors, and the high temperature of analysis often will lead to clay and sulphate dehydration. Mineral dehydration can lead to artificially high porosities and Sws. Programmed temperature series using the retort method can allow for distinction between bound and free water. Sondergeld et al. (2010a) compared shale gas reservoir Sws obtained from commercial labs using retort and Dean Stark methods, demonstrating substantial differences. They noted that there is no standardization of measurements for shale gas reservoirs.

For these extraction methods, sample preservation is critical (**Fig. 3**). In one well in tight gas study Area A, three 36 m cores were taken and subject to routine porosity, permeability and Dean Stark extraction (using toluene). 106, 1.5” diameter core plugs were cut from the preserved cores using liquid nitrogen as a lubricant. Sws ranged from 10.5 – 99.3%, oil saturations from 1.1 – 25.1% and gas saturations from 0 – 84.5%. Sws were generally < 30%. The reservoir, which has low permeability (see below), appears to be sub-normally saturated (desiccated) – the potential for phase trapping is considered high, and is investigated further below.

Lab-based NMR has also been used to estimate Sws in coal and shale. Guo et al. (2007) for example used the T₂ spectra from low-field NMR to detect adsorbed (fast relaxation, T₂ < 5 ms), capillary-bound (T₂ = 5-200 ms) and bulk (free) water (slow relaxation, T₂ > 200 ms). We anticipate this technology to play a more pivotal role in UGR fluid saturation and pore size analysis in the future.

Matrix Porosity and Pore Size Distribution. Porosity and porosity distribution estimates are critical for both storage and flow quantification in UGRs. Due to the complex nature of porosity in UGRs, the typically wide distribution of pore sizes (PSD) and shapes, and existence of pore sizes at the nanometer scale, measurement of porosity and pore size distributions can be a complicated affair (**Fig. 4**). Both fluid invasion methods, where a molecular probe is used to investigate the pore structure (connected pores only), and radiation methods, where x-ray or neutron scattering patterns are interpreted in terms of pore structure, have been used (Bustin et al. 2008a). If properly performed, porosity measurements (combined with saturation measurements) are useful for estimating free-gas storage, and PSDs (**Fig. 5**) can be used assess storage mechanism (free- versus sorbed), infer transport mechanisms and assist with establishing controls on fluid flow (ex. dominant pore throat size).

Typically a variety of methods is required to recreate the entire pore-size distribution of shale, coal and some tight gas reservoirs. For example, in the classic paper by Gan et al. (1972), a combination of mercury porosimetry and low-pressure nitrogen and carbon dioxide adsorption methods were applied to investigate PSDs in coal matrix porosity, and the data for each method, which covered a certain pore size range, were used to piece together the full pore size spectrum. Mercury intrusion data, where pore size is related to mercury injection pressures using the Washburn equation (Washburn 1921), were used to obtain a meso- (pore diameters between 2 – 50 nm) and macropore (pore diameters > 50 nm) distributions. Low pressure nitrogen adsorption isotherms were interpreted for pore size distribution in the mesopore range – micropore volume was inferred from the difference between total porosity and meso + macroporosity. Total porosity was established using by estimation of coal density using helium (for grain density) and mercury. Considerations for and limitations of isotherm, mercury intrusion and pycnometry measurements were also discussed by Gan et al. (1972). Much the same procedure was later applied by other researchers for coal (ex. Clarkson and Bustin 1999a) and most recently shale (Bustin et al. 2008a). It has been recognized for many years that molecular sieving (selected access to ultra-fine porosity based upon size of molecular probe) occurs in ultra-fine porous media such as activated carbons. Most recently, Ross and Bustin (2007) noted the impact of the selection of helium for void volume calculations used in adsorption isotherm measurement – due to size, helium can access smaller pores than typical reservoir gases, causing void volume measurements to exceed those measured with reservoir gases; if other reservoir gases are used for this purpose however, the impact of sorption must be included (Cui and Bustin 2009).

Radiation methods include scanning electron microscopy, transmission electron microscopy, small-angle x-ray and neutron scattering and optical microscopy. Optical microscopy allows only the largest pores in unconventional reservoirs to be observed, but is very useful for understanding of mode of occurrence and porosity types (ex. intergranular, intraparticle, slot porosity), mineralogic controls and affects of diagenesis (mechanical and chemical). Pores that can be observed with optical microscopy, assuming they are open at *in-situ* conditions, affect fluid flow and storage. Recently, backscattered scanning electron imaging, combined with focused ion beam (FIB) milling techniques, have allowed observations of porosity to be extended down to the nanopore range (actually lower mesopore range, using IUPAC definition), and have allowed porosity associations to be interpreted at this scale. Although occurrence of nanoporosity in kerogen has been known for many years (ex. Gan et al. 1972), we have only recently been able to “observe” pore sizes to ~ 4 nm with SEM. Some have even used the technique to create 3D volumes of porosity (Sondergeld et al. 2010b), but we note that these volumes are usually at the micron scale and would be difficult to scale-up for engineering purposes. Scanning transmission electron microscopy (STEM) methods have also recently been applied to shales, which allow even smaller pore sizes to be resolved, but scale-up of sample volume is challenging with this technique.

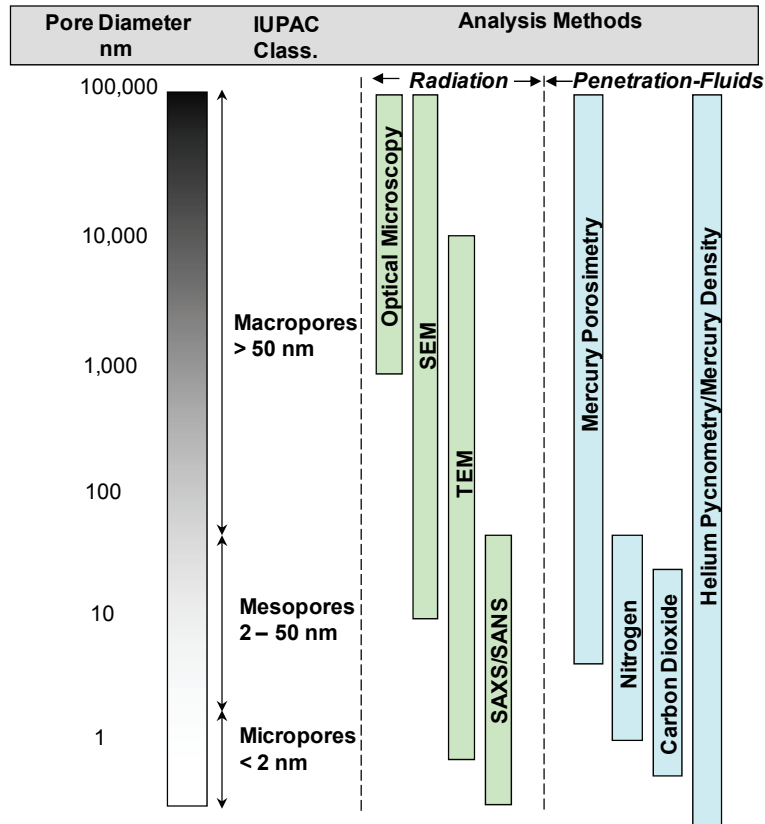
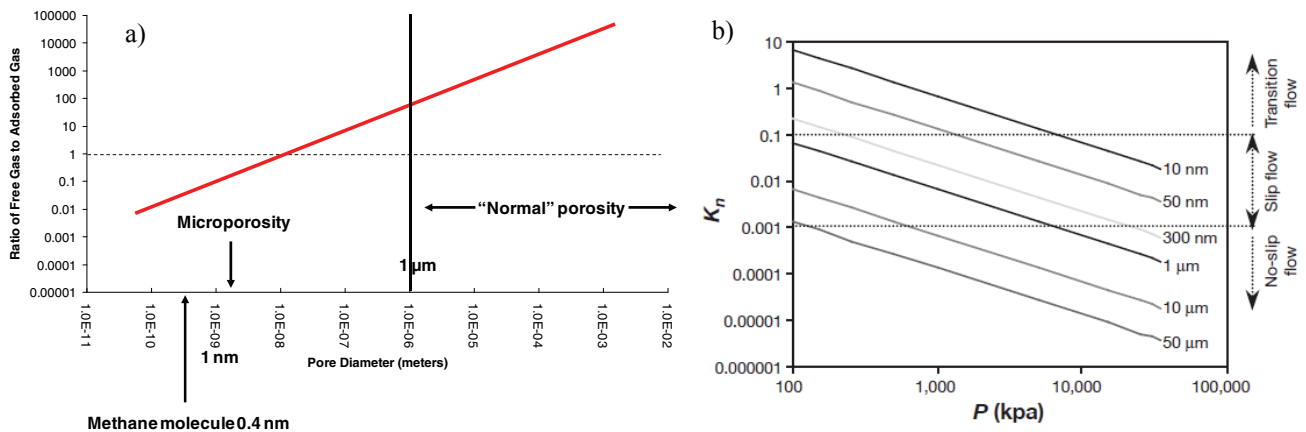


Fig. 4 — Methods used to estimate porosity and pore size distributions in unconventional gas reservoirs. Modified from Bustin et al. (2008b).



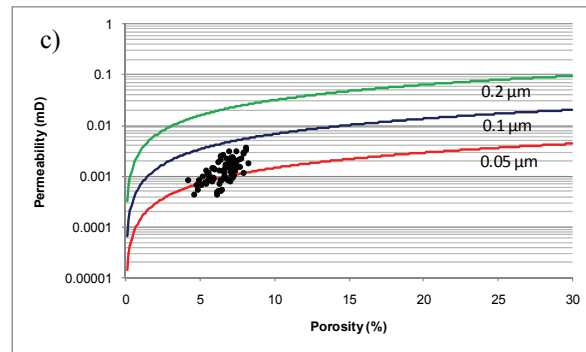


Fig. 5 — Uses of pore size distributions for unconventional reservoir characterization: a) inference of gas storage mechanism (modified from Beliveau 1993); b) inference of transfer mechanism (modified from Javadpour et al. 2007); c) and identification of dominant pore throat radius using a Winland-style plot.

Not included in Fig. 4, some researchers have also investigated the use of nuclear magnetic resonance (NMR) as a way to investigate pore structure in coal and shale. Recently, Sondergeld et al. (2010b) presented T2 spectra for Barnett shales and noted that “NMR is sensing pore bodies not accessed by mercury data” and calculated pore body radii from 5 nm to 150 nm.

Very recently, small-angle neutron (SANS) and ultra-small-angle neutron (USANS) measurements have been used out on coalbed methane reservoir samples to investigate matrix pore size distributions and the impact of CO₂ adsorption on pore structure (Melnichenko et al. 2009). In a SANS experiment (**Fig. 6**), a neutron beam is directed at a sample, and the neutrons are elastically scattered due to their interaction with nuclei of atoms in the sample – the scattering vector is related to a characteristic length scale (pore size) in the sample. The appeal of this method is that experiments can be performed at high pressure and temperature (simulating reservoir conditions), allowing for changes in pore structure to be observed as a function of pressure, and under certain conditions, open versus closed porosity may be distinguished. SANS experiments, combined with USANS, also enable a wide distribution of pore sizes to be investigated.

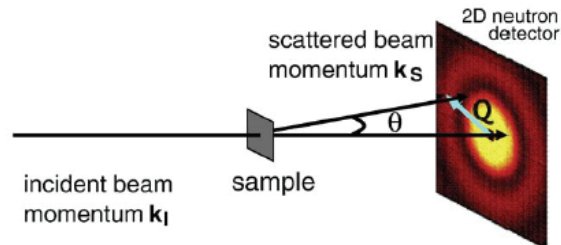


Fig. 6 — Diagram of a neutron scattering experiment. Source: Melnichenko et al. (2009)

The most common methods for estimating porosity and PSDs in shales and tight gas reservoirs remains helium pycnometry for grain density (combined with a measurement of bulk density) to estimate connected porosity, and mercury injection to obtain a PSD. As noted, use of helium may lead to errors in effective porosity estimation because helium kinetic diameter is smaller than most reservoir gases, so a greater percentage of total porosity will be investigated than is accessible with reservoir gases. If reservoir gases are used, corrections for adsorption must be made. Crushed versus whole core or core plugs could lead to different results for porosity, and because porosity is stress-sensitive (particularly for those samples that contain microfractures or slot porosity), it is best to measure porosity on core samples subject to confining stress. Mercury porosimetry suffers as a measure for pore size for several reasons. It is limited to pore sizes generally > 4 nm (and hence excludes the lower mesopore/micropores in coals and organic rich shale, which could dominate the matrix porosity), is likely to distort the pore structure of highly-compressible samples (organic rich shale and coal) because of the high-injection pressures required for measurement (up to 60,000 psi), and requires estimates of surface tension/contact angle for pore size calculations from the Washburn equation, which are not accurately known for UGRs (and may vary by sample type). A further consideration for porosity and PSD measurement is that UGRs are very heterogeneous, and hence a large number of samples, may be required to statistically characterize the reservoir – often sample sizes are greater than the scale of the measurement necessitating some averaging to occur.

Tight Gas Examples. Our tight gas study areas are used to illustrate the impact of sample heterogeneity and stress on porosity and lithology differences on PSDs. Further, flow mechanisms and storage mechanisms can be inferred, which influences basic reservoir engineering analysis.

In both areas, connected porosity was established using helium expansion. PSDs were obtained from mercury intrusion in Area A (43 coreplugs), while seldom applied techniques (for tight gas) of low-pressure N₂ adsorption and SANS (3 core samples) were tried for Area B. In Area B, routine porosity measurements were performed on full-diameter cores (37 samples), and routine porosities were also measured on 25 core plugs. Of the 25 core plugs, 10 plugs were selected for measuring porosities under hydrostatic stress (set to represent *in-situ* conditions) and of the 10 plugs, 3 were selected for measuring porosities under variable confining pressure. The 3 cores selected for variable confining pressure measurement were sub-sampled for N₂ adsorption analysis.

The impact of confining pressure for the three core plugs in Area B is significant (Fig. 7). The difference between porosities measured at “ambient” and net overburden conditions averaged about 11%, with some variability (8 – 19%) between samples (Fig. 7a), suggesting lithological differences plays a role (Fig. 7b).

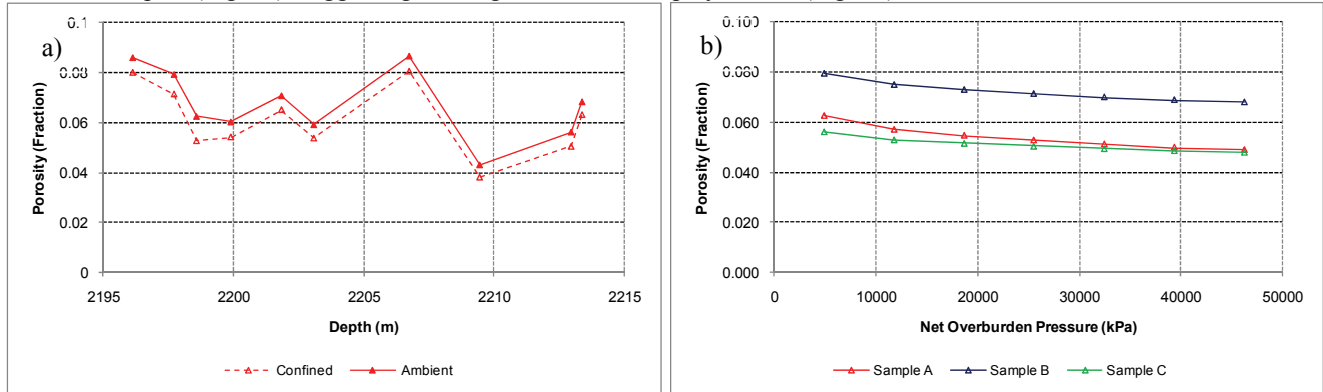


Fig. 7 — Impact of confining pressure (hydrostatic) on porosity for tight gas samples from Area B. (a) Comparison of porosities measured at ambient conditions and those at 14466 kPa (2098 psi) lab hydrostatic or 25468 kPa (3694 psi) reservoir confining pressure. “Ambient” conditions refer to measurements performed at 2758 kPa (400 psi) lab hydrostatic net confining pressure or equivalent reservoir net confining pressure of 4856 kPa (704 psi). (b) Influence of lithology and variable confining pressure on porosity.

Area B PSDs were obtained using nitrogen adsorption/desorption analysis (Fig. 8). This technique is seldom used for tight gas reservoirs (although more so for shale gas and coal), but proved useful for these samples. The adsorption/desorption hysteresis loops (Fig. 8b) can be interpreted in terms of a dominant pore shape (Gregg and Sing 1982), and the adsorption isotherms can be interpreted for PSDs (Fig. 8b) using BJH Theory (Clarkson and Bustin 1999a). Pores are interpreted to be slit-shaped, which is common in tight gas reservoirs (Shanley et al. 2004). The PSDs for two of the samples are bimodal, with the pore size fraction in the 50 – 100 nm range (500 – 1000 Angstroms). From the interpreted size range, non-Darcy (slip flow) can be important, particularly at low-pressures, which will influence the model choice used for simulation and production analysis. Free-gas storage is expected to dominate in this reservoir due to the absence of microporosity (< 2 nm diameter).

Although mercury injection data (MICP) were not collected in Area B for direct comparison with N₂ adsorption analysis, some data were collected on samples in Area A. Reservoir properties are variable in Areas A and B, therefore samples with similar routine permeabilities and porosities were selected to facilitate more direct comparison between PSD methods. An example PSD obtained from mercury injection in Area A (Fig. 9) exhibits a median pore size (~ 500 Angstroms) that is similar to the larger pore sizes obtained from Area B using N₂ adsorption (Fig. 8b). Thus N₂ adsorption is showing promise as a method to characterize UGR pore structure.

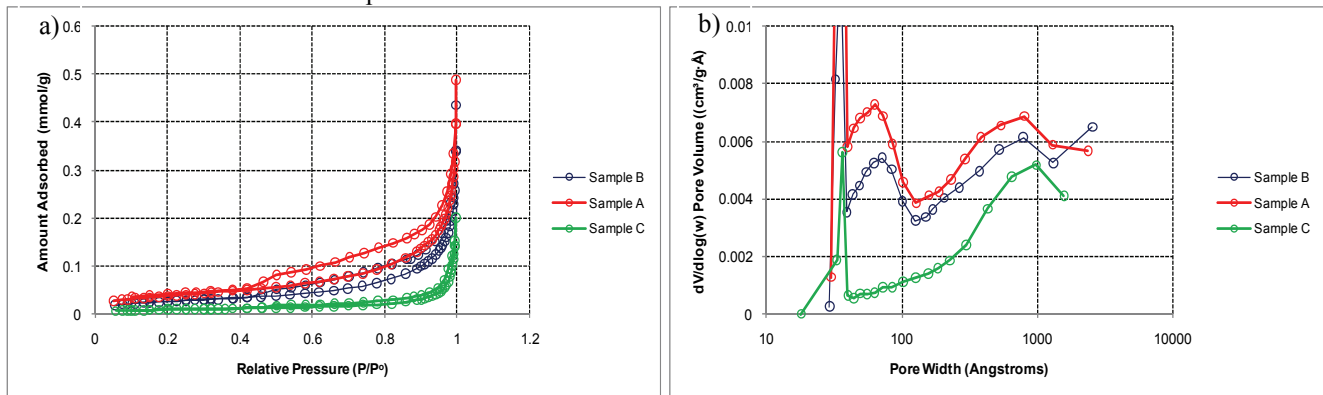


Fig. 8 — Nitrogen adsorption/desorption isotherms for 3 tight gas samples collected from core plugs from tight gas Area B (a), and interpreted pore size distributions (b) using BJH Theory. Note the bimodal pore size distributions for two of the samples, with larger pore sizes in the 50 – 100 nm (500 – 1000 Angstroms) range.

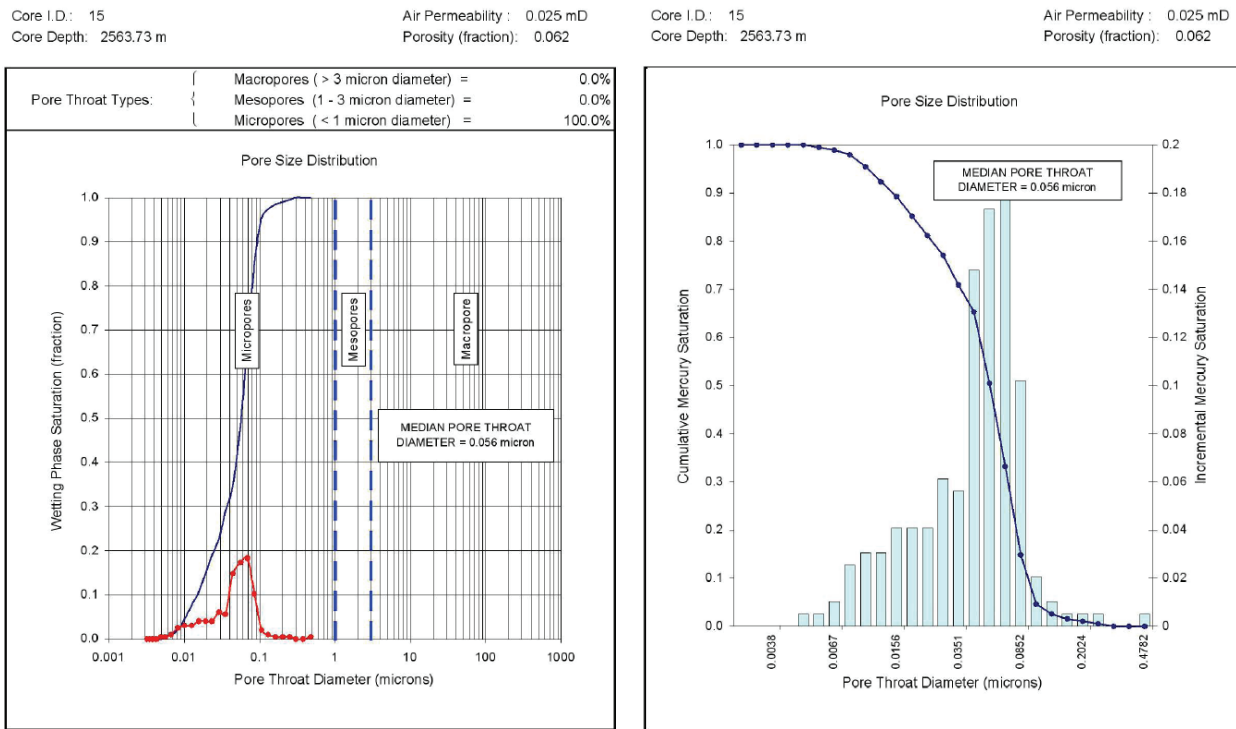


Fig. 9 — Example pore size distribution for tight gas sample in Area A using MICP. This sample has routine air permeability and porosity values comparable to the 3 samples in Area B. Note the pore size classification used in the plot on the left is not the same as IUPAC (Sing et al., 1985).

SANS and USANS data (Fig. 10) have also been recently been gathered on the same 3 tight gas samples from Area B shown in Fig. 8. The technique promises to provide an independent way to interpret PSDs in these samples and allowed a broad range of pore sizes to be probed by neutrons, from approximately 500 nm to 1.2 nm (Melnichenko, personal communication). At the time of writing, the SANS/USANS data for these samples are being interpreted in terms of surface area and pore size distributions; the results of this analysis will be reported on in the near future.

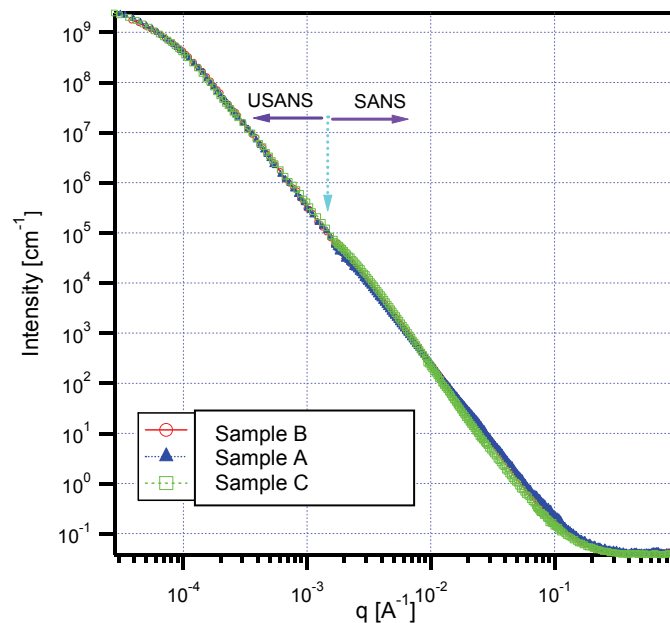


Fig. 10 — SANS/USANS data from 3 tight gas samples collected from core plugs cut in tight gas Area B. q is the scattering vector. Image courtesy of Liliin He and Yuri Melnichenko of Oak Ridge National Labs (2010).

Matrix Absolute Permeability. Both steady-state and non steady-state permeability measurements can be used, although the industry is currently favoring non steady-state measurement due to the relatively short measurement times. Pressure- and pulse-decay methods can be used – see Cui et al. (2009) for a summary of these methods and analysis techniques as applied to tight rock. Mercury intrusion has also been used for estimating permeability – a comprehensive review of permeability estimates using MICP for tight gas reservoirs was provided by Comisky et al. (2007).

As with porosity and saturation measurements, absolute permeability is affected by PVTxt. The nature of the pore structure has a direct control on the measurements, with pore throat dimension thought to be the major control on permeability in UGRs. Due to the ultra-fine nature of matrix porosity in most coals, shales and tight gas reservoirs, non-Darcy flow effects (slippage, transitional flow and diffusion) can be important under certain PVTx conditions (Civan, 2010 and Javadpour, 2009), and must be adjusted if the measurements are performed using gases. Further, the molecular sieving effect of nanopores in some shales and coal may require the use of reservoir gases versus helium - if reservoir gases are used, care must be taken to correct for adsorption effects (Cui et al. 2009).

As with porosity, a fundamental concern is the use of crushed versus core or core plug samples, although it appears that permeability is even more sensitive to sample size used – we discussed some of the concerns for both crushed and core samples in a previous section.

Permeability of UGRs is very stress sensitive, usually owing to the presence of microfractures. It is therefore important to ensure that measurements recreate the *in-situ* stress condition as accurately as possible.

A further consideration for absolute permeability is the issue of averaging. Permeability is a tensor, and the average permeability is dependent on direction. Scaling-up permeability requires assumptions about the reservoir architecture. For example, parallel bedding tends to lead to parallel flow, where the average permeability is controlled by high permeability streaks – in finely laminated tight gas reservoirs as in Areas A and B, these thin streaks may dominate flow. Although geometric average permeabilities are often used based on the assumption of a disordered heterogeneous system, this is often not consistent with the depositional architecture of many UGRs. For parallel bedding, an arithmetic average should be used, resulting in higher permeability due to the presence of thin high permeability streaks. If a sample contains parallel beds of contrasting permeability and porosity, the measured permeability at the average porosity is always greater than that based upon the composite of the individual beds (Byrnes, 2006). Further, issues of scale must always be considered.

Lastly, we note that there are a great many compositional controls on permeability in UGRs, due to the impact of component type and distribution on pore throat sizes and pore size distribution. For example, different clay types will impact permeability in tight gas reservoirs and shale, and lithology differences impact not only permeability but also stress-dependence. Kerogen content will also impact permeability in shales and coals. The organic matter composition which controls pore structure also affects permeability (Clarkson and Bustin 1997). Careful petrographic study is required to understand the controls on permeability in each reservoir type – we recommend the rock-typing procedure proposed by Rushing et al. (2008) as a way to systematically evaluate the controls on permeability which allows for log-calibration. Procedures for permeability and porosity evaluation will vary by reservoir type, however. In short, absolute permeability (measured with gas) is a function of gas pressure, temperature and composition (affects non-Darcy flow), confining pressure, and pore /pore throat size distribution. Javadpour (2009) discusses the impact of pore size, and gas pressure, temperature and molar mass on gas apparent permeability for shale gas reservoirs.

Tight Gas Examples. Our tight gas study areas are used to illustrate the impact of stress and compositional heterogeneity on absolute permeability measurements. The tight gas reservoir in Areas A and B generally consists of a finely interbedded very fine grained sandstone, siltstone and shale with a strong contrast in permeability from lamination to lamination. In Area B, several different permeability measurement types were performed, including routine permeabilities measured on a full-diameter core at 500 psia net confining pressure, pressure-decay probe (profile) permeability measurements on the slabbed core and pulse-decay permeability performed on 1” coreplugs taken at the locations of several of the probe permeability measurements. The routine permeability values have a lower resolution of 0.01 mD as a time-limit was placed on reaching steady-state, meaning that many of the datapoints were below the resolution of the instrumentation (**Fig. 11**).

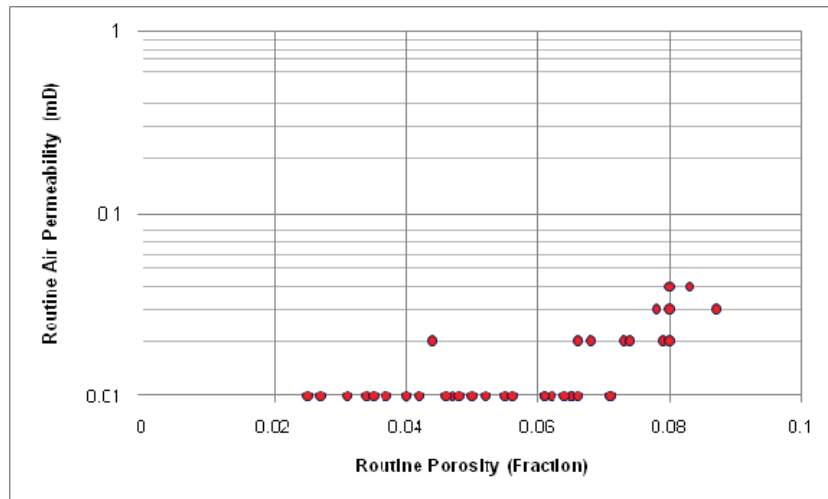


Fig. 11 — Crossplot of routine permeability and porosity for full diameter core in Area B.

Following routine measurements, profile permeability data were collected on the slabbed core using a PDPK-400® (CoreLab) probe permeameter at approximately 2.5 cm (1 inch) intervals. Details of the probe permeameter measurement procedures and theory are provided in Jones (1994). A total of 593 data points were collected, with measurements performed approximately parallel to bedding in an attempt to characterize fine-scale heterogeneities in the core (Fig. 12). The analyzed core is finely laminated and because profile data can be collected at a much finer scale than routine measurements, which are normally obtained from full-diameter core, some trends from probe data may not be observable with routine core data. In this data set (Fig. 12), permeabilities do not appear to show a strong change with depth, except perhaps in the uppermost 2 m of the dataset. Above 2209 m, cyclic (sinusoidal) changes in permeability appear to occur about every 2 m. Generally, the measurements show a modest range in values (slip-corrected permeabilities from ~0.001 to 0.03 mD), suggesting a fairly narrow range in dominant pore throat radius.

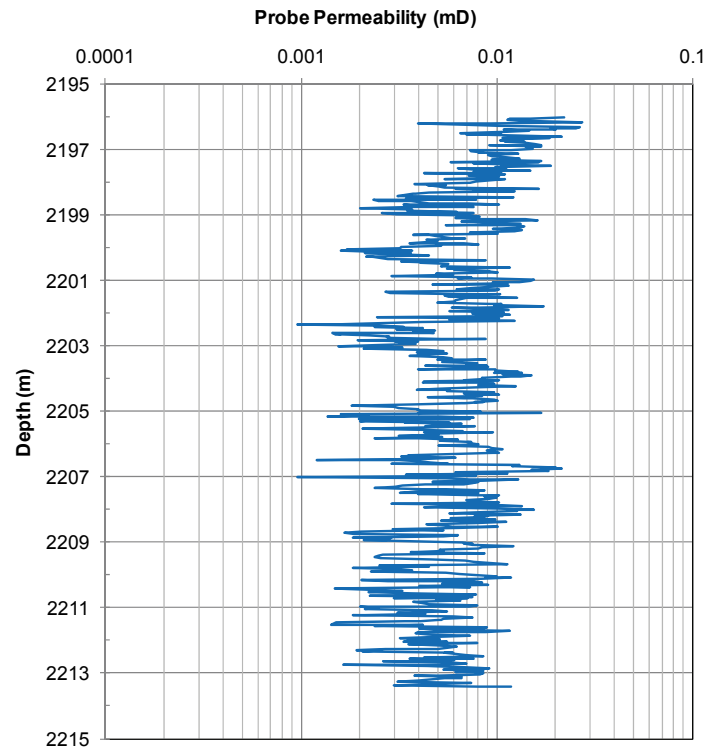


Fig. 12 — Plot of slip-corrected probe permeability with depth collected on slabbed core in tight gas Area B.

Although the profile permeabilities provide a quick way to characterize vertical (and potentially lateral) variation in permeability, the measurements are performed on unconfined core and hence are not representative of *in-situ* conditions. To investigate stress-dependence of permeability, the 10 core plugs cut for porosity measurement (discussed above) were also

used for pulse-decay permeability (Jones 1997) measurements under hydrostatic stress (set to represent *in-situ* conditions), and 3 were selected for measuring permeability under variable confining pressure.

Comparison of pulse-decay permeability measurements at ambient conditions and at *in-situ* conditions (Fig. 13a) reveals a very strong stress-dependence, with differences as great as 71%, however there is a much larger difference between probe permeameter measurements at atmospheric pressure compared to the pulse-decay measurements under stress. Much of the permeability loss is within the first few MPa of confining pressure, possibly due to the presence of open microfractures caused by stress relief (Fig. 13b). There is also some variation in stress-dependence by sample and hence lithology. The relationship between probe permeability measurements and pulse-decay measurements measured at confining pressure (Fig. 14) can be used to “adjust” the probe measurements to *in-situ* stress conditions – this is useful for core-log calibration, as discussed below.

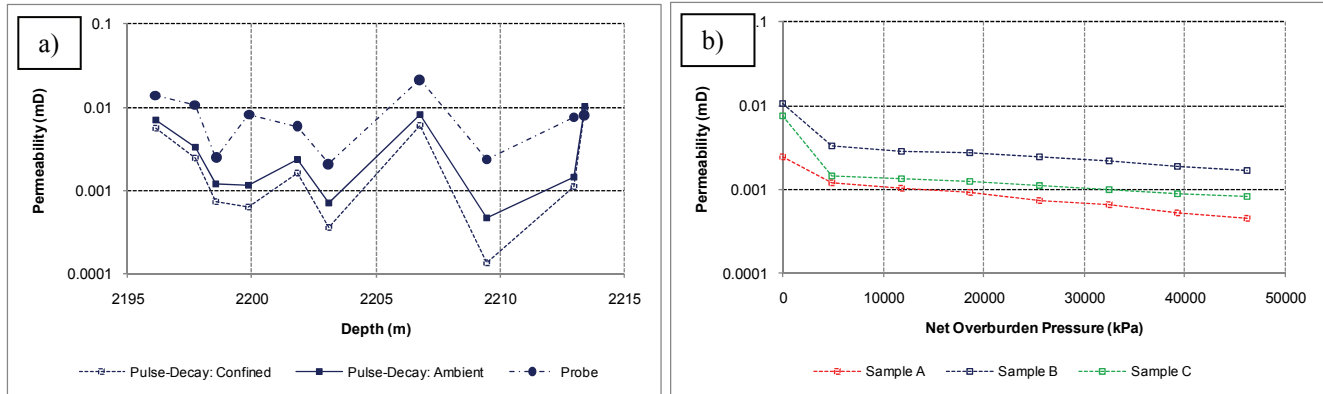


Fig. 13 — Impact of confining pressure (hydrostatic) on permeability for tight gas samples from tight gas Area B: (a) Comparison of pulse-decay permeabilities measured at ambient conditions and those at 14466 kPa (2098 psi) lab hydrostatic or 25468 kPa (3694 psi) reservoir confining pressure. “Ambient” conditions refer to measurements performed at 2758 kPa (400 psi) lab hydrostatic net confining pressure or equivalent reservoir net confining pressure of 4856 kPa (704 psi). Probe (profile) permeability values measured at the location of the plug ends are also shown. (b) Influence of lithology and variable confining pressure on permeability.

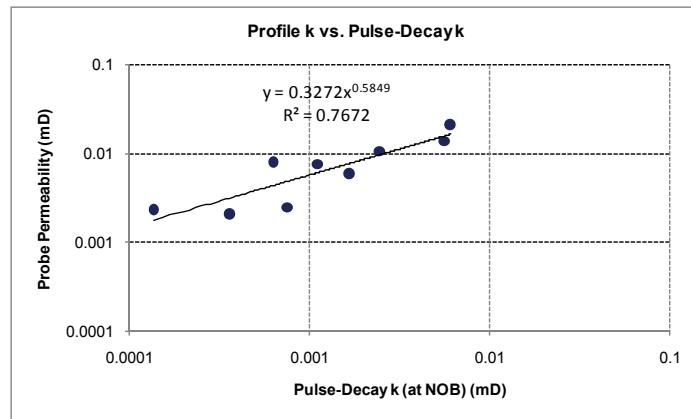


Fig. 14. Probe permeability vs. pulse-decay permeability measured at net overburden pressure, collected for core in tight gas Area B. The two values are weakly correlated, but differ substantially in absolute value due to differences in measurement conditions and volume of rock sampled.

Capillary Pressure and Relative Permeability. In tight gas and shale gas reservoirs, capillary pressure curves are used to quantify saturation distributions which are important for free-gas storage calculations. Further, it is well known that effective permeability to gas is strongly affected by water saturation, and that relative permeability curves are useful to establish the dependence of effective permeability on water saturation.

Newsham et al. (2004) observed that the combination of low connate S_{ws} and high capillary pressures in tight gas sands have prevented the application of conventional methods for estimation of capillary pressure curves – those authors recommended the use of hybrid methods (combined high-pressure porous plate and centrifuge methods with the vapor desorption techniques) to cover a wide range in S_{ws} . Both high pressure centrifuge and porous plate methods have an upper capillary pressure limit of 1000 psia, and must be combined with vapor desorption. Analysis times for both porous plate and vapor pressure methods tend to be long, and there are problems with obtaining a reasonable S_w estimate with the centrifuge method. However, these techniques offer an advantage over high-pressure mercury injection (MICP) because MICP uses a non-wetting, non-reservoir fluid (mercury), creating errors when converting to a more realistic air-brine system. Newsham et al. (2004) recommend using methods that use reservoir-like fluids. Some of the findings of Newsham et al. (2004) may also carry over to the inorganic framework of shale gas reservoirs, but the presence of organic matter will affect wettability, and

cause vapor adsorption when air-brine systems are used – some authors (Andrade et al. 2010) suggest that brine saturation is limited to the inorganic framework, but we suspect this is organic-matter type-dependent as coal (usually Type-III organic matter) is known to sorb water. To our knowledge, a detailed study of capillary pressure in shale gas reservoirs is yet to be published. In shale gas reservoirs, Andrade et al. 2010 suggest that instantaneous capillary equilibrium is not realistic, and that non-equilibrium formulations should be considered for simulation.

Relative permeability is similarly difficult to measure in UGRs. Steady-state and non steady-state techniques have been applied, with associated limitations. Usually, large differential pressures are required to initiate 2-phase flow in tight gas reservoirs, creating large saturation and pressure gradients. As with absolute permeability, non-Darcy flow effects must be accounted for, and the correction is known to vary with saturation and temperature (Rushing et al. 2003). Failure to correct for slippage may cause effective permeability to gas to be overestimated.

Some studies focus on gathering effective permeability to gas using the single-phase stationary method (water is held in sample by capillary pressures while gas flows). Effective permeability to gas can then be measured at different S_{ws} – a set of incremental phase trap experiments is discussed for our tight gas study Area A below.

Tight Gas Examples. Although tight gas sands often lack mobile water, water may be introduced to the system through hydraulic fracturing operations. The combination of a water-wet system and high capillary pressures causes water to be imbibed changing the effective permeability to gas, particularly near the fracture face. The impact of imbibed water on effective permeability to gas was investigated for 4 core samples in Area A (**Fig. 15**) using incremental phase trap experiments. The initially dried core samples were first weighed, then subject to a test temperature of 20°C and a net overburden pressure representative of the reservoir. The initial permeability to gas was measured at these (dry) conditions and used as the baseline permeability. Brine was injected to yield a $S_w = 10\%$, then humidified gas was flowed in both directions through the core to achieve an even saturation distribution. Saturations were estimated gravimetrically at each step. Gas permeability using the humidified gas was measured (at overburden pressure) to establish the impact of the trapped water.

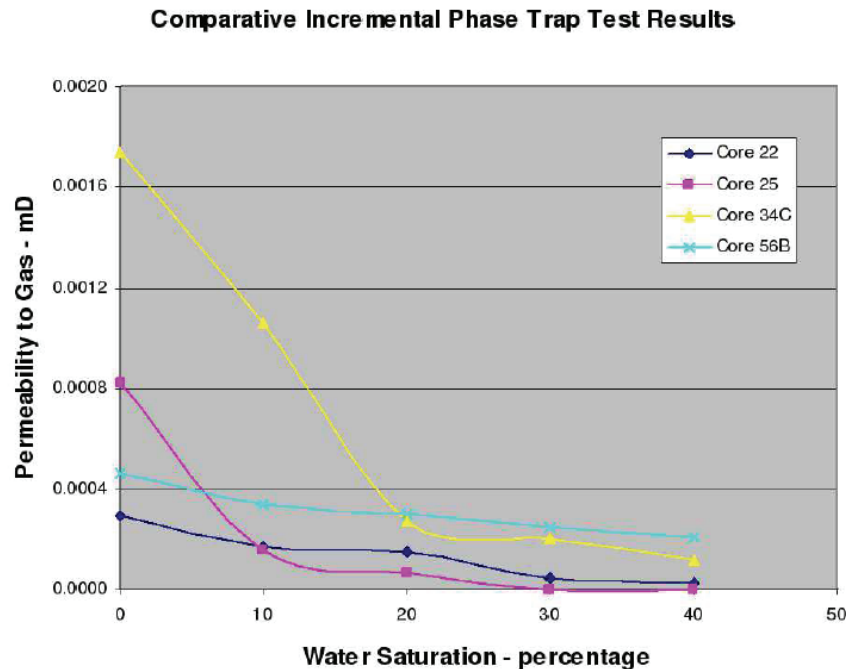


Fig. 15 — Effective gas permeability as a function of S_w for 4 Area A tight gas core samples. These gas permeabilities were measured at the maximum drawdown pressure of 20670 kPa.

The results suggest that gas permeability is more strongly affected by S_w for the highest permeability samples compared to the low permeability samples (Fig. 15). For all samples, permeabilities are less than 0.0004 md for S_w s exceeding 20%, thus imbibition of water during fracturing operations could have a serious affect on gas permeability.

Electrical Properties. Electrical properties provide a link between pore-scale petrophysical properties and log-derived properties. Conductance is affected primarily by movement of ions in the pore fluids which in turn is affected by pore structure, pore geometry, rock composition and temperature and hydrocarbon fluids. Two critical parameters, cementation factor (m) and saturation exponent (n) can be derived from core-based measurements and are required for saturation calculations using Archie's equation although Archie's equation may not be applicable for UGRs. Ions in clay-bound water may act as separate conductors, which must be included in S_w calculations; the conductance of the cores is measured using

fluids of varying salinity and plotted versus the salinity of the saturation fluid. “Pseudo” m and n may be derived from this plot and input into Archie’s equation.

m is not just a function of cementation, but is a function of pore geometry too. Aguilera (2008) derived m for tight gas sand reservoirs that contain naturally-fractured and/or slot porosity using a dual porosity model. He noted that the decrease in m with porosity may be indicative of a slot pore network (Fig. 16). Recently, Aguilera (2010) noted that the petrophysical model for shale gas reservoirs should include up to four porosity systems: fracture, inorganic matrix, organic matter, and porosity associated with the induced hydraulic fracture network. Clearly, theoretical m calculations for such systems could be complex.

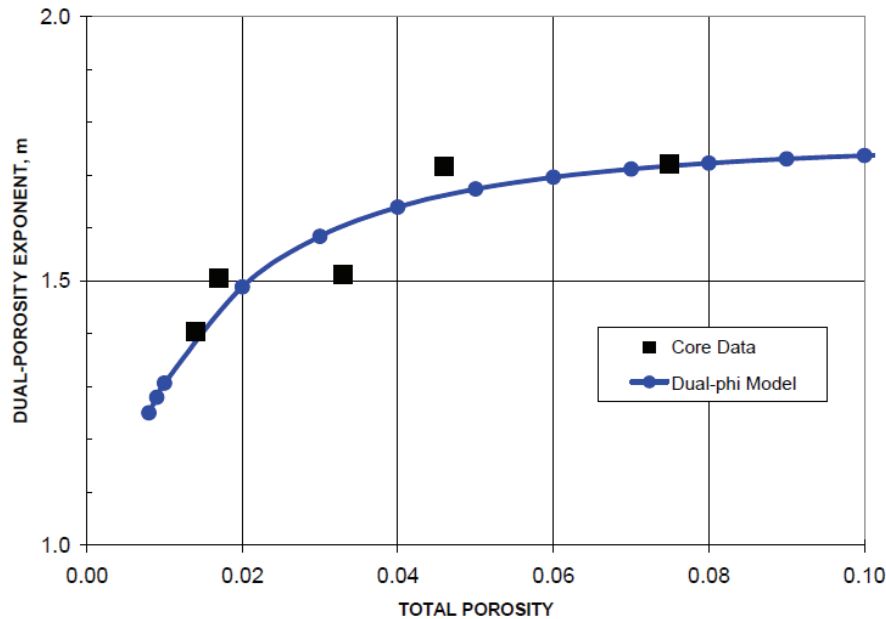


Fig. 16 — Plot of Archie cementation factor versus porosity showing decrease in cementation factor with porosity due to presence of natural fractures or slot porosity. Modified from Aguilera (2008).

Tight Gas Examples. Electrical properties were measured on samples Area A covering a range of rock properties. Samples were flushed with 5 pore volumes of brine to ensure $S_w = 100\%$, and resistivity readings were made until they were stable. Formation resistivity factor was measured at several overburden pressures (Fig. 17a). m ranged from 1.29 to 2.35, suggesting that some samples may have microfractures since m approached 1 at low porosities.

After completing the formation resistivity factor measurements, the samples were put into a porous plate desaturation cell, and placed in capillary contact with the synthetic brine. Humidified nitrogen was used to desaturate the samples at incrementally increasing capillary pressures. When capillary equilibrium was reached, the samples were placed in a core holder subject to net overburden pressure and the resistivity measured (Fig. 17b). Resistivity index was calculated by dividing the desaturated resistivity by the 100% saturated resistivity. n varied from 1.6 to 2.21, with a composite value of 1.87.

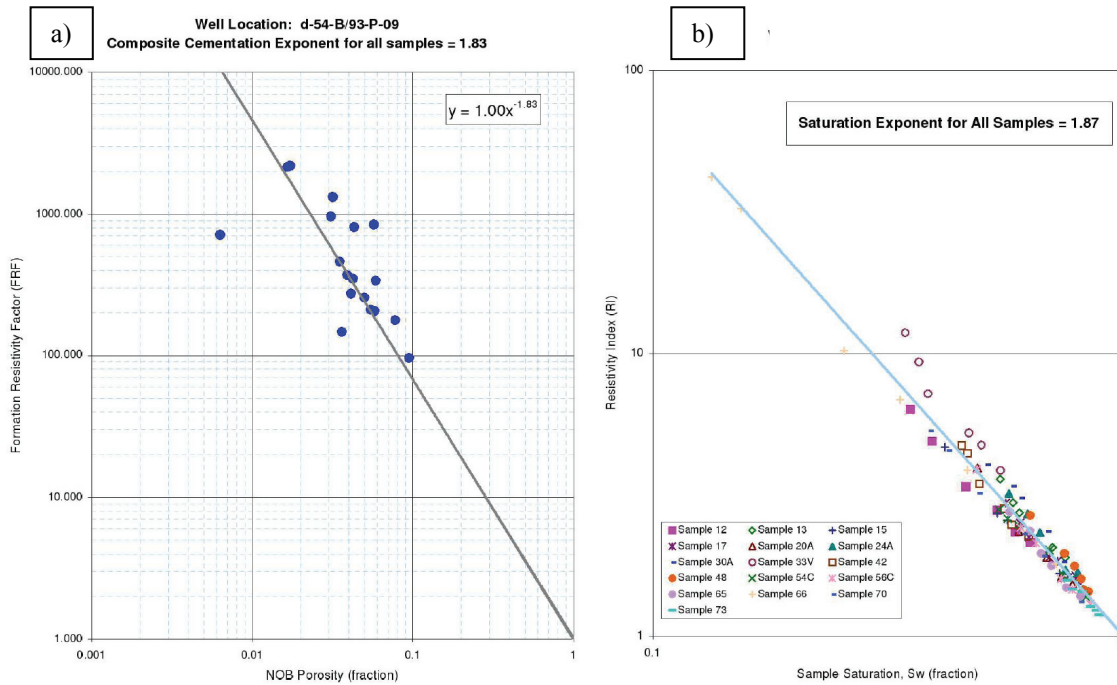


Fig. 17 — (a) Formation Resistivity Factor versus porosity and (b) Resistivity Factor versus Sw for 18 core samples in tight gas Area A.

To test the general applicability of the m and n parameters derived from Area A core, we used Archie’s equation to estimate Sws in Area B (**Fig. 18**). Although the macroscopic lithology for both areas appears similar, there are likely differences in mineralogy and pore structure however. Using $m = 1.83$ and $n = 1.87$ obtained from Area A does not yield a good match (red curve) to the Area B core data – however the match (green curve) using best-fit values $m = 1.38$ and $n = 1.81$ is reasonable and within the ranges obtained from Area A data. We note that the core-derived Sw values may be low because the samples were not preserved. This exercise shows the sensitivity of log-calculated Sw values to m , n values, and the danger of applying composite values from one UGR area to another.

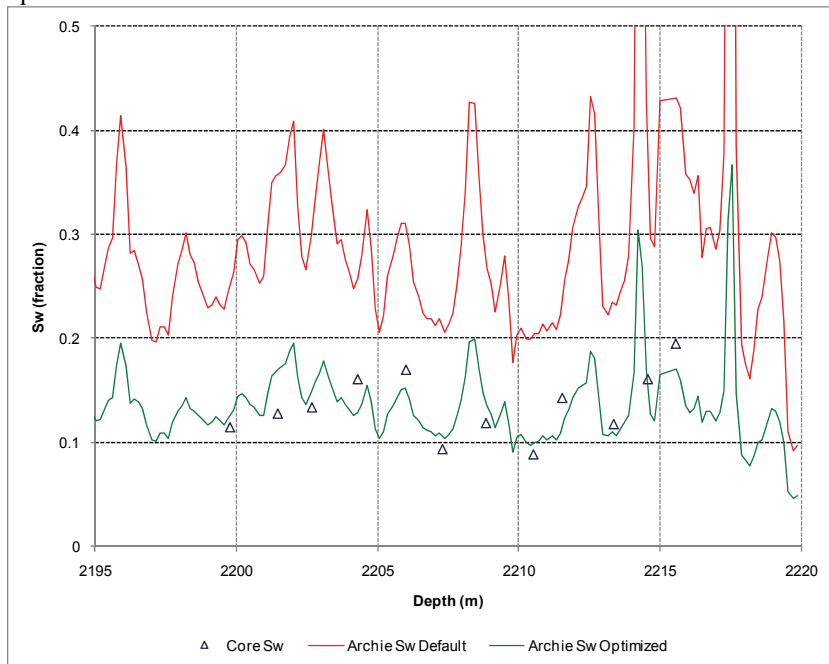


Fig. 18 — Comparison of log-derived Sw using Archie’s equation using composite m , n parameters derived from Area A core (red curve) and best-fit m , n parameters. Core data (blue triangles) are from Area B.

Gas Content and Adsorption Isotherms. Coalbed methane and organic-rich shale plays have a significant amount of gas stored in the sorbed state, requiring special measurements in the field/lab to quantify. A recent summary of CBM gas content and sorption isotherm measurements, along with a discussion of uncertainties, was provided by Clarkson and Bustin (2010). It is important to note that, like many of the measurements discussed above, there are no standards for measurements, although excellent guidance has been provided for CBM reservoirs by GRI publications in the 1990's. For example, inter-laboratory comparisons of sorption-isotherms show significant variance, despite the fact that the laboratories tend to follow the same general procedure. For sorption isotherm measurements, there are potential errors associated with sample preparation and conditioning (samples must be re-equilibrated with moisture, representing *in-situ* conditions), void volume measurement (which is necessary to correct calculations for volume occupied by sorbed gas), gas composition etc. For gas content measurements, the largest source of error is estimation of lost gas prior to sealing the sample uphole in a desorption canister. For CBM reservoirs, if the gas content measured from desorption canister testing equals the sorbed gas content as estimated by sorption isotherm measurements, the coals are said to be saturated; if gas content is less, then the coals are said to be undersaturated. For CBM reservoirs, sorbed gas storage is assumed to dominate, with generally little free-gas storage (although for some dry CBM plays, free gas storage may be significant), whereas with shale plays, this may not be the case. For the latter, free-gas storage in porosity must be estimated along with sorbed gas storage – Ambrose et al. (2010) provide good recent discussion on shale gas gas-in-place determination.

There are many controls on sorbed gas storage in CBM and organic-rich shales including: 1) pore pressure; 2) temperature (sorption decreases with increase in temperature); 3) moisture content (adsorption decreases with moisture content up to a moisture limit); 4) organic matter content (microporous structure in organic matter tends to drive the amount of sorption that occurs); 5) organic matter composition (different organic matter constituents referred to as macerals have different pore structures); 6) organic matter thermal maturity (OM pore structure changes with thermal maturity); 7) and gas composition (different gases have different sorption characteristics). Further, Hartman (2008) noted that some clays are thought to contribute to sorbed gas storage in shales and that for oil or wet-gas prone shales, entrained bitumen may affect sorption of gas. There has been much focus on quantifying total organic carbon (TOC) in the lab for shales, correlating lab-based sorption measurements to TOC, then using logs to predict TOC using a variety of methods (see below), but we suggest that there may be considerable error in this process if TOC is not the only driver for sorbed gas content. Nonetheless, TOC measurements are routinely performed for shales along with an estimate of thermal maturity, usually done using vitrinite reflectance (Ro) measurements.

Tight Gas Examples. In study Areas A and B, TOC is generally quite low (generally less than 1-2%) and sorbed gas storage was expected to be quite low. To test this, 5 fresh core samples were selected for gas desorption canister testing. The cumulative desorption at STP ranged from 1.7 to 231 cm³ after 10000 minutes of desorption time, confirming the very low sorbed gas storage that could be inferred from low TOC levels. No sorption isotherms were measured. In subsequent analysis, sorbed gas storage was therefore ignored.

Rock Mechanical Properties. A comprehensive discussion of mechanical properties of shales and anisotropy was provided by Sondergeld et al. (2010a). Several points raised by those authors are that shales are elastically anisotropic (requiring the measurement of up to 7 elastic constants if the samples are fractured normal to bedding); sample size must be appropriately selected; obtaining analysis on vertical, horizontal and 45° coreplugs can be challenging for shale and there may be sample inhomogeneity due to spatial spread of the samples; samples tend to be biased toward more mechanically competent materials; fresh core should be used (versus legacy core); and that commercial labs may not divulge all the details of the testing (# strain gauges used, orientation etc.); there are mineralogic controls on mechanical properties of shales; and confining pressure impacts Poisson's ratio. Bustin et al. (2008b) noted that Poisson's ratio and Young's modulus are a function of mineralogy and fabric which, in turn, are functions of sedimentology, provenance, diagenesis, and tectonics (**Fig. 19**). Barree et al. (2009) further note that saturation, stress history and anelastic strain (amongst other) factors affect static and dynamic measurements of elastic moduli for UGRs – they also urge caution when attempting to scale-up core-derived properties.

Clearly a goal of rock mechanical property measurements is to ascertain which portions of the reservoir are amenable to hydraulic fracturing (more brittle) – Britt and Schoeffler (2009) further emphasize the importance of mineralogy on shale rock mechanical properties and suggest that if shales contain > 35-40 % clay, they are not likely to be prospective. Those authors also recommend triaxial compression tests (for static Young's Modulus and Poisson's Ratio) and ultrasonic velocity tests for dynamic measures of those properties, which in turn can be used to distinguish brittle versus ductile shale (Rickman et al. 2008).

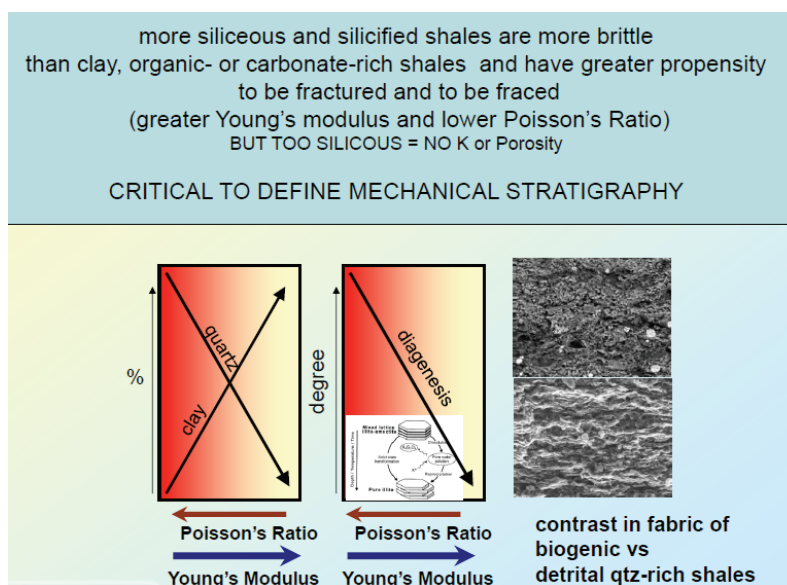
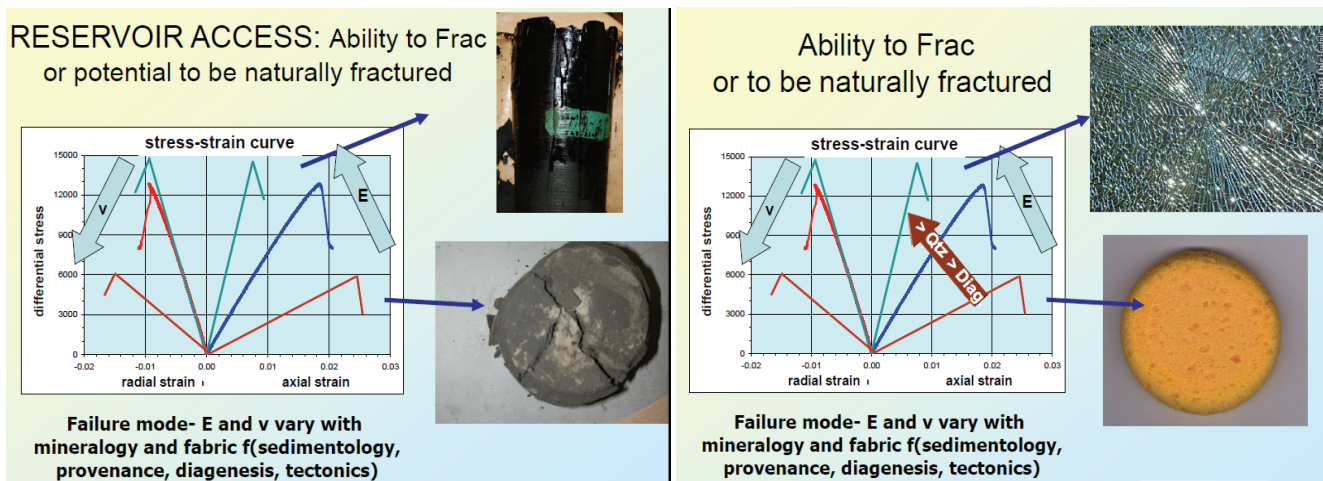


Fig. 19 — Illustration of the impact of mineralogy and fabric on rock mechanical properties of shale. From Bustin et al. (2008b).

Tight Gas Examples. No rock mechanical property testing was available for either of our tight gas study areas, but rock mechanical properties inferred from openhole logs suggest a high Young's Modulus ($> 4.5 \times 10^7$ kPa, or 6.5×10^6 psi) and low Poisson's ratio (~ 0.2), suggesting that the rock should be easily fractured (all other factors considered). Frac modeling utilizing these values is discussed in a later section.

Well Log Analysis

UGR log analysis has progressed dramatically over the past two decades. Excellent recent reviews for shale gas reservoirs for example have been provided (ex. Sondergeld et al. 2010a, Jacobi et al. 2008, Bartenhagen 2009), demonstrating that logs, if properly calibrated against core data (with its inherent uncertainties) can be a useful technique for estimating: properties to estimate free-gas storage (porosity and S_w for example); total organic carbon content (for estimating sorbed gas content); rock mechanical properties; and natural fracture properties. We refer to the cited reviews for in-depth coverage of these advances, including the complications and corrections required. One particular complication, which is generally consistent for all unconventional reservoir types, is the issue of resolution of logs relative to the heterogeneity often exhibited at the core scale. Core measurements are often performed on sample sizes significantly below log scale, so there needs to be some attempt to scale up the core measurements in a meaningful way to allow for calibration of log to core data. We discuss core-log calibration and cyclicity evaluation using one of our tight gas study areas.

Tight Gas Examples. For our tight gas example, we concentrate on the issue of scale-up for core-log calibration in the finely-laminated reservoir of Area B and assume that most of the gas is stored in the free-gas state. Limited TOC data in the area suggest that TOC is generally < 2 -3%, but no TOC was available for our core in Area B. To estimate TOC, we used Passey's (1990) method (Fig. 20), which confirms that above 2213 m, TOC values are $< 2\%$. We note that there are several methods available to estimate TOC content using logs (Sondergeld et al. 2010a).

As described above, profile permeability data were collected and adjusted to *in-situ* values using pulse-decay permeability measurements performed on core plugs which were subject to confining pressure. One approach for calibrating logs for the purposes of permeability prediction is to apply a running average to the profile data to yield a resolution similar to the logs and compare the trends of the log readings to the averaged profile data (Fig. 21). The density porosity values track the averaged profile permeameter data reasonably well. We used the corrected probe permeameter data (averaged) along with density porosity (with matrix density adjusted to match routine core porosity measurements) to assist with flow-unit identification (Fig. 22). r_{p35} values (predicted pore size at 35% mercury saturation) were estimated using Eq. 2 of Aguilera (2010) – the pore sizes estimates (assuming slit shaped pore geometry) appear consistent with the values obtained from nitrogen adsorption discussed above (~ 500 Angstroms).

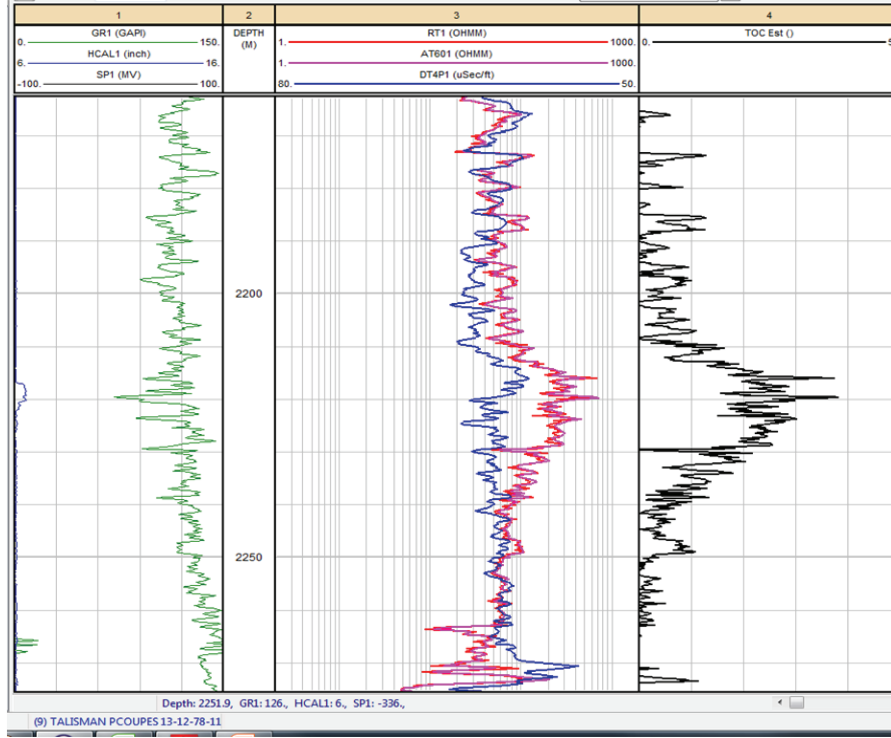


Fig. 20 — Estimation of TOC (4th track) at an Area B tight gas well location using Passey’s method (1990). Zone of interest is above 2213 m. Image courtesy of Howell, Javaid and Ogundele (2011).

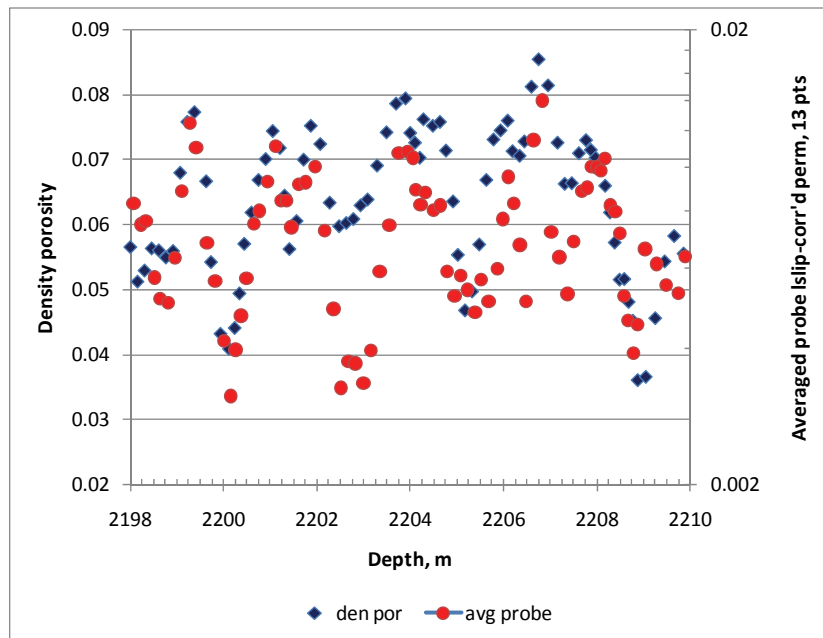


Fig. 21 — Comparison of smoothed probe permeabilities (13-point running average) and density porosity values in tight gas Area B.

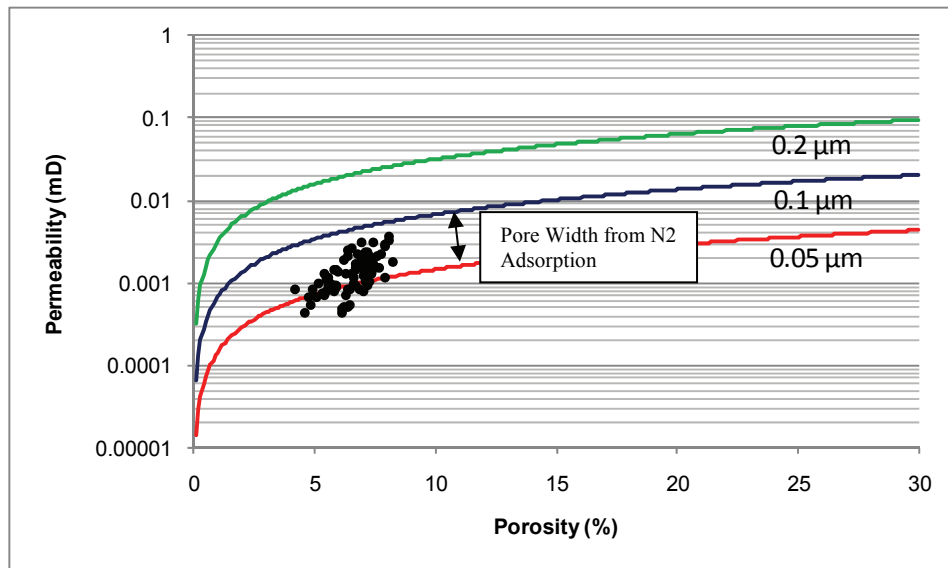


Fig. 22 — Winland-style plot of corrected (for *in-situ* stress) probe permeability data versus density porosity along with the lines based on several values of r_{p35} for Area B. The range of pore widths from N_2 adsorption analysis is also given.

A useful approach for establishing the appropriate scale for reservoir layering, is to interrogate trends in the core and log data and look for consistency between the two. In Fig. 12, there appear to be ~ 2 m cycles in the probe permeability measurements above 2209 m. To investigate cyclicality further, semivariograms (SVs) can be used (Jensen et al. 1996). For example, wireline bulk density (RHOB) and gamma ray (GR) SVs (Fig. 23) show different characteristics for the 2198—2218 m interval. The steadily increasing semivariance of the density SV reflects the trend of decreasing porosity with depth (Fig. 24). The GR SV, however, shows holes (decreases in the SV) at lags of approximately 2.6, 5.2, and 7.8 m, suggesting a strongly cyclic element to the GR response with wavelength of 2.6m. It is common in turbidite deposits to find meter-scale cyclicities and may be due to lobe shifts or variation in sediment input (e.g., Berg, 1986).

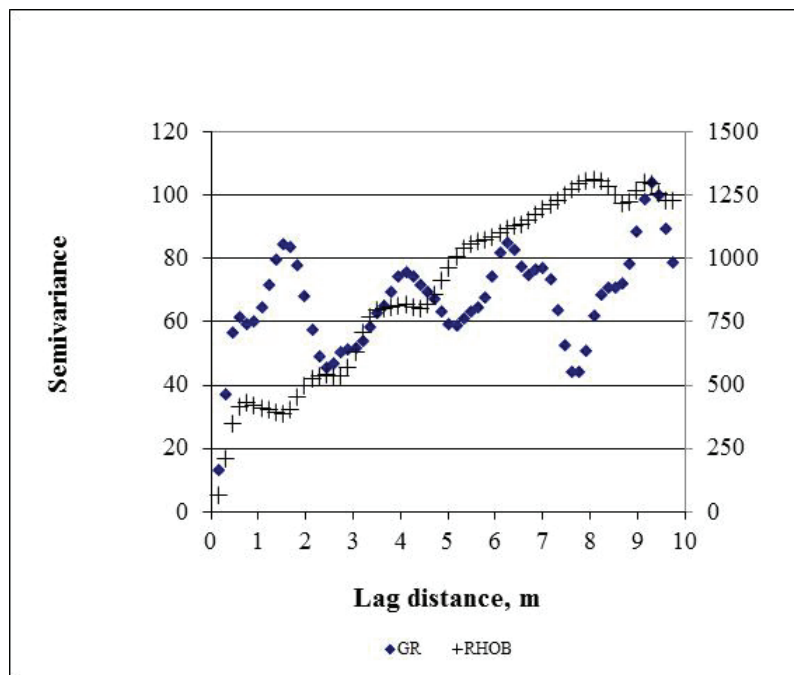


Fig. 23 — Semivariograms of wireline GR (left axis) and density (right axis) from interval 2198-2218 m in tight gas Area B.

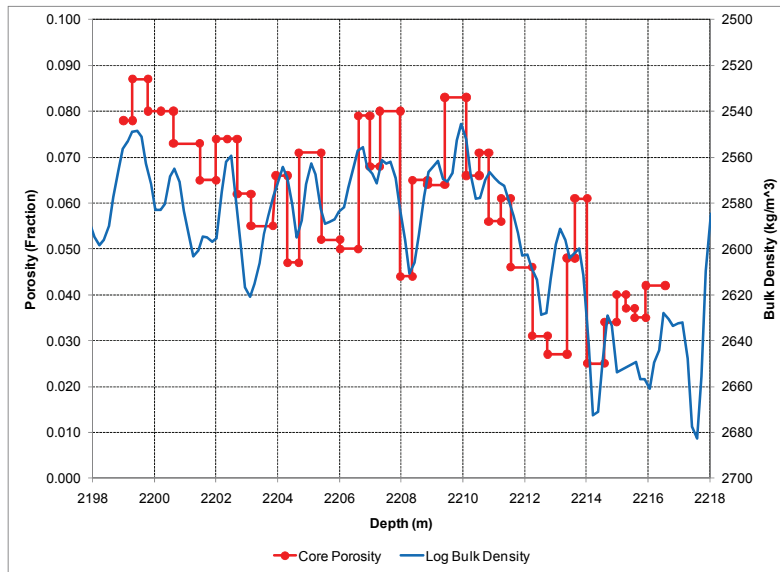


Fig. 24 — Wireline bulk density and full diameter core (routine) porosity versus depth in tight gas Area B.

Depending on what factors are controlling the formation permeability, we could see either a simple trend or cyclicity or both in the permeability variations in this interval. Analysis of the probe permeameter measurements does indeed reveal a cyclic element (Fig. 12). Fourier transform (FT) amplitudes of the probe data, averaged over a span of 7 cm, reveal a large peak at approximately 2.6 m wavelength, similar to that observed in the GR FT but not the RHOB FT (Fig. 25). All FTs also show a smaller peak at approximately 1 to 1.5 m wavelength. Cyclicities at these wavelengths are often difficult to identify in core or logs, and might be mistaken for random variations in the SVs. The probe FT also shows there is very little cyclicity at wavelengths between 0.2 and 1 m. Cyclicities at wavelengths smaller than 15 cm, which might be present from lamination-scale variations, are filtered out by the running average applied to the probe data. The small amplitude of the probe FT amplitude below 1 m suggests that the probe data can be averaged over 50 cm or larger lengths without loss of detail when scaling up the permeability for flow simulation models or correlations with other measurements. That is, except for variations at the lamination (cm) scale, averaging the probe data over 50 cm intervals will not result in a loss of information when scaling up.

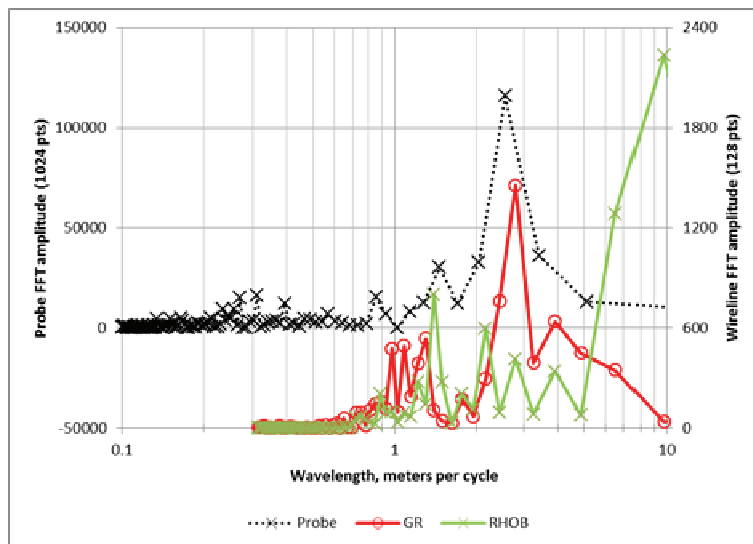


Fig. 25 — Fourier transform amplitudes of probe permeameter (left axis) and wireline GR and density (right axis) from interval 2198-2218 m in tight gas Area B.

Pre- and Post-Frac Well Test Analysis

Well-test analysis can be performed before and after hydraulic-fracture stimulation. Pre-frac tests are generally designed to obtain reservoir information, such as initial pressure and permeability, to aid in stimulation design. Post-frac analysis is generally designed to estimate hydraulic-fracture properties (frac half-length and conductivity) and, if a radial flow period is reached, an independent estimate of permeability. Post-frac analysis for tight gas and shale gas reservoirs often does not

yield an estimate of permeability because of the excessive times required to reach a radial flow period (due to very low permeability). An example case is shown for a tight gas well that was shut-in for 240 days (Fig. 26). The intended shut-in time for this well was 2 weeks, but the gauges were stuck in the hole and could not be retrieved until 240 days had elapsed. Even at the end of this extended buildup period, radial flow was not reached so that a unique estimate of permeability could not be determined from the test. Often operators are not willing to shut-in wells for extensive periods of time, so recently there has been an emphasis on the use of tests where the testing period is much shorter (ex. pre-frac tests). However, as we will illustrate with our tight gas example, if estimates of initial pressure and permeability can be derived from independent sources, then post-frac tests can be quite useful for obtaining quantitative estimates of hydraulic fracture properties, provided efforts are taken to reduce wellbore storage. Pre-frac testing (openhole and cased hole) can have a relatively short test time, and therefore a stronger chance of yielding permeability information, but generally suffer from a small radius of investigation compared to longer post-frac tests or rate-transient analysis (discussed later).

Of course there are many reservoir-related issues associated with UGR that complicate interpretations of well-tests, which will be discussed in more detail during the rate-transient section below. Specialized procedures for dealing with multi-phase flow and desorption, multi-layer behavior and dual porosity behavior are discussed elsewhere in the context of coalbed methane reservoirs (Clarkson and Bustin, 2010; Mavor and Saulsberry, 1996). The focus of this short discussion will be on pre- and post-frac testing of tight and shale gas reservoirs.

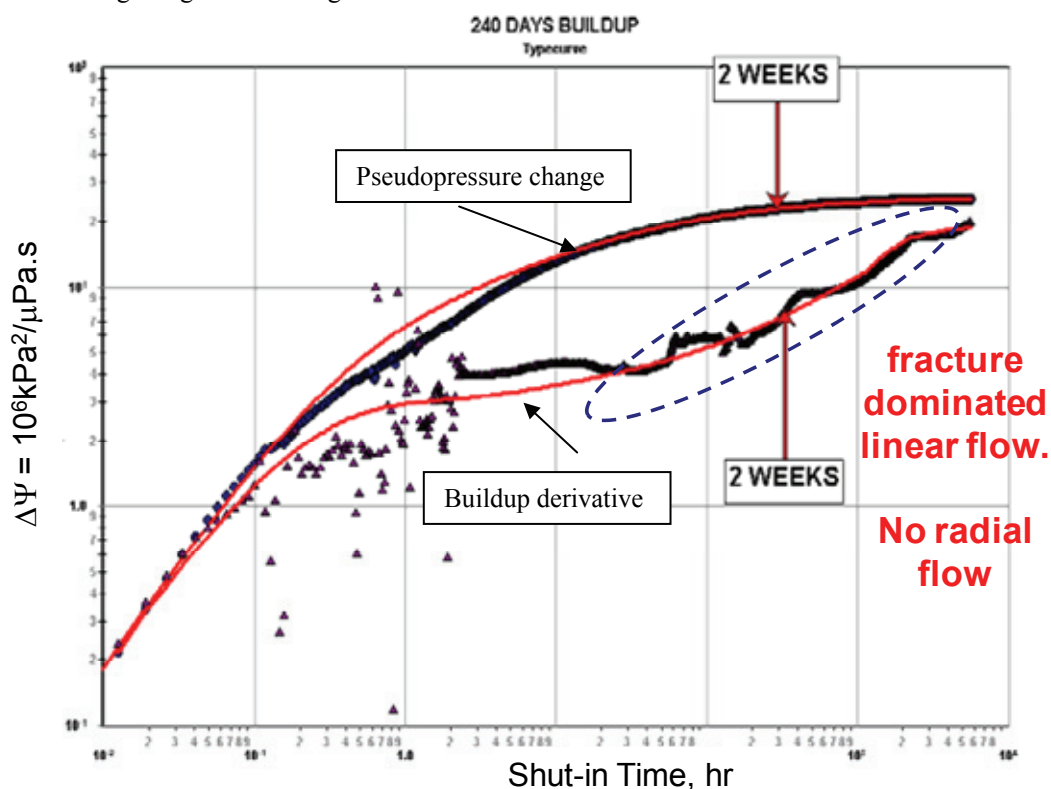


Fig. 26 — Pressure-buildup analysis of a tight gas well. The pressure gauge was stuck and could not be removed at the original planned time of 2 weeks. The result is a 240 day buildup that still shows no signs of radial flow. Image courtesy of Dr. Maghsood Abbadaszadeh.

Pre-frac Testing. Pre-frac tests can be performed openhole and cased hole. Openhole tests include drillstem testing (DST), and wireline formation tests such as the formation rate analyzer (FRA), modular dynamic test (MDT) and repeat formation test (RFT). The openhole tests are primarily useful for obtaining pressure information, but may suffer from the “supercharge” effect, causing errors in initial pressure estimates (Jahanbani and Aguilera 2009).

Cased-hole tests include slug and impulse tests, perforation inflow diagnostic (PID) tests, perforation inflow test analysis (PITA), closed chamber tests, flow-rate tester (FRT), mini-frac tests, and diagnostic fracture injection tests (DFIT). Mini-frac and DFIT tests have become popular in tight/shale gas (Thompson et al. 2009) and even coalbed methane operations (Ramurthy et al. 2002). For example, some operators have chosen to perforate the toe of eventual multi-fractured horizontal wells and perform DFIT tests to obtain closure pressure information (for frac design) and initial pressure, and potentially permeability information. The principles behind a minifrac test are illustrated in Fig. 27. Details of the DFIT analysis procedure are provided in Barree et al. (2007). The DFIT is essentially the analysis of a small frac job without proppant. G-function analysis combined with other techniques can be used to pinpoint closure pressure and closure mechanism, the latter being useful reservoir characterization purposes. The after fracture closure (ACA) data can be analyzed in a similar way to a conventional well test where the pressure transient propagating away from the fracture is analyzed. Special time functions

are used to assist with identification of flow regimes – as with conventional well tests, linear and pseudo-radial flow regimes may be analyzed, but only pseudo-radial flow will yield a permeability estimate. Limitations of these techniques from a reservoir point of view is that for very low permeability formations, closure may not occur for a long period of time (if at all), and even if it does, pseudoradial flow (and hence the chance to obtain a permeability estimate) may not be reached. Further, there may not be a direct comparison to conventional well-test techniques because of the difference in volume sampled. Nevertheless, if properly executed and sufficient time has been allowed, then an initial pressure and permeability estimate can be obtained.

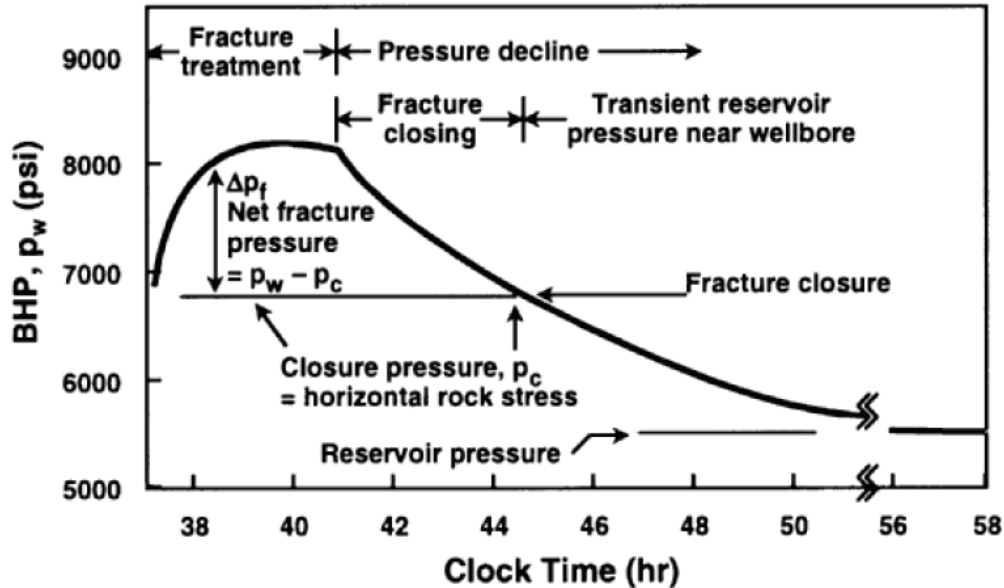


Fig. 27 — Illustration of typical mini-frac test. Reservoir information such as permeability can be obtained from the after-closure data.

Tight Gas Examples. Although we may seem to have been critical of the use of conventional post-fracture well-test analysis (such as flow and buildups) in tight gas and shale gas reservoirs, we believe these tests can still be very useful for obtaining hydraulic fracture information, provided efforts have been made to properly clean up the well after fracturing operations, and efforts have been made to reduce wellbore storage. Although pseudoradial flow is unlikely to be reached during the test in many tight gas cases, if an independent estimate of reservoir pressure is available (e.g. a pre-frac test), as well as permeability (e.g. rate-transient analysis, core or pre-frac test), then the post-frac test is irreplaceable as a way to quantify hydraulic fracture properties. An example is given in Fig. 28 for a hydraulically-fractured vertical well in Area B. The well was shutin for two weeks and exhibits a hydraulic fracture signature (linear flow), but no radial flow – assuming that radial flow is reached at the end of the flow period causes permeability to be overestimated (0.084 md), and hydraulic fracture half-length to be under estimated (91 ft). The permeability estimate from rate-transient analysis for this same well (after producing for 600 days), is 0.016 md, which is still considered to be over-estimated because radial flow is not thought to have been reached during the production period either. However, using the flow capacity kh (and with an assumption of h and k) derived from rate-transient analysis, a new estimate of hydraulic-fracture half-length may be derived (~ 200 ft), which is much closer to the RTA-derived values of 250-300 ft (discussed below). The somewhat shorter well-test derived values may be due to incomplete cleanup of the fracture post-stimulation. Nonetheless, we think that the short, post-frac well-test is justified, provided constraints on initial pressure and reservoir permeability are available, to provide an independent estimate of hydraulic-fracture properties. We also note that periodic testing of this nature could allow for effective half-length and conductivity to be monitored, perhaps for the purposes of identifying re-stimulation candidates.

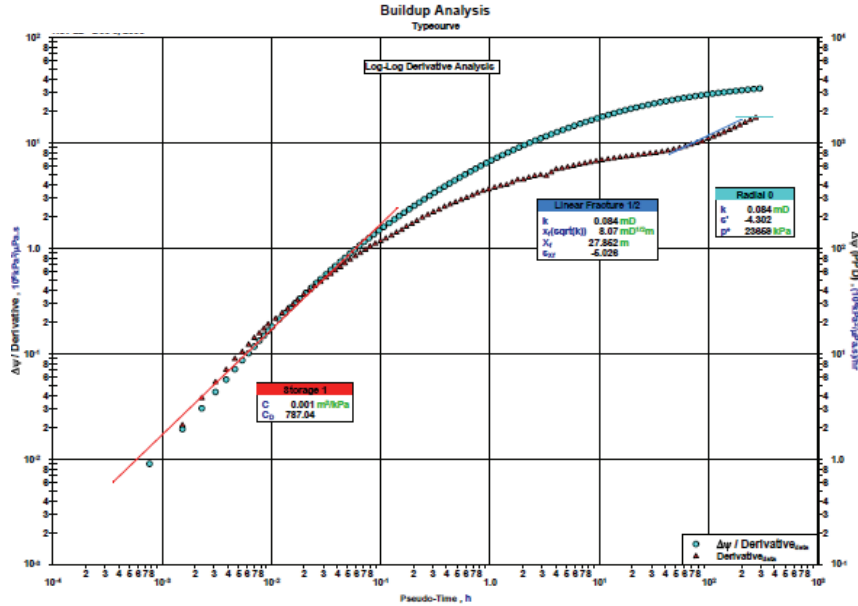
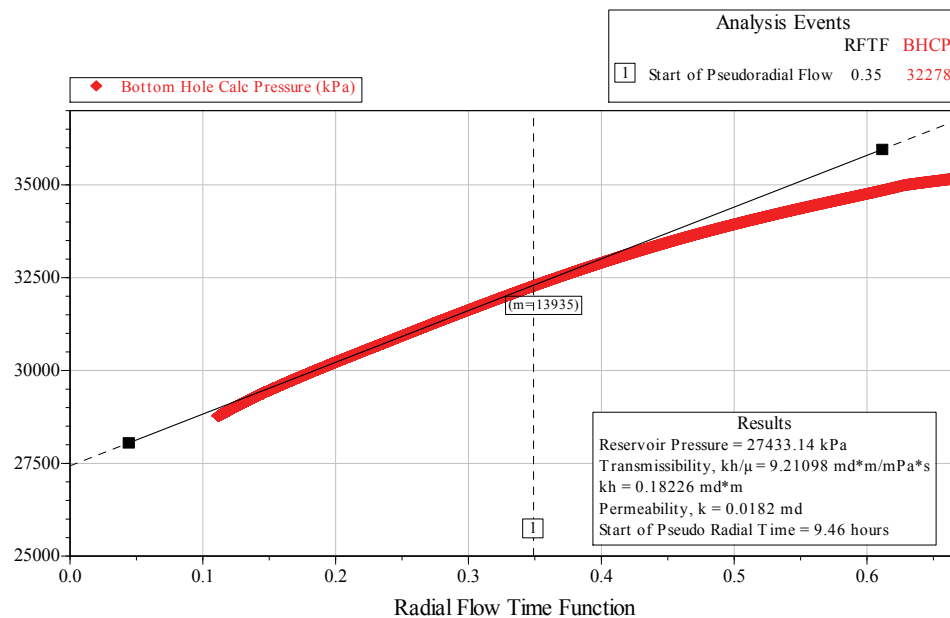


Fig. 28 — Example post-frac buildup analysis of a hydraulically-fractured vertical well in tight gas Area B. Note the short build-up times. A hydraulic fracture signature is evident from a formation linear flow period. The estimate of formation permeability is too high in this case (radial flow not reached), and hence hydraulic fracture half-length is underestimated. A more robust estimate for fracture half-length can be obtained using the RTA-derived permeability values.

Little pre-frac well-test was available in either tight gas study area (Area B or A), and what was available was of variable quality, mainly due to inadequate test lengths that did not allow pseudoradial flow to develop. Some exceptions exist, however, such as the DFIT test interpretation shown in **Fig. 29**, which exhibits an apparent radial flow period that could be interpreted for a *kh* and pressure value. The *kh* estimate for this well (0.182 md*m or 0.60 md*ft) is within the range of values obtained from rate-transient analysis (Clarkson and Beierle, 2010) and appears to be reasonable. As discussed above, ideally pre-frac tests can be used to obtain an independent estimate of initial pressure and permeability that can be used for analysis of short post-frac flow and buildup tests.



GohWin v1.6.5
02-Jul-09 14:17

Fig. 29 — Example after-closure analysis (ACA). In this example, the radial flow period is analyzed to obtain a permeability estimate.

Rate-Transient and Production Data Analysis

Rate-transient and production data analysis have undergone a rapid evolution recently in an attempt to make these methods applicable to UGRs. Both analytical and empirical methods have been advanced. In previous work (Clarkson et al. 2009, Clarkson and Beierle 2010), we categorized production analysis methods into: a) straight-line (flow-regime) methods; b) type-curve methods; c) analytical and numerical simulation and d) empirical methods. Straight-line analysis involves first the identification of flow-regimes, followed by analysis of the flow regime data on specialty plots to obtain hydraulic fracture or reservoir property information. Type-curve methods involve matching production data to analytical and/or empirical solutions to flow equations cast in dimensionless form. Analytical and numerical simulators can be “calibrated” to dynamic data (rates and pressures) to derive properties. Lastly, empirical equations can be fit to production data to yield a forecast.

When performing quantitative production analysis of UGRs, the analyst can encounter a wide range of reservoir characteristics that may need to be accounted for (or at least acknowledged) in the analysis including:

- Low matrix permeability, which causes transient flow periods to be extensive
- Dual porosity or dual permeability behavior, due to existence of natural fractures or induced hydraulic fractures (or both)
- Other reservoir heterogeneities, such as multi-layers (interbedded sand/silt/shale) and lateral heterogeneity
- Stress-dependent permeability, due to a highly compressible fracture pore volume
- Desorption of gas from the organic matrix
- Multi-mechanistic (non-Darcy) flow - in shale matrix, caused by gas-slippage along pore wall boundaries and diffusion (see Javadpour 2009), or in the hydraulic fractures due to inertial flow

Recent advances in these methods specifically for UGRs include:

1. Type-Curves developed for hydraulically-fractured wells
 - Infinite- and finite-conductivity fractures (ex. Pratikno et al. 2003, Agarwal et al. 1999)
 - Elliptical flow (Amini et al. 2007)
2. Straight-line (flow-regime) techniques adapted
 - To analyze flow regimes in tight gas, CBM and shale reservoirs (ex. Wattenbarger et al. 1998, Clarkson et al. 2009, Bello and Wattenbarger 2008)
3. Type-curve and straight-line methods modified to account for:
 - Desorption (Clarkson et al. 2007, and Gerami et al. 2007)
 - Multi-phase flow (Mohaghegh and Ertekin 1991, Clarkson et al. 2009)
 - Non-static permeability (Thompson et al. 2010)
 - Non-Darcy flow (Clarkson et al. 2011b)
4. Numerical and analytical simulators for CBM and shale
5. Improvements in flow-regime identification (ex. Ilk et al. 2005)
6. New empirical methods (ex. Power-Law Exponential) (Ilk et al. 2008)

Recently, rate-transient analysis methods have been used to analyze shale gas reservoirs to extract information about contacted surface area generated from hydraulic fracturing operations, and possibly hydraulic fracture spacing (Anderson et al. 2010). We note that RTA used on its own with no further information about fracture geometry could be very misleading. Whenever possible, production analysis should be combined with other surveillance data such as microseismic, production and tracer logs, so that flow regimes encountered during the analysis can be interpreted for physical meaning. In the tight gas example that follows, we discuss integration of data for a more meaningful analysis – for shale gas reservoir examples, we refer to Anderson et al. (2010).

Tight Gas Examples. In a previous paper (Clarkson and Beierle 2010), hydraulic-fractured vertical and horizontal wells were analyzed using rate-transient techniques, including straight-line, type-curve and analytical and numerical simulation in Area B. A detailed procedure for analysis was provided, emphasizing the integration of surveillance data such as microseismic, production and tracer logs. Rate-transient analysis of vertical wells was first performed to establish estimates of reservoir (ex. kh) and hydraulic fracture (effective length and conductivity) properties, prior to analysis of multi-fractured horizontal wells, which were used in later development. The consistency in stimulation treatments for both vertical and horizontal well hydraulic fracturing stages allowed for direct comparison of results. Both commingled and individual zone production rates were analyzed in multi-fractured horizontal wells. Detailed core and log analysis for Area B, discussed in previous sections, provided volumetric data as input, and very importantly, estimates of matrix permeability for comparison with RTA. Further, some pre-frac well-test analysis was performed on vertical wells in the area to provide for addition comparisons.

Straight-line analysis examples for a vertical and horizontal well (commingled stage) production data are summarized in Fig. 30a and b, and typecurve analysis in c and d. Flow-regime identification was first performed using semi-log and linear derivatives and other diagnostic plots (not shown) to ensure the correct flow regimes were being analyzed. We note that

plots containing superposition time functions contain a bias towards the flow regime assumed for superposition calculations, and should not be used for flow-regime identification. A planar hydraulic fracture model was chosen for the type-curve model due to the low-complexity of hydraulic fracture geometry as inferred from microseismic data (Clarkson and Beierle, 2010). Only linear flow analysis is shown, although (early) bilinear analysis was performed to estimate fracture conductivity for type-curve selection, and flowing material balance to obtain a minimum contacted gas-in-place (wells are still in transient flow). Additionally, although radial flow did not appear to be fully-developed in vertical wells, a maximum kh value was derived, and resulting permeabilities (with estimation of h) used in horizontal well analysis. The effective fracture half-length and conductivity from vertical well analysis is similar to that estimated from horizontal wells (noting that a total half-length from all stages is derived from the horizontal well analysis, and per stage values were derived from # stages). This consistency makes sense due to the similarity in fracture stage treatments for verticals and horizontal wells. The half-lengths from linear flow analysis are assumed to be over-estimated, due to use of pseudotime values in linear superposition time calculations that are anchored to pore volume average pressure – as noted by Nobakht and Clarkson (2011a,b), a corrected pseudotime yields more accurate values.

Type-curve estimates of hydraulic fracture lengths were slightly smaller for vertical wells – this is because the well is not yet in boundary-dominated flow, and hence ultimate drainage radius is underestimated. The use of material balance time combined with liquid loading behavior is believed to cause a false-boundary signature. The selected type-curve stem is the ratio of drainage radius to hydraulic fracture half-length, so if drainage radius is underestimated, so is hydraulic fracture half-length. Again, the reservoir engineer must be cautious regarding interpretation of flow regimes – errors in this interpretation will lead to errors in property estimates.

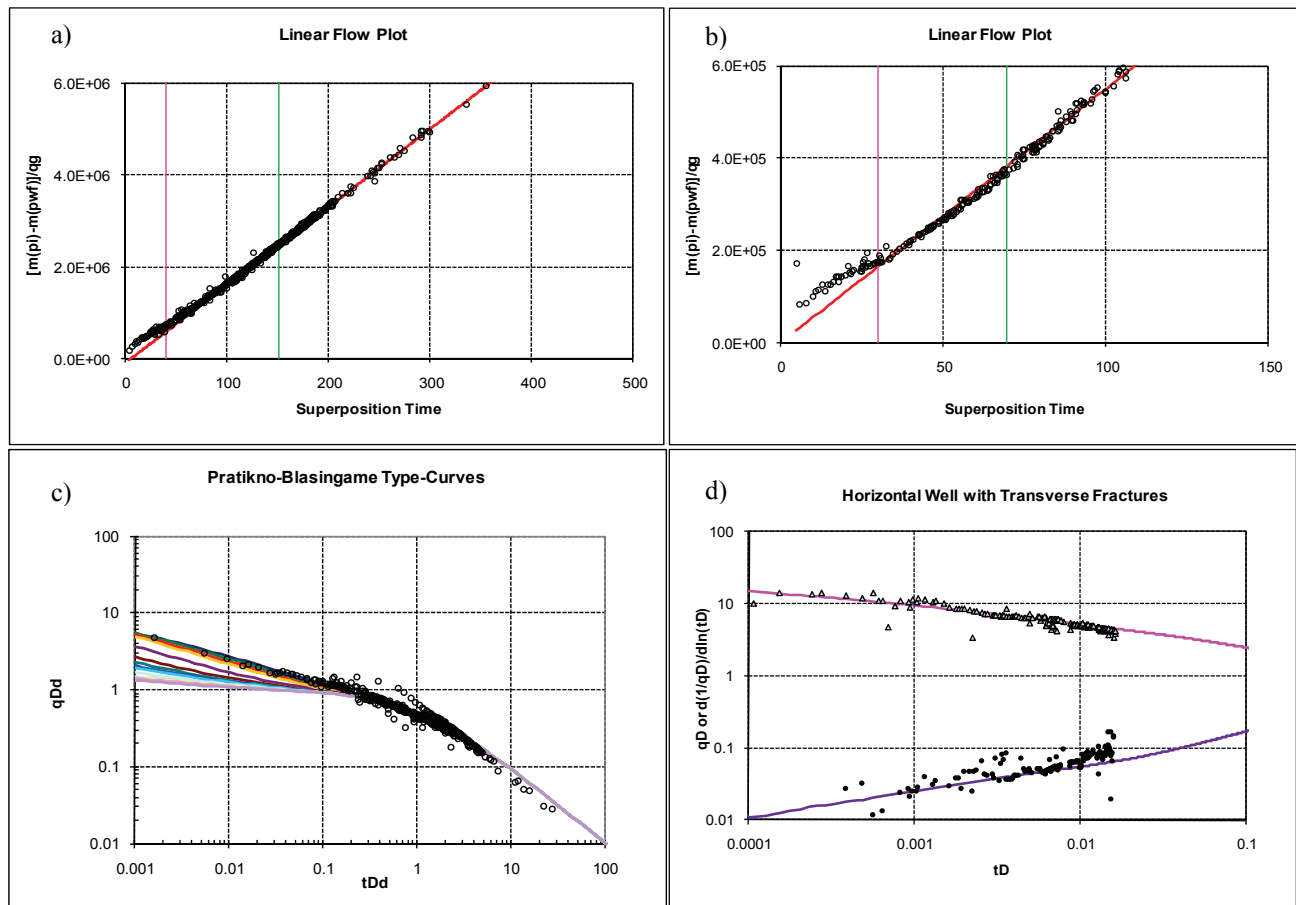


Fig. 30 — Linear flow analysis of vertical (a) and multi-fractured horizontal well (b), and type-curve analysis of vertical (c) and multi-fractured horizontal well (d) in Area B.

Analytical model history-matching and forecasting was performed to validate the rate-transient-derived reservoir and hydraulic fracture properties (not shown).

Once RTA work has been performed, it is important to compare property estimates to other sources, and potentially iterate until consistent results are obtained. Permeability values derived from RTA radial flow analysis of vertical wells, believed to yield a maximum value because radial flow was not reached, were compared to core and pre-frac well-test analysis. Slippage-corrected matrix permeabilities obtained from pulse-decay analysis under confining pressure and corrected profile permeabilities tended to be $< .01$ md, whereas values derived from RTA averaged $\sim .01$ md. The discrepancy could be caused by several factors – an overestimate of permeability from RTA due to radial flow not being

reached and/or underestimated net pay (we note this is necessary to obtain a permeability estimate from RTA), non-representative permeability values from core analysis, or heterogeneities that are larger in scale than the core (included in the averaging process for RTA). Additional factors affecting RTA-derived values include non-Darcy flow and stress-dependence of porosity and permeability. From core analysis, we note that the dominant pore throat sizes, combined with PT information, suggest that slippage-flow may be important in this reservoir. Conventional RTA analysis assumes Darcy-type flow behavior; correction for slippage in this case is expected to yield only small changes in permeability, but may be significant for shale gas cases – a method for correcting for non-Darcy flow in RTA is described by Clarkson et al. (2011b). The small stress-dependence of permeability for this reservoir at higher pressures is not expected to affect the analysis significantly, but this may not be true for some shale (ex. Thompson et al. 2010) and CBM reservoirs (Clarkson et al. 2008). A further complication for CBM and some shale cases is the impact of desorption, which if not corrected for, can also affect reservoir/hydraulic fracture property estimates. In this tight gas area, TOC values are calculated to be quite small (Fig. 20), and hence adsorption insignificant, which will not be the case of many shale gas plays and certainly not for CBM. In this study area, the values for permeability agree well within an order of magnitude, despite discrepancies in the measurement volumes etc., which is quite good compared to some UGR. Pre-frac well-test analysis, yielded a range of results (.002 - .02 md) within the range of RTA and core analysis, providing an additional consistency check.

Hydraulic-fracture property estimates derived from RTA were also compared to other sources (Fig. 31). Hydraulic fracture modeling (discussed in more detail later), yielded a fracture half-length that is consistent with type-curve and linear flow analysis (“RTA-type-curve” and “RTA-straight-line”, respectively, in Fig. 31). The fracture half-length derived from post-frac well-test analysis (labeled “flow/BU” in Fig. 31) is somewhat smaller (~ 200 ft), but still in reasonable agreement with RTA and frac modeling – as discussed above, the shorter well-test derived half-length may be due to incomplete cleanup of the fracture. Fracture half-lengths from microseismic data, interpreted by three different vendors, yielded consistently larger values. We note that post-frac- and RTA-derived values represent propp’d hydraulic fracture lengths (but static, versus dynamic values, respectively) and microseismic values represent created hydraulic fracture lengths, but not necessarily propp’d or conductive. Care must be taken by the reservoir engineer to use values of fracture-length that allow the performance of the wells to be recreated – in this field case, the RTA-derived values are consistent with well performances obtained, although as noted the half-lengths are likely an overestimate due to the incorrect pseudotime calculations. We believe the flowing effective half-lengths are likely between 250-300 ft. Microseismic data provides a boundary on upper limit values, and the geometries can be used to assist with model selection. Fracture conductivities derived from post-frac analysis were significantly greater than that derived from RTA, suggesting that flowing conductivities (which include multi-phase flow, non-Darcy flow etc.) as derived from RTA are significantly less than static values – an excellent discussion of differences of hydraulic fracture properties derived from various sources was provided by Barree et al. (2005).

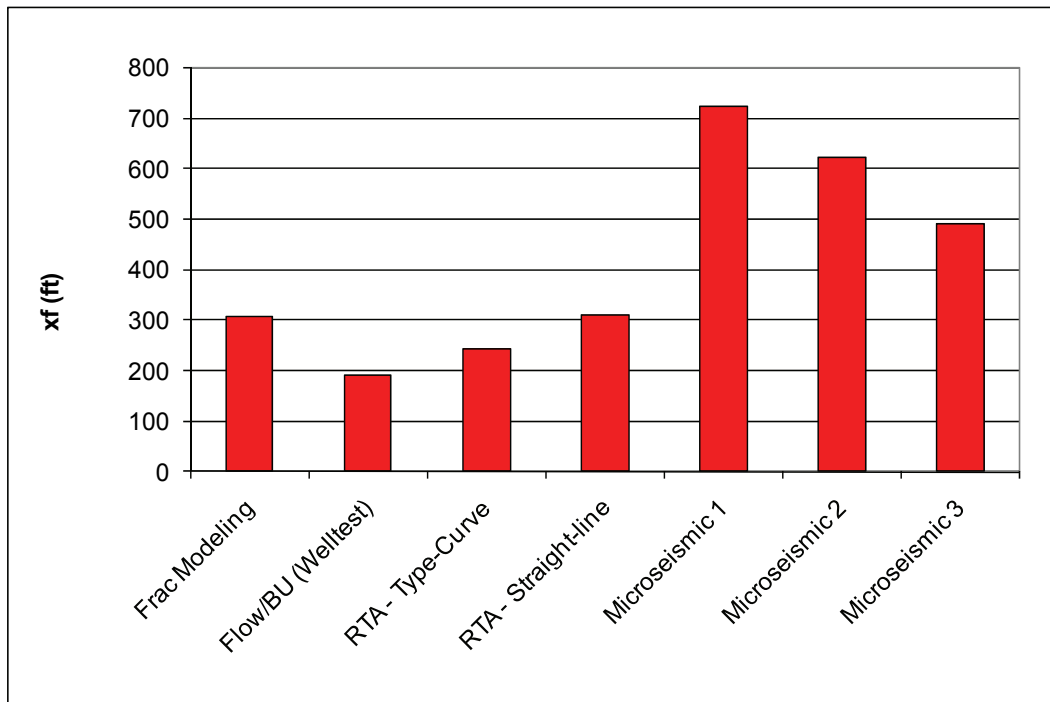


Fig. 31 — Comparison of hydraulic-fracture half-lengths (x_f) derived for a vertical well in Area B from various sources. “Frac modeling” refers to the modeling of fracture length using a commercial hydraulic fracture simulator, using net pressure data etc. “Flow/BU...” refers to the post-frac well-test, and “RTA – Type-Curve” and “RTA-Straight-line” refer to analysis of rate-transient data using typecurve and straight-line (flow-regime) analysis, respectively. “Microseismic 1, 2 and 3” refer to estimates from microseismic data, as interpreted from 3 different vendors.

Lastly, although not discussed in Clarkson and Beierle (2010), empirical (decline-curve) analysis was also performed on several wells in Area B. Multi-segmented Arps (1 segment for transient flow, 1 for boundary flow) and Power-Law Exponential (PLE) decline analysis was performed – only the latter is shown (Fig. 32). The Power-Law model provides a very good fit to the (transient) data. The EUR for the wells were adjusted to be consistent with that obtained from analytical and numerical modeling (which have estimated boundaries imposed). We used the approach of Rushing et al. (2007) to constrain individual well reserve estimates.

In Fig. 32, note that the loss-ratio ($1/D$) and derivative of loss-ratio (b) decline with time, as expected during transient flow. Ultimately, during boundary dominated flow, both parameters will stabilize to constant values. We note that the modeled value for b is > 2 , and close to 4, indicative of low conductivity fractures, as suggested by Kupchenko et al. (2008). Very recently, Ilk et al. (2011) compared correlated RTA model-derived properties to parameters in the PLE.

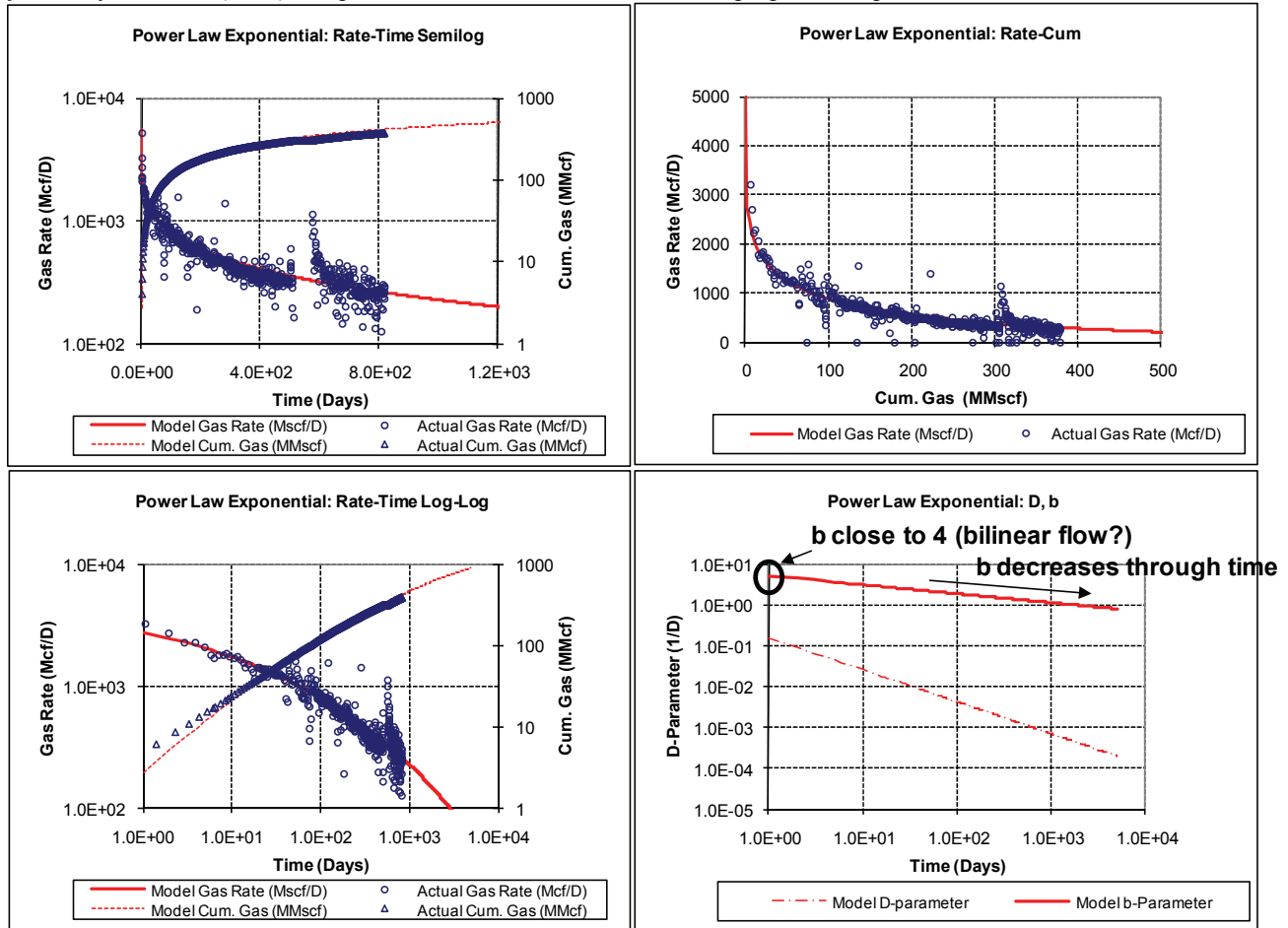


Fig. 32 — Power-Law Exponential decline analysis of vertical well in Area B. Rate-time plots on semi-log and log-log plots are shown in (a) and (c), a rate-cum. plot in (b) and model trends for D and b are shown in (d).

Hydraulic Fracture Modeling

For unconventional reservoirs, the completion/stimulation is critical to successful development, hence a lot of emphasis must be placed on the careful characterization of hydraulic fractures/hydraulic fracture network and incorporation into reservoir modeling. Several methods for estimating hydraulic fracture properties are given in Table 2. Rate- and pressure-transient analysis can be used to estimate hydraulic fracture properties such as effective length and conductivity but these techniques require some understanding of hydraulic fracture geometry to properly interpret the data, meaning that surveillance data such as microseismic will be required (Fig. 33). In relatively low-complexity fracture scenarios, planar hydraulic models used for RTA/PTA should be sufficient to extract quantitative estimates of hydraulic fracture properties provided good data quality and that the appropriate flow regimes are represented. In more complex fracture scenarios (as may be obtained for naturally-fractured reservoirs such as CBM and some shales, (Fig. 33)), resulting in a “stimulated reservoir volume” (SRV) as opposed to a discrete hydraulic fracture with an elevated conductivity relative to the background reservoir, the physical meaning of the extracted information from RTA/PTA becomes less clear. Some authors (ex. Anderson et al. 2010) have interpreted linear flow data in terms of contacted (by the hydraulic fracture) matrix surface area and if the boundaries of the SRV had been reached during the test, fracture spacing may be interpreted if a hydraulic fracture geometry is assumed (or inferred) from microseismic data. In the complex fracture geometry scenario, hydraulic fracture properties derived from RTA/PTA are at best semi-quantitative, and may not be of great use for hydraulic fracture design.

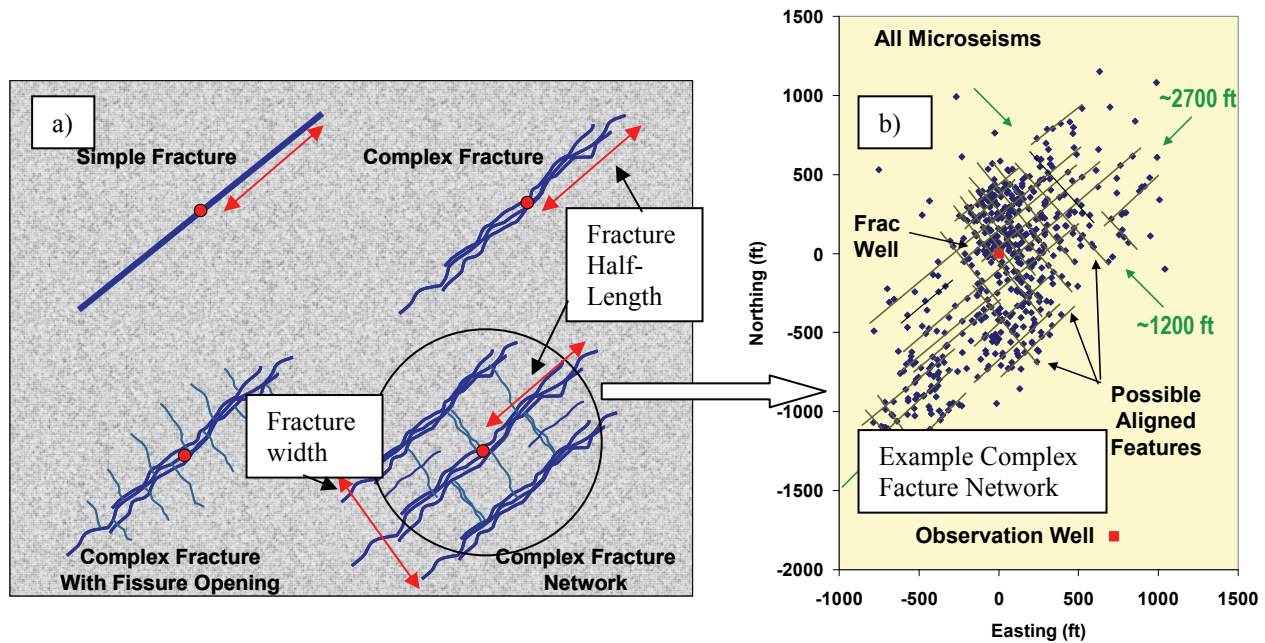


Fig. 33 — (a) Illustration of spectrum of possible fracture geometries that may be encountered in shale and (b) evidence for complex fracture geometry in Barnett Shale. Modified from Warpinski et al. (2008). Cipolla et al. (2008) used a fracture complexity index, which is the ratio of fracture width to length as determined from the microseismic cloud, to establish the degree of frac complexity – complex fracture networks have nearly equal width and length.

Similarly, hydraulic fracture modeling, which uses pressures monitored during the frac job, minimum stress profile, rock mechanical properties, fluid properties, injection rate, proppant concentration and slurry information to predict propp'd hydraulic fracture length and conductivity, is well established for conventional reservoirs, but is problematic for shale gas or CBM reservoirs that exhibit a complex fracture geometry. As mentioned, complex fracture geometry may in some cases be related to the existence of natural fractures - conventional fracture simulators often assume a bi-wing, planar frac geometry and simplified physics for hydraulic fracture propagation, although there is a variability in rigor for existing commercial simulators. When complex fracture geometries are created, simple planar models may not be appropriate. Microseismic data is a promising technique for inferring hydraulic fracture geometry, but does not provide fracture conductivity distribution information (within natural or hydraulic fractures), which is necessary to understand fluid transport properties of the induced hydraulic fracture network. As discussed above, in the complex fracture scenario, rate-transient analysis can be combined with microseismic data and other surveillance to provide gross estimates of fracture properties such as spacing and contacted matrix surface area, but generally fails to provide an understanding of vertical and areal distribution of fracture conductivity (due to proppant placement), which is necessary for detailed well and reservoir optimization work.

Hydraulic fracture models that accommodate more complex fracture geometry are starting to be developed. Recently, a semi-analytical method for simulating complex fracture growth has been introduced (ex. Xu et al., 2010), which is referred to as a Wire-mesh model. The hydraulic fracture network is represented by an elliptical region with two sets of parallel vertical fractures that are uniformly spaced. The model can be used to predict the evolution in fracture geometry, treating pressure, fracture width and proppant placement in the fracture network over time. The model can be constrained by using image logs, 3D seismic, core and outcrop studies estimate fracture network parameters. Further, microseismic data can be used to provide a constraint on overall fracture network dimensions. This approach, while promising, requires a great deal of data to implement and calibrate – these data are often available for pilot studies, but not necessarily during full development.

The most rigorous approaches for modeling complex fracture geometries involve the use of coupled fluid flow and transport models, with geomechanical simulation (Cipolla et al. 2010). These approaches could allow for the prediction of microseismic events during the pumping of the frac job, which can be compared against the actual time-lapse microseismic data, predict proppant distribution (and hence fracture conductivity), as well as the overall dimensions of the fracture network. Such approaches are in their infancy, however, but we look forward to significant advancements in this area. These approaches however would require a very complete description of the existing natural fracture network, and other reservoir properties, necessitating detailed geological, petrophysical and geophysical input.

In the following, we again look at the relatively simple tight gas scenario.

Tight Gas Examples. As we noted for the Area B study area, low complexity hydraulic fracture geometries were inferred from microseismic data, and this assumption was used in RTA/PTA work. The same assumption was used for modeling fracture length and conductivity using data collected during the hydraulic fracture treatment, allowing existing commercial hydraulic fracture simulators to be used. The hydraulic simulation results for 1 of 2 fracturing stages of a vertical well is given in Fig. 34 – this is the same well for which the fracture half-length comparison was performed in Fig. 31. This

well was treated with a polymer-free, water-based stimulation fluid (some breaker required to reduce viscosity before production) with 4% KCL at a rate of 2.5 m³/min for the lower stage and 1.5 m³/min for the upper stage. Approximately 70,000 kg of 20/40 mesh Jordan sand and 10,000 kg of a resin coated ceramic proppant were used. The hydraulic fracture model was calibrated by matching fracture treatment data. The estimated average fracture half-length for both stages is 94 m (308 ft), which is shown in Fig. 31, but ranges from 86.2 m (lower stage) to 101.8 m (upper stage). The estimated fracture conductivity is ~ 2950 md*ft, which is much higher than that obtained from RTA, which is ~ 50 md*ft. The difference in the two conductivity values may be due to non-Darcy, multi-phase flow and other effects realized during production of the well (Barree et al. 2005).

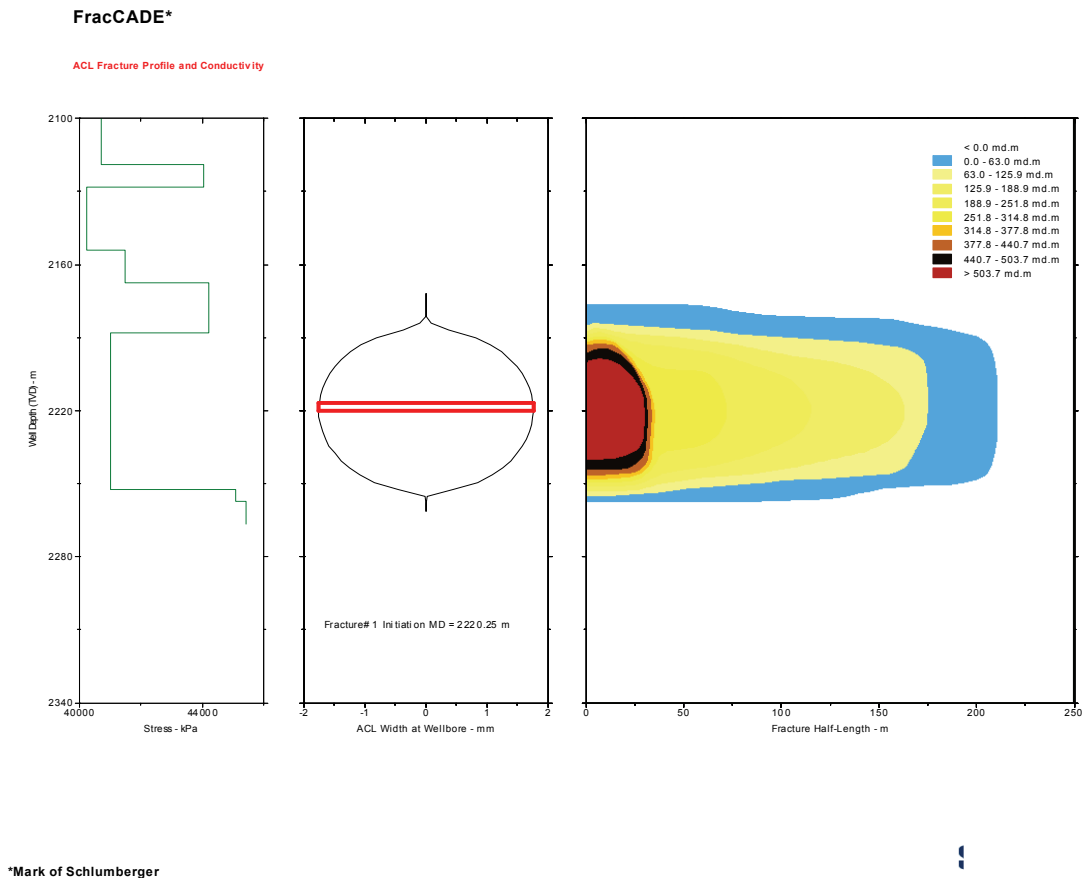


Fig. 34 — Example hydraulic fracture model, assuming planar hydraulic fracture geometry, used to predict fracture length and conductivity for Area B vertical well.

Because the fracture conductivity obtained from RTA allows for a better match of production data, future fracture design runs using the frac model utilized the effective conductivity number obtained from RTA (Fig. 35). The match point for x_f and conductivity is also shown in this plot, serving as a calibration point for modeling sensitivities. The agreement between RTA and frac modeling provides greater confidence in the analysis. Hydraulic fracture model predictions of fracture geometry (half-length) and conductivity as a function of proppant tonnage using the calibrated model are also shown and are used for economic analysis. Larger job sizes will lead to longer hydraulic fractures, but at an added cost of materials/horsepower. Forecasts associated with each fracture design scenario must be generated using simulation, then economic analysis performed to select the optimal design, as discussed in a later section.

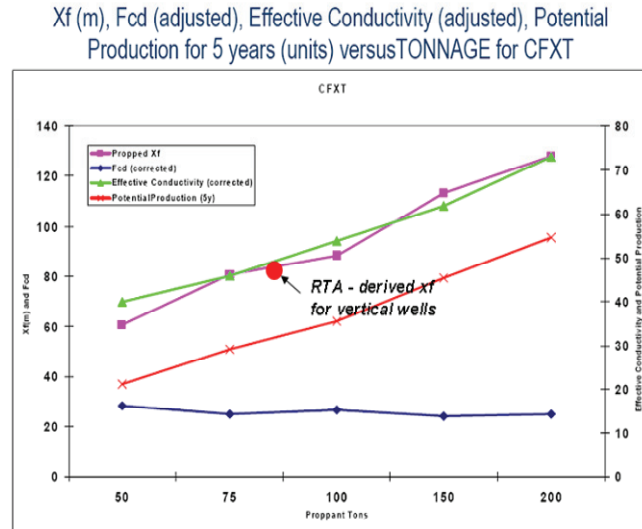


Fig. 35 — Hydraulic fracture sensitivities to proppant tonnage using a calibrated hydraulic fracture simulator. The agreement between RTA and the frac model provides greater confidence for model calibration. Sensitivities to job size are used to estimate the optimal frac half-length.

Reservoir Modeling

Following the reservoir/hydraulic fracture characterization stages, the first attempt at reservoir modeling can be performed, usually starting with individual well simulation, to check the results of individual well RTA/PTA, followed by field simulation. We note again that Fig. 1 illustrates an iterative process, with modeling efforts potentially requiring the analyst to revisit various stages of the characterization process to reconcile differences between the model and actual well performance. The first objective is to calibrate the resulting simulation model against existing dynamic data (production and flowing and shut-in pressure information), then forecasting the wells against operational constraints in the future to create a “base” case. The modeling step can be handled deterministically or stochastically (Rushing and Newsham 2001) – we do not wish to discuss the mechanics of the process, but rather some of the considerations and recommendations specific to unconventional gas reservoirs.

Based upon our experience, we offer the following advice for those who wish to perform simulation modeling for unconventional reservoirs:

1. For models requiring inclusion of hydraulic fractures (most unconventional gas reservoir modeling scenarios), **use fine gridding near the fractures and small time steps** to ensure that pressure and saturation changes are captured accurately. Many commercial simulators offer local-grid-refinement options, logarithmic or unstructured gridding options to capture these effects properly. An ideal way to test whether or not the gridding is appropriate is to analyze the rate/flowing pressure output from the simulator in a well-testing package to make sure the flow regimes can be identified properly (1/2 slope on semi-log derivative for linear flow etc.) and the sequence makes sense. An example of a multi-fractured horizontal well completed in a single-porosity, single-layer homogenous isotropic tight gas formation is given below (**Fig. 36**) using KAPPA’s Topaze® software. The flow-regimes are easily identified and the sequence is what is expected.

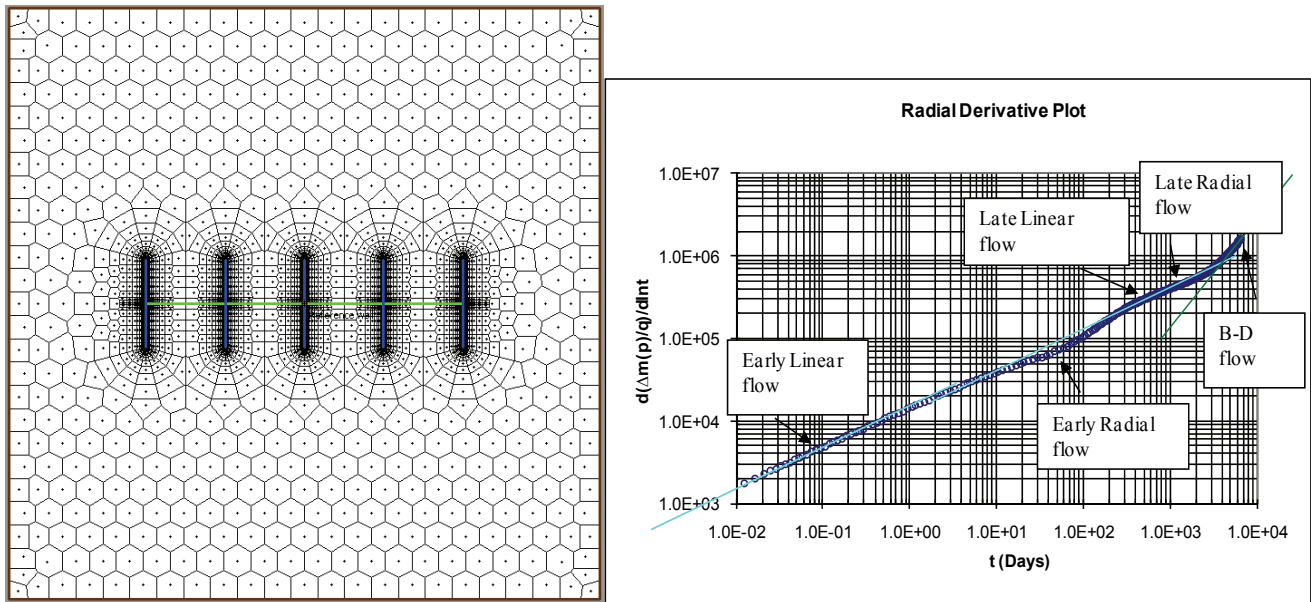


Fig. 36 – (a) Gridding used in numerical simulation of multi-fractured horizontal well completed in a tight gas reservoir, and (b) sequence of flow regimes identified from derivative analysis of the rate-transient signature.

2. **Select the right tools for the job.** UGRs exhibit a wide range in reservoir characteristics, including adsorbed gas storage (CBM and organic-rich shale), non-Darcy transport, dual porosity or dual permeability, multi-phase flow etc. Thus ensure the simulator you are using captures the reservoir behavior you require and contains the advanced gridding options discussed above. We will revisit this point below for shale gas reservoirs.
3. **Pick the simplest tool that gets the job done.** If there are too many inputs in the model that cannot be defined correctly because of lack of/poor quality data, then you may not be further ahead than using a simpler method/tool for forecasting, particularly for single-well scenarios. For example, CBM reservoirs are inherently complex reservoirs, but in some scenarios, where dual porosity effects can be ignored (sorption times are small), simple tank-type simulators may be adequate to capture the salient features of single-well performance, as illustrated in Clarkson and McGovern (2005), and more recently in Roadifer et al. (2009). For shale gas reservoirs, there have been a number of “hybrid” single-well forecasting approaches introduced, that combine analytical transient flow modeling (often linear flow) with Arps’ decline forecasts once boundaries are reached (ex. Nobakht et al. 2010, Ambrose et al. 2011). An example is shown below, using an approach analogous to Nobakht et al. (2010), where linear flow is first analyzed on square-root of time plot to obtain a slope and intercept value for forecasting transient linear flow, followed by analytical (material balance) forecasting of boundary-dominated flow (Fig. 37). Additional information, such as microseismic data, may be required to constrain the potential drainage limits of the reservoir. Such approaches can yield a reasonable “first pass” forecast to assist with development planning and for comparison with more rigorous approaches. When detailed hydraulic fracture and reservoir characterization data are available, then more complex and rigorous tools may be desirable to assist with development planning – this is discussed in the context of shale gas reservoirs below.

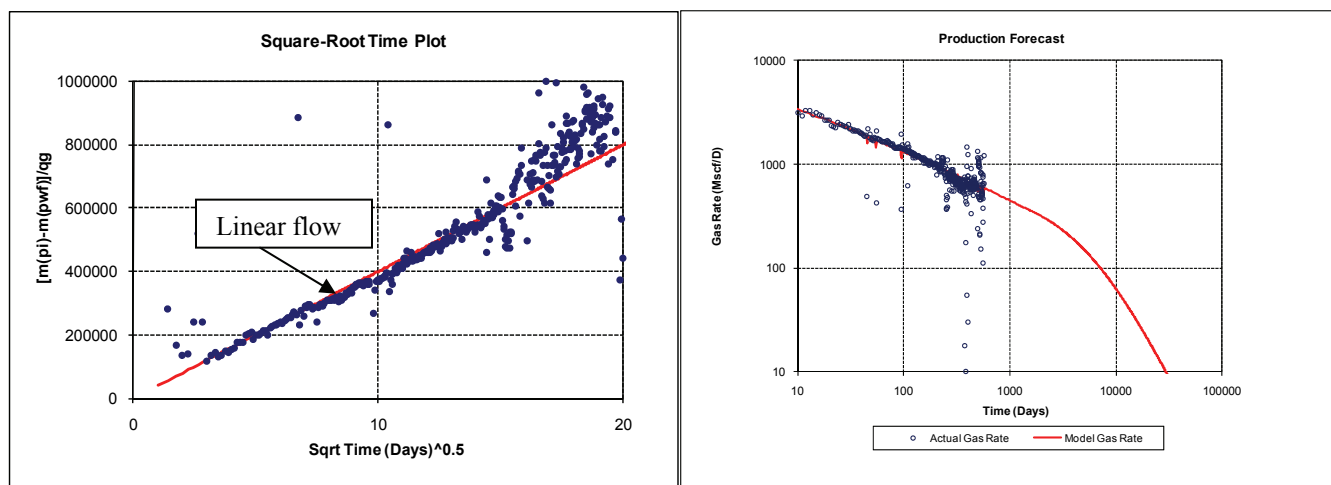


Figure 37 — (a) Square-root of time plot used to analyze linear flow period for a shale gas reservoir and (b) resulting forecast. From Clarkson et al. (2011a).

4. **Perform rate-transient analysis first.** It should be obvious from the above that we are proponents of starting with simpler approaches for modeling, then progressing to more complex approaches should the data warrant it. Rate-transient analysis using simple analytical methods may yield information useful for constraining inputs (ex. contacted matrix surface area or hydraulic fracture half-length and conductivity) to more rigorous numerical simulation approaches and is easier to setup – this is a logical first step in well-performance analysis, and there has been great advancement in this area for UGRs as described above.
5. **Incorporate surveillance data to assist with history-matches.** As described in Clarkson and Beierle (2010) for tight gas and Cipolla et al. (2010) for shale gas, besides the usual static (PVT, porosity, reservoir thickness etc.) and dynamic data (flowing pressures and production rates), UGRs require additional surveillance data to both assist with model selection and constrain model history-matches. Examples include microseismic data to assist with definition of hydraulic fracture geometry, production and tracer logs to assist with allocation of stage production rates, pressure observation wells etc. The complexity of UGRs necessitate that additional constraints be placed on simulation, which is in part fulfilled with surveillance data.
6. **Constrain volumetric (static) model as much as possible.** It should be evident from the reservoir characterization discussion above that there can be a great deal of uncertainty associated with any static model generated for UGRs due to all the issues related to reservoir sample and log analysis. Core-log calibration is critical for constraining petrophysical models, and stochastic methods are often required to represent static model uncertainty.
7. **Use field simulation where well-to-well interference effects need to be captured and where there is significant lateral and vertical heterogeneity.** Fully calibrated field models are the ultimate tool in the reservoir engineer's tool kit – they are extremely time consuming to construct and calibrate, but the fully calibrated model can be used for field development studies (well spacing, orientation, geometry, enhanced recovery), establish incremental versus accelerated reserves, and when coupled with a surface model, assist with pipeline network and surface facility design.
8. **Use stochastic models when there is a large uncertainty in model inputs.** These are particularly useful for exploration scenarios, as discussed by Clarkson and McGovern (2005) and Roadifer et al. (2003) for CBM reservoirs.
9. **Constrain simulation with surface/wellbore model for forecasting.** Fully integrated reservoir/surface network models are most useful to constrain forecasts as the reservoir model is constrained by surface gathering system restrictions. A fully calibrated integrated model can be used for both surface facilities optimization (compression, pipeline etc.) as well as subsurface.
10. **Use flow simulation or coupled flow/geomechanical models to model flowback of fracturing fluids.** Large volumes of fluid are typically pumped during hydraulic fracturing operations in shale gas and tight gas reservoirs. A useful exercise is to use flow or coupled flow/geomechanical models to model first the injection of fracture fluids, then the flowback of water and gas to gain insight into the mechanisms of water retention, and model effective permeability to gas changes due to imbibition of water. In Fig. 38, we used a flow simulator to model this process for a hypothetical shale reservoir. A horizontal well model was first created using Eclipse® and logarithmic gridding. A dual porosity model was used (matrix permeability = 300 nd, fracture permeability = .05 md, matrix porosity = 5%, fracture porosity = 0.5%) and discrete hydraulic fractures were input into the model to create a preferred fracture growth direction. A strong pressure-dependent permeability was input for

pressures above initial reservoir pressure (during injection) to allow water to move away from the fractures, creating “complexity”. The input irreducible S_w (50%) was different than initial S_w (20%) to allow water to be trapped. During the fracture simulation, water was injected into the well at a high rate at pressures above initial reservoir pressure for 50 minutes/per stage. A snapshot of fracture pressure after injection is shown in Fig. 38a indicating that water was propagated a significant distance away from the fracture, an indicator of fracture complexity. Injection rates used in the simulator were a bit higher than typical for many shale plays (142 bbls/min average rate), but total fluid injection (7000 bbls/stage) was reasonable. Flow back of the well for several months after a brief shut-in was simulated. The resulting water and gas production profiles (Fig 38b) are qualitatively similar to flowback we have observed for some shale gas reservoirs, with realistic load recoveries (30% after 30 days), and flowback gas and water production profiles. This exercise demonstrates that flow simulators may be “tricked” to model the flowback process, but we contend that coupled flow/geomechanical simulation is more rigorous and should be used if the data support the effort (see below). In the future we will incorporate gas and water compositional data into the flowback modeling process to improve uniqueness of the results.

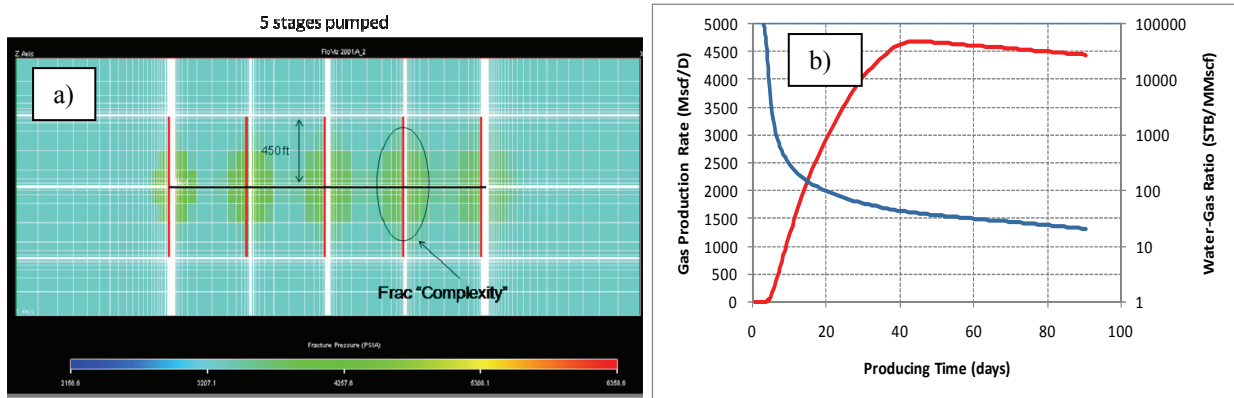


Fig. 38 — Use of a flow simulator to model water injection and flowback. (a) gridlock (fracture) pressures after injection and (b) flowback characteristics of gas and water.

Perhaps the greatest challenge facing reservoir engineers modeling UGRs is modeling systems that exhibit a complex fracture geometry. Discrete, low-complexity fractures, although requiring special gridding, are relatively straight forward to implement, but may require conductivity to be adjusted to achieve a match, reflecting the dynamic nature of hydraulic fracture effective permeability during initial flow back and at later stages of production. Complex fractures are more difficult to model. Several simulation approaches may be used to represent the reservoir/hydraulic fracture system in these cases as discussed by Cipolla et al. (2010) for shale gas reservoirs, including use of a 1) dual porosity/estimated stimulated volume (ESV) approach, the ESV being estimated using microseismic data; 2) modeling of the hydraulic fracture network using the Wire-mesh approach mentioned above and 3) fracture plane extraction approach as described in Cipolla et al. (2010). Cipolla et al. (2010) compared these approaches and noted that despite the fact that each of them could be used to successfully history-match well data, the forecasts from each method were significantly different due to the differences in drainage volumes predicted by each approach (Fig. 39). Clearly a model bias exists, and adds to the uncertainty in accurately predicting well production. Cipolla et al. (2010) also emphasize the integration of data (geological, geophysical, petrophysical and engineering) to constrain the modeling efforts, which is most important for UGRs.

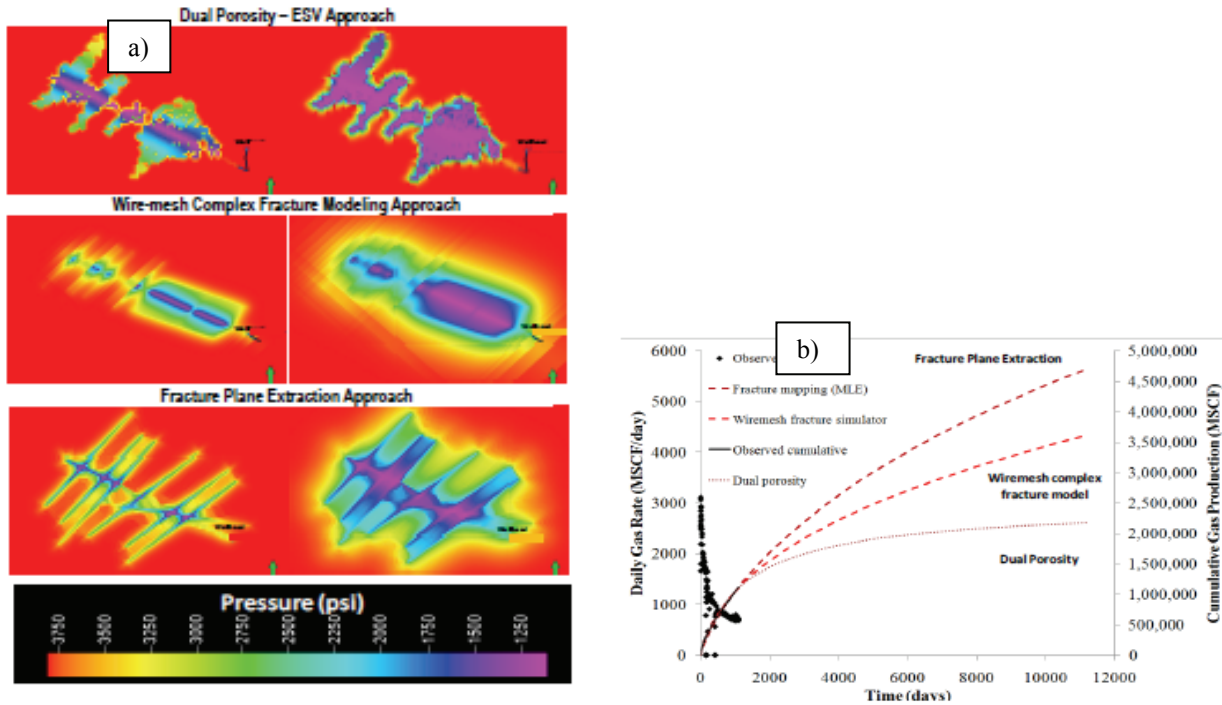


Fig. 39 — History-matching and forecasting shale gas production using 3 different modeling approaches. In (a), gridblock pressures on the left-hand side correspond to pressures at the end of the history-matching period, and gridblock pressures on the right-hand side correspond to pressures after 30 years. (b) illustrates the impact of model choice on cumulative production. Modified from Mack et al. (2010).

Once the “base case” has been generated from calibration of the reservoir model corresponding to the existing development scenario, additional development scenarios can be generated by performing sensitivities to well-spacing and orientation, fracture spacing, frac size etc. The next step is to perform economic analysis of each scenario to establish the optimal development plan.

Tight Gas Examples. After completion of the reservoir and hydraulic fracture characterization steps for Area B, single-well numerical simulation modeling of existing vertical and horizontal well producers was attempted using all the data that had been compiled and interpreted to that point. An example horizontal well match is given in Fig. 40, noting that fine gridding was required to match the well performance (Fig. 40a). In this example, the total hydraulic fracture half-length derived from RTA and permeability mapping from offset vertical wells were used as input into the match – only a slight adjustment to fracture conductivity was required to achieve the match. The example demonstrates the value of performing RTA first to estimate reservoir and hydraulic fracture properties (Tip 4 above) to be used in numerical simulation. Ideally, little tweaking to the numerical model should be required at this stage.

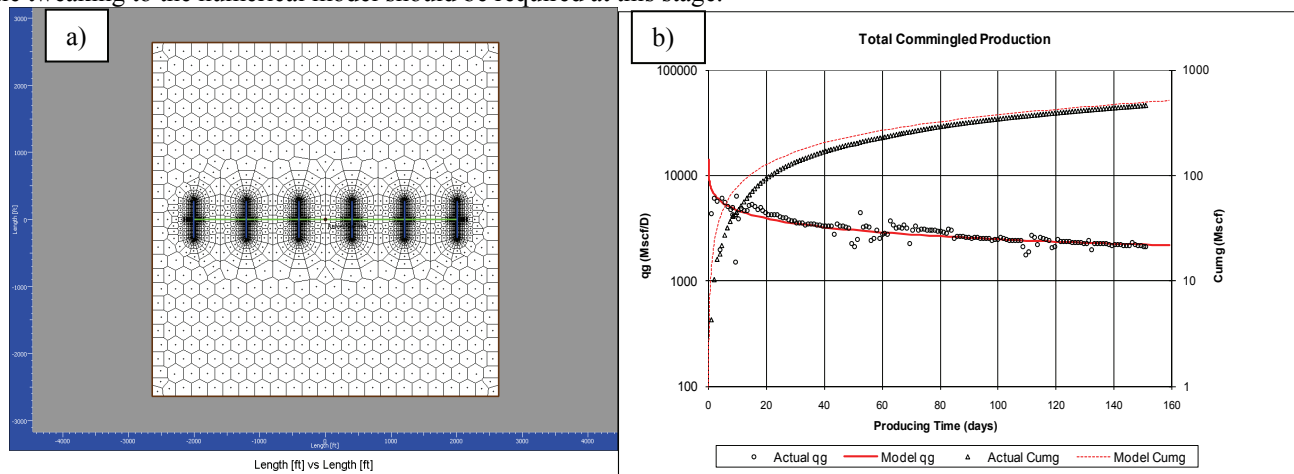


Fig. 40 — Single-well history-match for multi-fractured horizontal well in tight gas Area B. (a) shows the grid geometry and (b) illustrates the history-match of the gas production rate data, given a constant flowing bottomhole pressure assumption. The history match used parameters derived from rate-transient analysis as input.

The next step in the simulation process was the development of a 3-D geocellular model using petrophysical and geologic data for the purposes of generating static and dynamic properties for reservoir simulation (**Fig. 41**) – the static model was generated using interpreted well logs and geostatistical methods to extrapolate reservoir properties between wells.

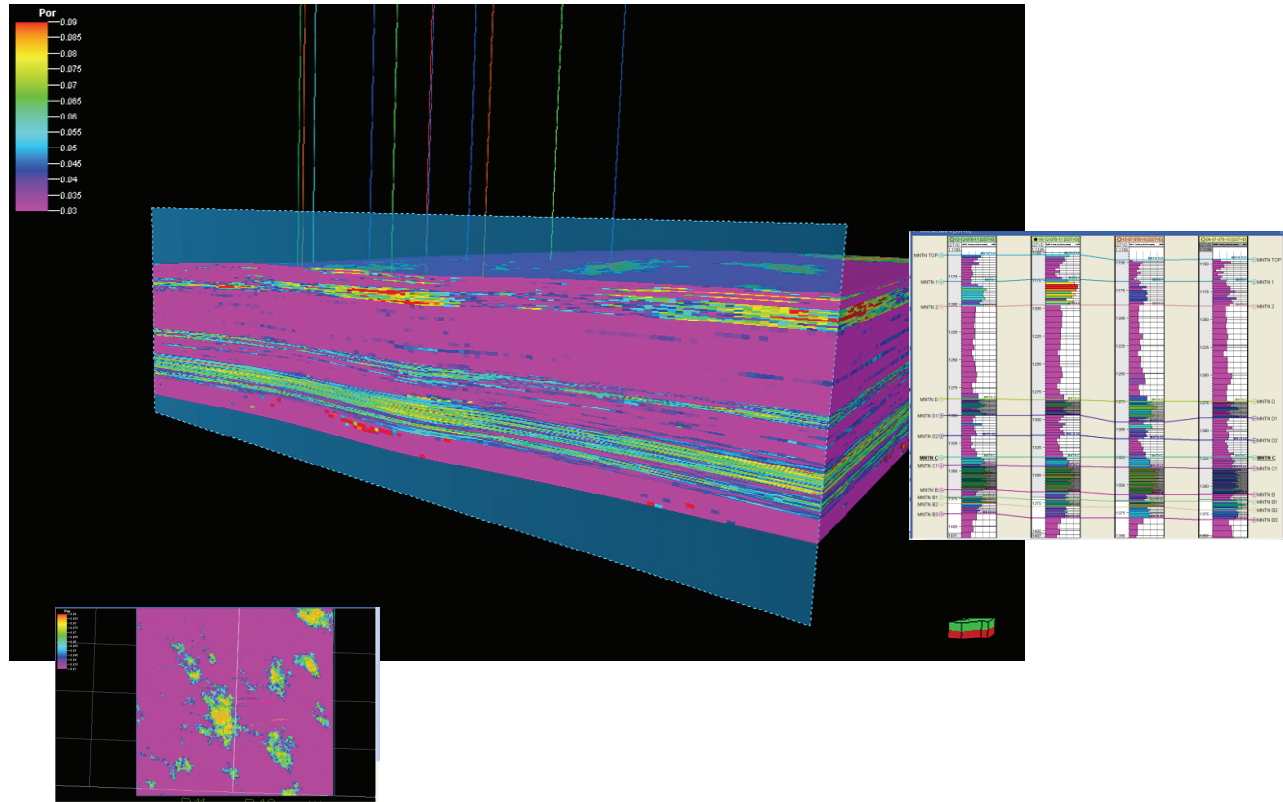


Fig. 41 — Geological model constructed for modeling field performance in Area B. Porosity distribution is shown. Image courtesy of Leyva, Yazdi and Murdoch (2010).

For permeability modeling, kh values obtained from RTA transient analysis were mapped using geostatistical (SGS) methods (**Fig. 42**). Because radial flow was not reached for vertical wells, the kh values are likely to be optimistic, but serve as a starting point for field simulation. Hydraulic fracture half-length and conductivity values from vertical and horizontal well RTA work were also used for input.

As with the single-well models, the input values derived from RTA and used in the field model provided reasonable history-matches for the vertical and horizontal wells without significant changes to the model. The next step was to generate production forecasts for all wells in the study area, under current operating conditions to serve as a “base case”. **Fig. 43** illustrates a forecast for one of the multi-fractured horizontal wells in the study area, along with a snapshot of gridblock pressures over time to illustrate the radius of investigation over time.

At present, we are using the calibrated reservoir model to generate multiple scenarios corresponding to: well-spacing, hydraulic-fracture spacing, conductivity and length, flowing pressure etc. Economic analysis will be used to establish the optimal development plan for the field.

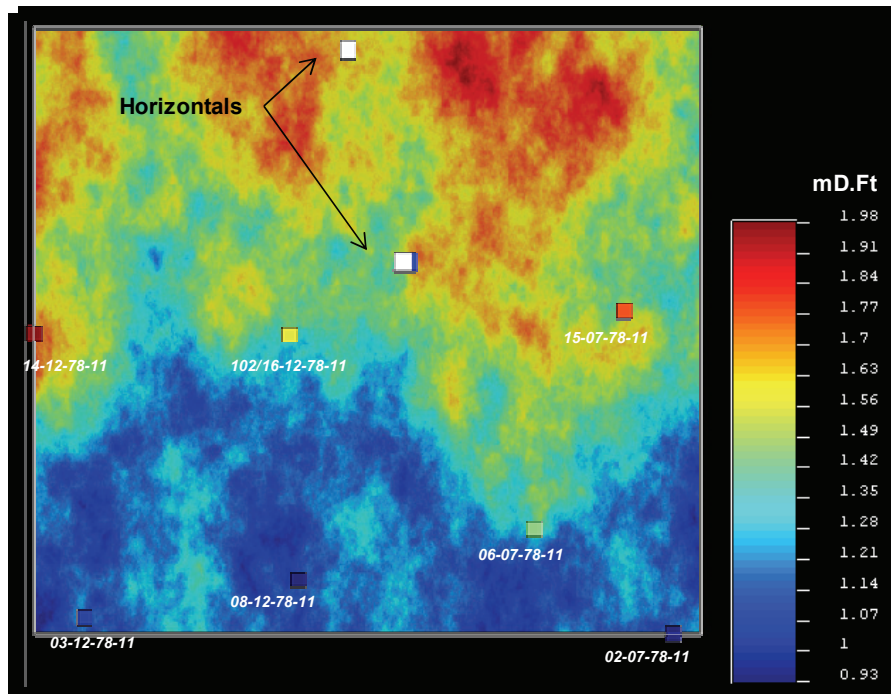


Fig. 42 — kh map constructed for a portion of our Area B tight gas field using kh values from rate-transient analysis of vertical wells. Vertical well locations are shown, along with wellhead locations of multi-fractured horizontal wells in the area. Image courtesy of Leyva, Yazdi and Murdoch (2010).

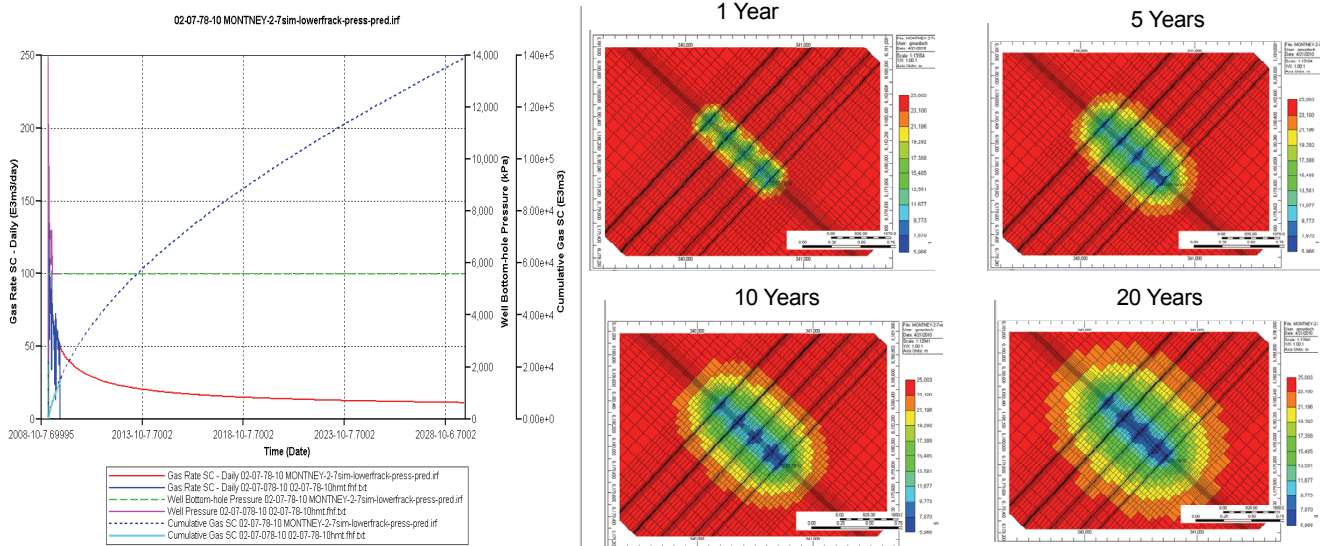


Fig. 43 — Use of field model for forecasting well production. (a) is a forecast for a multi-fractured well generated using the field model, and (b) is the resulting gridblock pressures viewed over time. Image courtesy of Leyva, Yazdi and Murdoch (2010).

Economics and Development Planning

Economic analysis of forecasts generated from simulation is necessary to make informed decisions about optimal development planning. Each of the scenarios generated during the modeling stage require different levels of capital investment and may have different operating costs. The calculated revenue generated for each development scenario is offset by costs specific to that development scenario, and hence the optimal scenario is one that adds the most value. There are also regulatory and environmental considerations. As an example, we look at the relatively simple case of optimizing hydraulic fracture length for a single well scenario, assuming planar fracture geometry (Fig. 44). A numerical simulator was used to generate forecasts as a function of hydraulic fracture half-length - stimulation costs for each fracture design scenario were evaluated by estimating the corresponding treatment volumes with a hydraulic fracture simulator. Details associated with this example provided in Voneiff and Gatens (1993). Longer fracture half-lengths translate into greater production, but the

increased revenue is offset by increased cost associated with the hydraulic fracture treatment (more sand etc.). An optimal hydraulic fracture size that maximizes value can be identified using this approach. A similar approach can be used to identify optimal number of fractures in multi-fractured horizontal wells (see Meyer et al. 2010), well-spacing etc. Further, surface facility, compression and wellbore design can be optimized in a similar way (using calibrated reservoir models) – an example of compression design for CBM wells was provided in Clarkson and McGovern (2005).

Uncertainty in the reservoir and hydraulic fracture model parameters (ex. permeability etc.) may require that a stochastic approach be used to generate a range of forecasts for each change in design parameter (ex. fracture half-length) - this will lead to a distribution of forecasts being generated for each scenario. This process is described in Economides et al. (1994) for hydraulic fracture design.

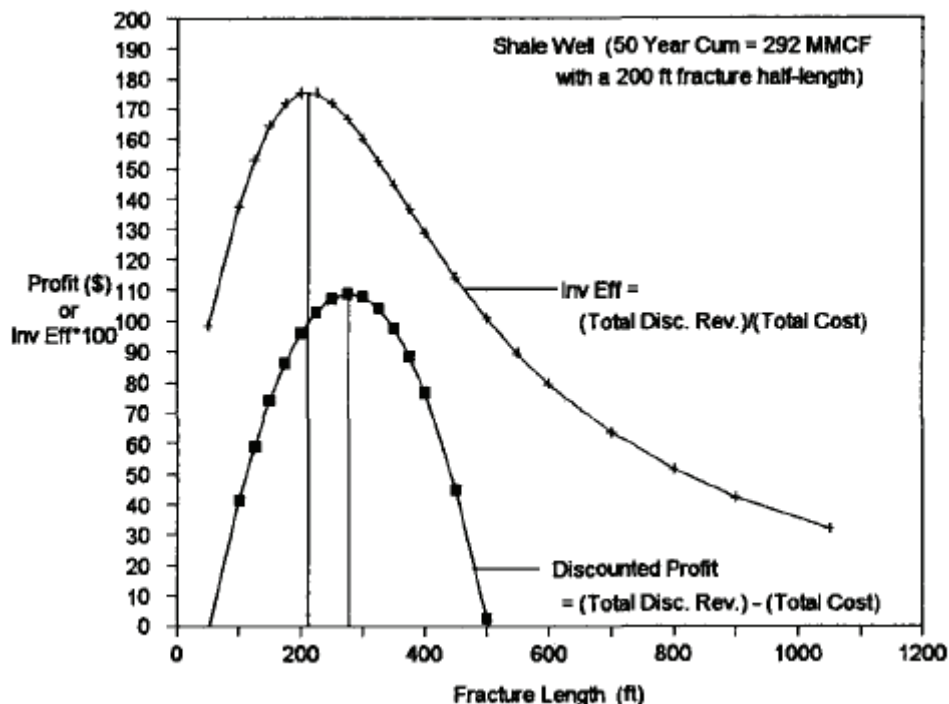


Fig. 44 — Using simulation and economics to optimize hydraulic fracture length. Example from Voneiff and Gatens (1993).

Alas, field development must consider many more parameters than can be covered in this article. The reader is referred to an excellent summary (Reynolds and Munn 2010) of field development considerations for the Horn River Basin, British Columbia, including pad design considerations, hydraulic fracture treatments, production and operations challenges, infrastructure issues, and development costs and economics.

Discussion

In this paper we have discussed many of the issues related to UGR evaluation that we think the reservoir engineer must be familiar with and concerned about when performing field development optimization. Clearly we are unable to go into detail on all critical topics, and there are several that we have not discussed at all. For example, PVT properties of reservoir fluids were not discussed, but we feel this is also an important aspect of UGR evaluation. Given the current favorable pricing for oil and hydrocarbon liquids, many E&P companies are pursuing UGR plays with a significant liquid hydrocarbon yield. PVT evaluation of these fluids is a critical aspect of modeling, and understanding fluid composition of course is critical to valuing assets. It is unclear how liquid hydrocarbons are transported through unconventional reservoirs (ex. shales), and how pore structure affects selective transport of these fluids. The thermodynamic properties of these fluids within the ultrafine pore structure are also poorly understood. Sorption properties of heavy hydrocarbons on shale has not been investigated in detail. Finally, even for dry gas scenarios, the current trend to deeper and hotter plays means that conventional PVT correlations for gaseous components and their mixtures will be challenged. There is still much research to be performed in the area of fluid PVT in UGRs.

Another aspect of UGRs that was not discussed in detail includes geological and geophysical (G&G) evaluation. An excellent discussion of integrated geologic and engineering workflows for UGRs was provided by Newsham and Rushing (2001) and Rushing and Newsham (2001), much of which is still relevant today. Some UGR are referred to as “engineering plays” because of the emphasis placed on drilling and completions strategies. We contend however that G&G evaluation of these plays is critical, from micro- to macro-scale. At the microscale, for example, an understanding of mineralogic and organic matter type/thermal maturity and diagenetic effects on pore structure is critical for understanding transport and storage processes in UGRs – these types of studies are commonly performed by geoscientists. At the macro-scale,

understanding the depositional and structural controls on natural fracture development and distribution, and other controls on reservoir quality is also in the domain of geoscientists. Also, there is the huge contribution that microseismic has made to helping us understand geologic controls on induced hydraulic fracture networks. Our workflow in Fig. 1 is premised on the fact that much important G&G evaluation is part of the process.

Although we touched on it, we would also like to reinforce the importance of careful wellbore architecture, completion and stimulation design in UGR. We refer you to excellent recent summaries by King (2010), Cramer (2008), Britt and Smith (2009) and Mayerhofer (2008).

Conclusions

In this manuscript, we have attempted to provide guidance to the practicing reservoir engineer on understanding data sources, data uncertainty and evaluation methods for unconventional gas reservoirs. Some new and emerging evaluation methods were also introduced. To guide the discussion, we provided a comprehensive workflow illustrating one approach to optimizing field development – examples of each step were provided using tight gas reservoirs in Western Canada. The following discussion points were raised for each step of the process:

Reservoir Sample Analysis

- Sample collection, preservation and conditioning has a critical impact on measured properties for UGRs
- There are no standards for many analyses run on UGRs, so the reservoir engineer must always question the conditions of lab measurement and understand the sensitivity of those properties being measured to PVTxt
- Use of crushed samples versus core: resulting permeability and porosity values will be vastly different because of both the conditions of the samples and conditions of measurement, and there are advantages and disadvantages to both. We think core plug analysis offers significant advantages because *in-situ* conditions can be more effectively preserved or recreated
- The pore structure of UGRs is complex, and proper characterization requires methods that span a large pore size range. New methods (for UGRs) such as USANS/SANS are showing great promise for characterizing pore structure under realistic PT conditions
- Combined profile/pulse-decay permeability measurements appears to be an effective way of characterizing fine-scale permeability heterogeneity in tight gas reservoirs
- There are many controls on gas storage in UGRs; sorbed gas storage often cannot be characterized by TOC alone
- Electrical properties, although not commonly measured for UGRs, are important for properly calculating Sw
- Measurement of rock mechanical properties of UGRs is critical to ascertain which portions of the reservoir are amenable to hydraulic fracturing (more brittle), but as with other measured core properties, scale-up to reservoir is a challenge for UGRs

Log Analysis

- There are new petrophysical tools and workflows that have greatly aided with estimation of those properties affecting free-gas and sorbed gas storage, hydraulic fracturing etc., however well-logs must be calibrated to core data to provide quantitative estimates
- Scale-up of core data to logs continues to be a difficult process for UGRs because core-scale heterogeneities (ex. laminations) often are below the resolution of logging tools
- Innovative methods presented in this work for finely-laminated tight gas reservoirs appear effective for establishing the appropriate scale(s) for reservoir layering

Well Test Analysis

- The unique properties of UGRs continue to challenge conventional well-test analysis techniques: in particular for tight gas and shale gas reservoirs, the radial flow period, which allows a unique estimate of permeability to be obtained, is often not reached in a reasonable timeframe
- Pre-frac testing is useful for establishing estimates of reservoir pressure and sometimes permeability – the shorter time frame of these tests make them desirable, but they sample a smaller volume of the reservoir
- If reservoir pressure and permeability can be established from independent sources, conventional post-fracture well-tests with identified hydraulic fracture signatures can still be useful for quantifying hydraulic fracture properties
- Analysis of flowback data (immediately after hydraulic fracturing operations) is a promising avenue for obtaining hydraulic fracture properties (ex. Ilk et al. 2010)

Rate-Transient and Production Data Analysis

- There have been significant advances in rate-transient and production data analysis for UGRs, accounting for the unique reservoir and hydraulic fracture properties
- Rate-transient analysis must incorporate surveillance data such as microseismic and production logs to yield meaningful results – in the complex fracture geometry scenarios, hydraulic fracture properties derived from RTA/PTA are at best semi-quantitative, and may not be of great use for hydraulic fracture design
- Results of RTA must be compared to other sources (core, well-test) before using derived properties in simulation modeling

Hydraulic Fracture Modeling

- Hydraulic fracture modeling, which uses pressures monitored during the frac job, minimum stress profile, rock mechanical properties, fluid properties, injection rate, proppant concentration and slurry information to predict propp'd hydraulic fracture length and conductivity, is well established for conventional reservoirs, but is problematic for shale gas or CBM reservoirs that exhibit a complex fracture geometry
- Microseismic data analysis is a promising technique for inferring hydraulic fracture geometry, but does not provide fracture conductivity distribution information (within natural or hydraulic fractures)
- Hydraulic fracture models that accommodate more complex fracture geometry are starting to be developed
- The most rigorous approaches for modeling complex fracture geometries involve the use of coupled fluid flow and transport models, with geomechanical simulation

Reservoir Modeling

- 10 tips for reservoir simulation of UGR:
 1. Use fine gridding near the fractures and small time steps and test appropriateness of gridding using well-test analysis techniques (derivative analysis to identify flow regimes and sequence)
 2. Select the right tools for the job
 3. Pick the simplest tool that gets the job done
 4. Perform rate-transient analysis first
 5. Incorporate surveillance data to assist with history-matches
 6. Constrain volumetric (static) model as much as possible
 7. Use field simulation where well-to-well interference effects need to be captured and where there is significant lateral and vertical heterogeneity
 8. Use stochastic models when there is a large uncertainty in model inputs
 9. Constrain simulation with surface/wellbore model for forecasting
 10. Use flow simulation or coupled flow/geomechanical models to model flowback of fracturing fluids
- Perhaps the greatest challenge facing reservoir engineers modeling UGRs is modeling systems that exhibit a complex fracture geometry – there are several approaches available to model this scenario, but forecasts may differ substantially
- Simulation is an immensely useful tool but requires constraint using results of reservoir/hydraulic fracture characterization methods – iteration may be required with various steps of the optimization workflow to arrive at satisfactory calibrated model that can serve as a starting point for development sensitivities

Economics and Development Planning

- Economic analysis of forecasts generated from simulation is necessary to make informed decisions about optimal development planning
- Each of the scenarios generated during the modeling stage require different levels of capital investment and may have different operating costs
- The calculated revenue generated for each development scenario is offset by costs specific to that development scenario, and hence the optimal scenario is one that adds the most value

Unconventional gas reservoirs require the reservoir engineer to integrate a vast amount of data from disparate sources, and to be intimately involved in the process of the data collection and evaluation. Further, with the amount of new technology being put forward to assist with the development of UGRs, the reservoir engineer must be on top of all new developments.

Acknowledgements

Chris Clarkson would like to acknowledge Encana for support of his Chair position in Unconventional Gas at the University of Calgary, Department of Geosciences. Jerry Jensen holds the Schulich Chair in Geostatistics at the University of Calgary. The authors would like to thank Dr. Azfar Hassan and Dr. Pedro Pereira for performing N₂ adsorption experiments and Lou Monahan and Raymond Chan of CoreLab for assisting with permeability measurements.

This work utilized facilities supported in part by the National Science Foundation under Agreement No. DMR-0454672. We acknowledge the support of the National Institute of Standards and Technology, U.S. Department of Commerce, in providing the neutron research facilities (USANS) used in this work. Research (SANS) at Oak Ridge National Laboratory's High Flux Isotope Reactor was sponsored by the Laboratory Directed Research and Development Program and the Scientific User facilities Division, Office of Basic Energy Sciences, U. S. Department of Energy.

Nomenclature

Field Variables

A_{cm}	= Total matrix surface area contacted by hydraulic fracture, ft ²
b	= Arps' decline exponent, dimensionless
D	= reciprocal of loss ratio, D ⁻¹
E	= Young's modulus, psi
F_c	= Fracture conductivity, md-ft
h	= Formation thickness, ft
I	= Intensity of scattering (neutron coherent cross section $I(q)$), cm ⁻¹
k	= Permeability, mD
m	= cementation factor, dimensionless
$m(p)$	= Real gas pseudopressure, psi ² /cp
n	= saturation exponent, dimensionless
p	= Pressure, psia, kPa or MPa
r_{p35}	= Pore throat aperture at 35% cumulative pore volume (mercury saturation in capillary pressure test), microns
q	= Scattering vector, Å ⁻¹
q_g	= Gas production (surface) flowrate, MSCF/D
S_w	= Water saturation, dimensionless
x_f	= Fracture half length, ft

Dimensionless Variables

F_{cD}	= Dimensionless fracture conductivity
q_D	= Dimensionless rate
r_{eD}	= Dimensionless wellbore radius for hydraulically-fractured well type-curves
t_D	= Dimensionless time

Greek Variables

μ_g	= Gas viscosity, cp
ν	= Poisson's Ratio, dimensionless
ϕ	= Porosity, fraction

References

- Agarwal, R.G., Gardner, D.C., Kleinsteiber, S.W., and Fussell, D.D. 1999. Analyzing Well Production Data Using Combined Type Curve and Decline Curve Concepts. *SPEEE* 2 (5): 478–486. SPE-57916-PA.
- Aguilera, R., 2008. Role of Natural Fractures and Slot Porosity on Tight Gas. SPE Paper 114174 at the SPE Unconventional Reservoirs Conference, Keystone, Colorado, 10-12 February.
- Aguilera, R., 2010. Flow Units: From Conventional to Tight Gas to Shale Gas Reservoirs. SPE Paper 132845 presented at the Trinidad and Tobago Energy Resources Conference held in Port of Spain, Trinidad, 27–30 June 2010.
- Ambrose, R.J., Clarkson, C.R., Youngblood, J., Adams, R., Nguyen, Phuong, Nobakht, M., Biseda, B. 2011. Life-Cycle Decline Curve Estimation for Tight/Shale Gas Reservoirs. Paper SPE 140519 presented at the SPE Hydraulic Fracturing Technology Conference and Exhibition held in the Woodlands, Texas, 24–26 January.
- Ambrose, R. J., Hartman, R. C., Diaz-Campos, M., Akkutlu, Y., and Sondergeld, G. H., 2010, New Pore-Scale Considerations for Shale Gas in Place Calculations, SPE paper 131772 presented at the SPE Unconventional Gas Conference held in Pittsburgh, Pa., February 23-25.

- Amini, S., Ilk, D. and Blasingame, T.A. 2007. Evaluation of the Elliptical Flow Period for Hydraulically-Fractured Wells in Tight Gas Sands – Theoretical and Practical Considerations. Paper SPE 106308 presented at the SPE Hydraulic Fracturing Technology Conference, College Station, Texas, 29–31 January.
- Anderson, D.M., Nobakht, M., Moghadam, S. and Mattar L. 2010. Analysis of Production Data from Fractured Shale Gas Wells. Paper SPE 131787 presented at the SPE Unconventional Gas Conference, Pittsburgh, Pennsylvania, 23–25 February.
- Andrade, J., Civan, F., Devegowda, D., Sigal, R. 2010. Accurate Simulation of Shale-Gas Reservoirs. Paper SPE 135564 presented at the SPE Annual Technical Conference and Exhibition held in Florence, Italy, 19-22 September.
- Barree, R.D., Cox, S.A., Gilbert, J.V., and Dobson, M. 2005. Closing the Gap: Fracture Half-Length from Design, Buildup and Production Analysis. *SPE Production & Facilities* (November 2005): 274-285. SPE-84491-PA.
- Barree, R.D., Barree, V.L., and Craig, D.P. 2007. Holistic Fracture Diagnostics. Paper SPE 107877 SPE Rocky Mountain Petroleum Technology Conference, Denver, Colorado, 16–18 April.
- Barree, R.D., Gilbert, J.V., and Conway, M.W. 2009. Stress and Rock Property Profiling for Unconventional Reservoirs. Paper SPE 118703 presented at SPE Hydraulic Fracturing Technology Conference and Exhibition held in the Woodlands, Texas, 19–21 January.
- Bartenhagen, K. (2009). Wireline Evaluation Techniques of Shale Gas Reservoirs. *Schlumberger Presentation*. Oklahoma City, OK: Schlumberger Limited.
- Beliveau, D. 1993. Honey, I Shrunk the Pores. *JCPT* **32**: 15-17
- Bello, R.O. and Wattenbarger, R.A. 2008. Rate Transient Analysis in Naturally Fractured Shale Gas Reservoirs. Paper SPE 114591 presented at the CIPC/SPE Gas Technology Symposium 2008 Joint Conference, Calgary, Alberta Canada, 16-19 June.
- Berg, R.R.: *Reservoir Sandstones*, Prentice-Hall, Englewood Cliffs, N.J. (1986), 481 p.
- Britt, L.K., and Schoeffler, J. 2009. The Geomechanics of a Shale Play: What Makes a Shale Prospective! Paper SPE 125525 presented at the 2009 SPE Eastern Regional Meeting, Charleston, WVA, 23-25 September.
- Britt, L.K., and Smith, M.B. 2009. Horizontal Well Completion, Stimulation Optimization, and Risk Mitigation. Paper SPE 125526 presented at the 2009 SPE Eastern Regional Meeting, Charleston, WVA, 23-25 September.
- Byrnes, A.P. 2006. Rock Properties of Tight Gas Sandstones. Shortcourse Notes.
- Bustin, R. M., Bustin, A. M. M., Cui, X., Ross, D. J. K., and Murthy Pathi, V. S., 2008a. Impact of Shale Properties on Pore Structure and Storage Characteristics, SPE paper 119892 presented at the SPE Shale Gas production Conference held in Fort Worth, Texas, 16-18 November.
- Bustin, R. M., Bustin, A., Ross, D., Chalmers, G., Murthy, V., Laxmi, C., and Cui, X. 2008b. Shale Gas Opportunities and Challenges. Search and Discovery Articles # 40382 (2009). Adapted from oral presentation at AAPG Annual Convention, San Antonio, Texas, 20-23 April.
- Cipolla, C.L., Warpinski, N.R., Mayerhofer, M.J., Lolon, E.P., and Vincent, M.C. 2008. The Relationship Between Fracture Complexity, Reservoir Treatment and Fracture Treatment Design. Paper SPE 115769 presented at the 2008 SPE Annual Technical Conference and Exhibition, Denver, CO, 21-24 September.
- Cipolla, C.L., Williams, M.J., Weng, X., and Maxwell, S. 2010. Hydraulic Fracture Monitoring to Reservoir Simulation: Maximizing Value. Paper SPE 133877 presented at the SPE Annual Technical Conference and Exhibition held in Florence, Italy, 19-22 September.
- Civan, F., 2010. Effective Correlation of Apparent Gas Permeability in Tight Porous Media. *Transp. Porous Media* **82**: 375-384.
- Clarkson, C.R., and Beierle, J.J. 2010. Integration of Microseismic and Other Post-Fracture Surveillance with Production Analysis: A Tight Gas Study. Paper SPE 131786 presented at the SPE Unconventional Gas Conference held in Pittsburgh, Pennsylvania, 23-25 February.
- Clarkson, C.R., and Bustin, R.M. 1997. Variation in Permeability with Lithotype and Maceral Composition of Cretaceous Coals of the Canadian Cordillera. *The International Journal of Coal Geology* **33**: 135-151.
- Clarkson, C.R., and Bustin, R.M., 1999a. The Effect of Pore Structure and Gas Pressure Upon the Transport Properties of Coal: A Laboratory and Modeling Study. 1. Isotherms and Pore Volume Distributions. *Fuel* **78**: 1333-1344
- Clarkson, C.R., and Bustin, R.M., 2010. Coalbed Methane: Current Evaluation Methods, Future Technical Challenges. Paper SPE 131791 presented at the SPE Unconventional Gas Conference held in Pittsburgh, Pennsylvania, 23-25 February.
- Clarkson, C.R., and McGovern, J.M. 2005. Optimization of Coalbed Methane Reservoir Exploration and Development Strategies Through Integration of Simulation and Economics. *SPEE* **8** (6): 502–519. SPE-88843-PA.
- Clarkson, C.R., Bustin, R.M., and Seidle, J.P. 2007. Production-Data Analysis of Single-Phase (Gas) Coalbed-Methane Wells. *SPEE* **10** (3): 312–331. SPE-100313-PA.
- Clarkson, C.R., Jordan, C.L., Gierhart, R.R., and Seidle, J.P. 2008. Production Data Analysis of CBM Wells. *SPEE* **11** (2): 311–325. SPE-107705-PA.
- Clarkson, C.R., Jordan, C.L., Ilk, D. and Blasingame, T.A. 2009. Production Data Analysis of Fractured and Horizontal CBM Wells. Paper SPE 125929 presented at the 2009 SPE Eastern Regional Meeting held in Charleston, West Virginia, 23-25 September.

- Clarkson, C.R., Aguilera, R., Pedersen, P.K. and Spencer, R. 2011a. Shale Gas Production Analysis and Forecasting Production. Shale Gas Series, Part 7: Shale Gas Production Analysis and Forecasting. Canadian Society of Petroleum Geologists Reservoir (March 2011).
- Clarkson, C.R., Nobakht, M., Kaviani, D. and Ertekin, T. 2011b. Production Analysis of Tight Gas and Shale Gas Reservoirs Using the Dynamic-Slippage Concept. Paper SPE 144317 presented at the North American Unconventional Gas Conference and Exhibition held in The Woodlands, Texas, 12–16 June.
- Comisky, J.T., Newsham, K.E., Rushing, J.A., and Blasingame, T.A. 2007. A Comparative Study of Capillary-Pressure-Based Empirical Models for Estimating Absolute Permeability in Tight Gas Sands. Paper SPE 110050 presented at the SPE Annual Technical Conference and Exhibition held in Anaheim, California, 11-14 November.
- Cramer, D.D. 2008. Stimulating Unconventional Reservoirs: Lessons Learned, Successful Practices, Areas for Improvement. Paper SPE 114172 presented at the 2008 Unconventional Reservoirs Conference, Keystone, CO, 10-12 February.
- Cui, X., Bustin, A.M.M., and Bustin, R.M. 2009. Measurements of Gas Permeability and Diffusivity of Tight Reservoir Rocks: Different Approaches and their Applications, *Geofluids* (2009) 9, 208–223.
- Dake, L.P.: *Fundamentals of Reservoir Engineering*, Elsevier (1978).
- Economides, M.J., Hill, A.D., and Ehlig-Economides, C.: *Petroleum Production Systems*, Prentice Hall PTR, New Jersey (1994).
- Gan, H., Nandi, S.P., and Walker, P.L., 1972. Nature of the Porosity in American Coals. *Fuel* **51**: 272-277.
- Gerami, S., Pooladi-Darvish, M., Morad, K., and Mattar, L. 2007. Type Curves for Dry CBM Reservoirs With Equilibrium Desorption. Paper 2007-011 presented at the Petroleum Society's Canadian Petroleum Conference, Calgary, Alberta, Canada, 12–14 June.
- Gregg, S.J. and Sing, K.S.W. *Adsorption, Surface Area and Porosity*, second edition: Academic Press, New York (1982), 303 pp.
- Guo, R., Mannhart, K., and Kantzas, A. 2007. Characterizing Moisture and Gas Content of Coal by Low-Field NMR. *The Journal of Canadian Petroleum Technology* 46 (10): 49-54.
- Ham, Y. and Kantzas, A. 2008. Measurement of Relative Permeability of Coal: Approaches and Limitations. Paper SPE 114994 presented at the CIPC/SPE Gas Technology Symposium 2008 Joint Conference, Calgary, Alberta, Canada, 16–19 June.
- Hartman, C., Bhatta, Nimesh, and Lasswell, P. 2008. Recent Advances In The Analytical Methods Used For Shale Gas Reservoir Gas-In-Place Assessment. Oral Presentation, SPE Shale Gas production Conference held in Fort Worth, Texas, 16-18 November.
- Howell, G., Javaid, M., Ogundele, P. 2011. University of Calgary Geology/Chemical and Petroleum Engineering 698 Capstone Project 2011.
- Ilk, D., Valko, P.P., and Blasingame, T. A. 2005. Deconvolution of Variable-Rate Reservoir Performance Data Using B-Splines. Paper SPE 95571 presented at the 2005 Annual SPE Technical Conference and Exhibition, Dallas, TX, 09-12 October.
- Ilk, D., Rushing, J.A., Perego, A.D., and Blasingame, T.A. 2008. Exponential vs. Hyperbolic Decline in Tight Gas Sands – Understanding the Origins and Implications for Reserve Estimates Using Arps' Decline Curves. Paper SPE 116731 presented at the SPE Annual Technical Conference and Exhibition, Denver, CO, 21–24 September.
- Ilk, D., Currie, S.M., Symmons, D., Rushing, J.A., Broussard, N.J. and Blasingame, T.A. 2010. A Comprehensive Workflow for Early Analysis and Interpretation of Flowback Data from Wells in Tight Gas/Shale Reservoir. Paper SPE 135607 presented at the SPE Annual Technical Conference and Exhibition, Florence, Italy, 19–22 September.
- Ilk, D., Rushing, J.A., and Blasingame, T.A. 2011. Integration of Production Analysis and Rate-Time Analysis via Parametric Correlations – Theoretical Considerations and Practical Applications. Paper SPE 140556 presented at the SPE Hydraulic Fracturing Technology Conference and Exhibition held in the Woodlands, Texas, 24–26 January.
- Jacobi, D., Gladkikh, M., LeCompte, B., Hursan, G., Mendez, F., Longo, J., Ong, S., Bratovich, M., Patton, G., Shoemaker, P., 2008. Integrated Petrophysical Evaluation of Shale Gas reservoirs. SPE paper 114925 presented at the CIPC/SPE Gas technology Symposium Joint Conference held in Calgary, Canada, 16-19 June.
- Jahanbani, A., and Aguilera, R. 2009. Well Testing in Tight Gas Reservoirs. *The Journal of Canadian Petroleum Technology* **48** (10): 64-70.
- Javadpour, F., Fisher, D., and Unsworth, 2007. Nanoscale Gas Flow in Shale Gas Sediments. *JCPT* **46** (10): 55-61.
- Javadpour, F., 2009. Nanopores and Apparent Permeability of Gas Flow in Mudrocks (Shales and Siltstones). *JCPT* **48** (8): 16-21.
- Jensen, J. L., Corbett, P. W. M., Pickup, G. E., and Ringrose, P. S. 1996. Permeability Semivariograms, Geological Structure, and Flow Performance. *Mathematical Geology*, **28**(4): 419-435.
- Jones, S.C., 1994. A New, Fast, Accurate Pressure-Decay Probe Permeameter. *SPE Formation Evaluation* **9**: 193-199.
- Jones, S.C., 1997. A Technique for Faster Pulse-Decay Permeability Measurements in Tight Rocks. *SPE Formation Evaluation* **12**: 19-26.
- King, G.E. 2010. Thirty Years of Gas Shale Fracturing: What Have We Learned? Paper SPE 133456 presented at the SPE Annual Technical Conference and Exhibition, Florence, Italy, 19–22 September.

- Kupchenko, C.L., Gault, B.W., and Mattar, L. 2008. Tight Gas Production Performance Using Decline Curves. Paper SPE 114991 presented at the CIPC/SPE Gas Technology Symposium 2008 Joint Conference, Calgary, Alberta Canada, 16-19 June.
- Leyva, I., Yazdi, M.M. and Murdoch, G. 2010. University of Calgary Geology/Chemical and Petroleum Engineering 698 Capstone Project 2010.
- Mack, M., Cipolla, C.L., and Maxwell, S. 2010. Geomechanical Explanations for Microseismic Images in Shale Plays. Poster presentation at the AAPG/SEG/SPE/SPWLA Hedberg Research Conference entitled "Critical Assessment of Shale Resource Plays", Austin, TX, 5-10 December, 2010.
- Mavor, M.J.: Coalbed Methane Reservoir Properties. *A Guide to Coalbed Methane Reservoir Engineering*, Gas Research Inst. Report GRI-94/0397, Chicago (1996).
- Mavor, M.J., and Saulsberry, J.L. 1996. Testing Coalbed Methane Wells. *A Guide to Coalbed Methane Reservoir Engineering*, Gas Research Inst. Report GRI-94/0397, Chicago (1996).
- Mayerhofer, M.J., Lolon, E.J., Warpinski, N.R., Cipolla, C.L. and Walser D. 2008. What is Stimulated Reservoir Volume? Paper SPE 119890 presented at the SPE Shale Gas Production Conference, Fort Worth, TX, 16–18 November.
- Melnichenko, Y.B., Radlinski, A.P., Mastalerz, M., Cheng, G., and Rupp, J. 2009. Characterization of CO₂ Fluid Adsorption in Coal as a Function of Pressure using Neutron Scattering Techniques. *International Journal of Coal Geology* 77 (69): 1-11.
- Meyer, B.R., Bazan, L.W., Jacot, R.H., and Lattibeaudiere, M.G. 2010. Optimization of Multiple Transverse Hydraulic Fractures in Horizontal Wells. Paper SPE 131732 presented at the SPE Unconventional Gas Conference, Pittsburgh, Pennsylvania, 23–25 February.
- Mohaghegh, S.D., and Ertekin, T. 1991. Type-Curve Solution for Coal Seam Degasification Wells Producing Under Two-Phase Conditions. Paper SPE 22673 presented at the SPE Annual Technical Conference and Exhibition, Dallas, Texas, 6-9 October.
- Newsham, K.E., Rushing, J.A., Lasswell, P.M., Cox, J.C. and Blasingame, T.A. 2004. A Comparative Study of Laboratory Techniques for Measuring Capillary Pressures in Tight Gas Sands. Paper SPE 89866 presented at the SPE Annual Technical Conference and Exhibition held in Houston, Texas, 26-29 September.
- Nobakht, M. and Clarkson, C.R. 2011a. A New Analytical Method for Analyzing Production Data from Shale Gas Reservoirs Exhibiting Linear Flow: Constant Pressure Production. Paper SPE 143989 presented at the North American Unconventional Gas Conference, The Woodlands, Texas, Texas, 14–16 June.
- Nobakht, M. and Clarkson, C.R. 2011b. A New Analytical Method for Analyzing Production Data from Shale Gas Reservoirs Exhibiting Linear Flow: Constant Rate Production. Paper SPE 143990 presented at the North American Unconventional Gas Conference, The Woodlands, Texas, Texas, 14–16 June.
- Nobakht, M., Mattar, L., Moghadam, S. and Anderson, D.M. 2010. Simplified Yet Rigorous Forecasting of Shale/Tight Gas Production in Linear Flow. Paper SPE 133615 presented at SPE Western Regional Meeting held in Anaheim, California, 27–29 May.
- Passey, Q. R., Creaney, S., Kulla, J. B., Moretti, F. J., Stroud, J. D., 1990. A Practical Model for Organic Richness From Porosity and Resistivity Logs. *AAPG Bulletin*, December.
- Pratikno, H., and Blasingame, T.A. 2003. Decline Curve Analysis Using Type-Curves – Fractured Wells. Paper SPE 84287 presented at the SPE Annual Technical Conference and Exhibition, Denver, Colorado, 5–8 October.
- Ramurthy, M., Marjerisson, D.M., and Daves, S.B. 2002. Diagnostic Fracture Injection Test in Coals to Determine Pore Pressure and Permeability. Paper SPE 75701 presented at the Gas Technology Symposium, Calgary, Alberta, Canada, 30 April – 2 May.
- Reynolds, M.M., and Munn, D.L. 2010. Development Update for an Emerging Shale Gas Giant Field – Horn River Basin, British Columbia, Canada. Paper SPE 130103 presented at the SPE Unconventional Gas Conference, Pittsburgh, Pennsylvania, 23–25 February.
- Rickman, R., Mullen, M., Petre, E., Grieser, B., Kundert, D. 2008. A Practical Use of Shale Petrophysics for Stimulation Design Optimization: All Shale Plays are Not Clones of the Barnett Shale. Paper SPE 115258 presented at the SPE Annual Technical Conference and Exhibition held in Denver, Colorado, 21-24 October.
- Roadifer, R., Moore, T.R., Raterman, K.T., Farnan, R.A., and Crabtree, B.J. 2003. Coalbed Methane Parametric Study: What's Really Important to Production and When? Paper SPE 84425 presented at the SPE Annual Technical Conference and Exhibition held in Denver, Colorado, 5-8 October.
- Roadifer, R., and Moore, T.R. 2009. Coalbed Methane Pilots – Timing, Design, and Analysis. *SPEREE* (October 2009): 772-782. SPE-114169-PA.
- Ross, D.J.K. and Bustin, R.M. 2007. Impact of Mass Balance Calculations on Microporous Shale Gas Reservoirs. *Fuel*, vol. 85, p 2596-2706.
- Newsham K.E., and Rushing J.A. 2001. An Integrated Work-Flow Model to Characterize Unconventional Gas Resources: Part I – Geological Assessment and Petrophysical Evaluation. Paper SPE 71351 presented at the SPE Annual Technical Conference and Exhibition held in New Orleans, Louisiana, 30 September- 3 October.

- Rushing J.A. and Newsham K.E. 2001. An Integrated Work-Flow Model to Characterize Unconventional Gas Resources: Part II – Formation Evaluation and Reservoir Modeling. Paper SPE 71352 presented at the SPE Annual Technical Conference and Exhibition held in New Orleans, Louisiana, 30 September- 3 October.
- Rushing J.A., Newsham K.E., and Van Fraassen, K.C., 2003. Measurement of Two-Phase Gas Slippage Phenomenon and Its Effect on Gas Relative Permeability in Tight Gas Sands. Paper SPE 84297 presented at the SPE Annual Technical Conference and Exhibition held in Denver, Colorado, 5-8 October.
- Rushing J.A., Newsham K.E., Perego, A.D., Comisky, J.T. and Blasingame T.A., 2007. Beyond Decline Curves: Life-Cycle Reserves Appraisal Using an Integrated Workflow Process for Tight Gas Sands. Paper SPE 109836 presented at the SPE Annual Technical Conference and Exhibition held in Anaheim, California, 11-14 November.
- Rushing J.A., Newsham K.E., and Blasingame T.A., 2008. Rock Typing – Key to Understanding Productivity in Tight Gas Sands. Paper SPE 114164 presented at the SPE Unconventional Reservoirs Conference, Keystone, Colorado, 10-12 February.
- Shanley K.W., Cluff R.M., and Robinson J.W. 2004. Factors Controlling Prolific Gas Production from Low-Permeability Sandstone Reservoirs: Implications for Resource Assessment, Prospect Development, and Risk Analysis. *AAPG Bulletin* **88**: 1083 – 1121.
- Sing, K.S.W., Everett, D.H., Haul, R.A.W, Moscou, L., Pierotti, R.A., Rouquerol, J., and Siemieniowska, T. 1985. *Pure and Appl. Chem.* **57**: 603
- Sondergeld, C.H., Newsham, K.E., Comisky, J.T., Rice, M.C. and Rai, C.S. 2010a. Petrophysical Considerations in Evaluating and Producing Shale Gas Resources. Paper SPE 131768 presented at the SPE Unconventional Gas Conference, Pittsburgh, Pennsylvania, 23–25 February.
- Sondergeld, C.H., Ambrose, R.J., Rai, C.S. and Moncrieff, J. 2010b. Microstructural Studies of Gas. Paper SPE 131771 presented at the SPE Unconventional Gas Conference, Pittsburgh, Pennsylvania, 23–25 February.
- Thompson, D., Rispler, K., Stadnyk, S., Hoch, O., and McDaniel, B.W. 2009. Operators Evaluate Various Stimulation Methods for Multizone Stimulation of Horizontals in Northeastern British. Paper SPE 119620 presented at SPE Hydraulic Fracturing Technology Conference and Exhibition held in the Woodlands, Texas, 19–21 January.
- Thompson, J.M., Nobakht, M. and Anderson, D.M. 2010. Modeling Well Performance Data From Overpressured Shale Reservoirs. Paper CSUG/SPE 137755 presented at the Canadian Unconventional Resources & International Petroleum Conference, Calgary, Alberta, 19–21 October.
- Voneiff, G.W. and Gatens, J.M. III 1993. The Benefits of Applying Technology to Devonian Shale Wells. Paper SPE 26890 presented at the 1993 SPE Eastern Regional Conference and Exhibition, Pittsburgh, Pennsylvania, 2–4 November.
- Warpinski, N.R. 2009. Microseismic Monitoring: Inside and Out. SPE Distinguished Author Series, JPT, November 2009.
- Warpinski, N.R., Mayerhofer, M.J., Vincent, M.C., Cipolla, C.L., and Lonon, E.P. 2008. Stimulating Unconventional Reservoirs: Maximizing Network Growth While Optimizing Fracture Conductivity? Paper SPE 114173 presented at the 2008 Unconventional Reservoirs Conference, Keystone, CO, 10-12 February.
- Washburn, E.W. 1921. The Dynamics of Capillary Flow. *Physical Review* **17** (3): 273-283.
- Wattenbarger, R.A., El-Banbi, A.H., Villegas, M. E. and Maggard, J.B. 1998. Production Analysis of Linear Flow Into Fractured Tight Gas Wells. Paper SPE 39931 presented at the SPE Rocky Mountain Regional/Low-Permeability Reservoirs Symposium, Denver, Colorado, 5–8 April.
- Xu, W., Thiercelin, M., Ganguly, U., Weng, X., Gu, H., Onda, H., Sun, J., and Le Calvez, J. 2010. Wiremesh: A Novel ShaleFracture Simulator. Paper SPE 132218 presented at the CPS/SPE International Oil & Gas Conference and Exhibition in China held in Beijing, China, 8-10 June.